

THESIS D 2002

This is to certify that the

thesis entitled

Development Of A Mechanical Probe For NonDestructive Apple Firmness Evaluation

presented by

Hussain A. Ababneh

has been accepted towards fulfillment of the requirements for

Doctoral degree in Agricultural Engineering

MSU is an Affirmative Action/Equal Opportunity Institution

O-7639

Date ____

LIBRARY Michigan State University

PLACE IN RETURN BOX to remove this checkout from your record.

TO AVOID FINES return on or before date due.

MAY BE RECALLED with earlier due date if requested.

DATE DUE	DATE DUE	DATE DUE

6/01 c:/CIRC/DateDue.p65-p.15

DEVELOPMENT OF A MECHANICAL PROBE FOR NONDESTRUCTIVE APPLE FIRMNESS EVALUATION

Ву

Hussain Ahmad Amin Ababneh

A DISSERTATION

Submitted to

Michigan State University

in partial fulfillment of the requirements

for the degree of

DOCTOR OF PHILOSOPHY

Department of Agricultural Engineering 2002

ABSTRACT

DEVELOPMENT OF A MECHANICAL PROBE FOR NODESTRUCTIVE APPLE FIRMNESS EVALUATION

By

Hussain Ahmad Amin Ababneh

Fruit firmness is an important quality attribute of apples. It is important for consumer satisfaction, proper fruit storage, and shelf life. Therefore, it is considered a crucial parameter in the postharvest system. The Magness-Taylor pressure tester is widely accepted in the fruit industry for firmness measurement. However, it is destructive since it requires penetration of steel probe into the fruit flesh. The overall objective of this study was to develop a firmness tester that would be consistent with the Magness-Taylor measurement without causing fruit damage.

Since firmness is a measure of apple tissue strength in resisting probe penetration, the measurement of the bioyield strength of tissue was used to predict apple firmness. A mechanical probe composed of a cylindrical steel probe with rubber bonded at the end was pressed against fruit skin at a quasi-static rate, applying quasi-uniform pressure on the constant contact area. The Instron machine was used to detect the load drop due to the tissue failure.

A finite element (FE) model of the apple-probe contact was used to analyze the effect of various parameters on the contact stress distribution. It

provided guidelines for designing the probe to produce a quasi-uniform stress distribution.

Based on the FE results, six probes were built and evaluated experimentally. The probes were pressed against the fruit at a constant speed. The Instron testing machine was programmed to stop when a small drop in the contact force was suddenly detected due to tissue bioyielding. The force at the bioyield point was well correlated to the MT firmness measurement.

The 1/4" diameter probe with 1/8" rubber thickness was found to be the optimal probe. It was repeatable, produced minimum damage, and had the maximum correlation coefficient with the MT firmness measurement of 0.853 in comparison with the 0.919 of the MT firmness measurements on apposite sides of the fruit.

DEDICATION

This dissertation is dedicated to my wife Nabila Alomari, my daughter Judy, and son Hamzah to the memory of the time when we started our family.

ACKNOWLEDGMENTS

I would like to express my sincere gratitude to my admirable major professor, the Chairman of the Agricultural Engineering Department Prof. Ajit K. Srivastava for his guidance, suggestions and financial support. His wonderful scheme of technical analysis attracts my interest and made me delighted that he accepted me as a graduate student, and he would remain my academic example.

I am grateful to Dr. Renfu Lu my co-major professor, Agricultural Engineering Department –USDA for his assistance in the finite element study, experimental design and providing with the fruit samples.

My deepest thanks to Dr. Daniel E. Guyer, Agricultural Engineering Department for his serving as a member of my committee and providing valuable suggestions about the possible factors that might affect the bioyield test measurements.

I extend thanks for Dr. Randolph Beaudry, Department of Horticulture, who assisted me in recognizing the postharvest system and the biological structure of fruits.

I want also to extend my appreciation to Dr. Clark J. Radcliffe,

Department of Mechanical Engineering, for his serving in my committee

and providing valuable suggestions about the contact problem and the prospective online application of the probe in apple sorting.

Finally, I am thankful for Richard Wolthuis and Steve Marquie,
Agricultural Engineering Department for their technical assistance in
experimental construction and data acquisition.

TABLE OF CONTENTS

Abstract	ii
Dedication	iv
Acknowledgement	v
Table of Contents	vii
Table of Figures	xi
List of Tables	xiv
Chapter 1	
Introduction	1
1.1 Introduction	1
1.2 The Standard Firmness Test	2
1.3 Objectives	5
Chapter 2	
Literature Review	6
2.1 Acoustic and Impact Tests	
2.2 Quasi-Static Loading	7
2.3 The behavior of Apple Material	
2.4 Failure Criteria	13
2.5 Finite Element Studies	14
2.6 Summary	14
Chapter 3	
Theory of Contact between Bodies	16
3.1 Hertz Contact Theory	17
3.2 Assumptions for Apple-Probe Contact	18
3.3 Analysis	19
3.3.1 Concentrated Normal Force	23
3.3.2 General Axi-Symmetric Pressure Distribution	25

3.3.2.1 Uniform Pressure (n=0)	26
3.3.2.2 Uniform Normal Displacement (n= -1/2)	30
3.3.2.3 Hertz Pressure (n=+½)	31
3.3.3 Normal Stress at Any Point	35
3.3.4 The Viscoelestic Contact	35
3.3.5 Onset of Bioyield	37
3.4 Summary	40
Chapter 4	
Finite Element Simulation of the Contact Problem	42
4.1 The Concept of the Finite Element Method	43
4.2 Probe Design Considerations	45
4.3 Objectives	47
4.4 The Finite Element Model	48
4.5 Results and Discussion	53
4.5.1 Validation of the Finite Element Solution	53
4.5.2 Development of Bioyield Failure Criterion	56
4.5.3 Effects of Probe and Fruit Parameters	68
4.5.3.1 Rubber Elastic Modulus	68
4.5.3.2 Probe Diameter	70
4.5.3.3 Rubber Tip Thickness	71
4.5.3.4 Probe Edge Fillet Radius	71
4.5.3.5 Apple Size	73
4.5.3.6 Apple Skin	76
4.5.3.7 Friction	77
4.6 Summary and Conclusions	78
Chapter 5	
Experimental Evaluation	80
5.1 Introduction	80

5.2 Objectives	80
5.3 Materials and Methodology	81
5.3.1 Measuring Apple Material Properties	83
5.3.1.1 The Compression Test	83
5.3.1.2 The Stress Relaxation Test	85
5.3.2 The MT Firmness Test and The Bioyield Test	85
5.3.2.1 The Magness-Taylor Firmness Test	85
5.3.2.2 The Bioyield Point Test	87
5.3.2.3 The Mechanical Probes	88
5.3.3 Testing Procedure	90
5.4 Results and Discussion	92
5.4.1 Typical Bioyield Test	92
5.4.2 The Modulus of Elasticity	94
5.4.3 The Stress Relaxation Function	94
5.4.4 The Bioyield Point Test and Firmness Prediction	98
5.4.4.1 Regression Analysis	100
5.4.4.2 The Small-Thick Probe	105
5.5 Summary and Conclusions	119
Chapter 6	
Overall Summary, Conclusions and Recommendations	122
6.1 Summary	122
6.2 Conclusions	124
6.3 Recommendations	125
References	126
Appendices	132
Appendix A. The Testing Codes	
A.1 The Relaxation Testing Code	134
A.2 The Bioyield Point Testing Code	136

Appendix B. The Bioyield Test Results	138
B.1 Golden Delicious	139
B.2 Red Delicious	143
B.3 Fuji	147
B.4 Gala	151

TABLE OF FIGURES

<u>Figu</u>	<u>re</u> <u>Pa</u> ç	<u>je</u>
3.1	Coordinate system for the contact problem	17
3.2	Hertz contact of two convex bodies showing the principal axes	21
3.3	Concentrated force acting at the surface of a half-space	24
3.4	General axi-symmetric pressure distribution	26
3.5	Integration of the effect of pressure applied over a circular	
	area at point B(r, 0) located: (a) Inside the circle $[r < a]$	
	(b) Outside the circle $[r>a]$	27
3.6	Rigid cylindrical die loaded against half-space (Boussinesq problem)	30
3.7	Comparison of stress distributions at the surface and along the axis	
	of symmetry due to (left) uniform pressure and (right) Hertz	
	pressure on a circular area of radius a (Johnson 1985)	34
3.8	Variation of the pressure distribution against dimensionless	
	radius at particular times (Lee and Radok, 1960)	37
3.9	von Mises failure criterion in two-dimensional body	40
4.1	Probe geometry	46
4.2	Comparison of apple bioyield test by a cylindrical steel probe	
	with and without rubber tip	47
4.3	The finite element model showing the model components, the	
	boundary condition, and the path AB in the zoomed view of	
	the contact area	52
4.4	Uniaxial compression of cylindrical samples of apple and rubber,	
	the horizontal and vertical lines identify the linear	54
4.5	Comparison of the FD-curve of experimental and FE simulation	
	results of a particular apple	56
4.6	Displacement in the axial direction (mm)	62
4.7	Component of stress in the axial direction , σ_X (MPa)	63
4.8	Shear stress concentration under the outer edge (MPa)	64

4.9	Axial component of total strain (ϵ_{11})	65
4.10	Total strain energy density (J/cm ³)	66
4.11	Equivalent von Mises Stress, the white line indicates the locus	
	of local maximum stress	67
4.12	Effect of rubber modulus of elasticity on the normal	
	stress distribution	69
4.13	Effect of probe diameter on the normal contact stress distribution	70
4.14	Effect of rubber tip thickness on the normal contact stress	
	distribution	72
4.15	Effect of fillet radius on the normal contact stress distribution	72
4.16	Effect of fruit size on the normal contact stress distribution	75
4.1	7 Effect of skin modulus of elasticity on the normal contact	
	stress distribution	75
4.18	B Effect of skin thickness on the normal contact stress distribution	77
4.19	Effect of friction on the compression and shear stress distributions	78
5.1	The bioyield point test setup using the Instron Universal	
	Testing Machine	82
5.2	Preparation of the cylindrical sample	84
5.3	Compression test or relaxation test of the sample between	
	two parallel plates	84
5.4	The Magness-Taylor firmness test	86
5.5	The mechanical probes used in the bioyield test	89
5.6	Locations of the MT firmness and bioyield tests at opposite	
5.7	Locations of the MT firmness and bioyield tests at opposite sides	
	of the fruit. The circular areas are reserved for the MT tests, and	
	the bioyield tests are conducted at the spots marked by (x) using	
	the probe abbreviated next to the mark	91
5.8	Typical force-deformation relationship of the bioyield test	
	generated by the small-thick probe	93

5.8	The generalized Maxwell model of two simple elements96
5.9	The stress relaxation curve of apple material97
5.10	Correlation of the MT firmness with the force at the bioyield point
	measured by the small-thick probe (SK)107
5.11	Correlation of the MT firmness with the force at the bioyield point
	measured by the medium-thick probe (MK)108
5.12	Correlation of the MT firmness with the force at the bioyield point
	measured by the large-thick probe (LK)
5.13	Correlation of the MT firmness with the force at the bioyield point
	measured by the small thin probe (SN)110
5.14	Correlation of the MT firmness with the force at the bioyield point
	measured by the medium-thin probe (MN)111
5.15	Correlation of the MT firmness with the force at the bioyield point
	measured by the large-thin probe (LN)112
5.16	Comparison of the MT firmness measurements at opposite sides
	of the fruit of four apple varieties113
5.17	Correlation of the MT firmness with the stress at the bioyield point
	measured by three probe diameters (1/4, 3/8, and 7/16 inch), with
	constant rubber thickness to diameter ratio of ½114
5.18	Correlation of the MT firmness with the stress at the bioyield point
	measured by three probe diameters (1/4, 3/8, and 7/16 inch), with
	constant rubber thickness to diameter ratio of ¼
5.19	Variation of the deformation required for tissue bioyield with
	the diameter of the probe for thin and thick rubber tips116
5.20	Scatter plot of MT firmness versus the bioyield force measured by the
	small-thick (SK-probe), showing the prediction interval (PI) and
	confidence interval (CI), based on 95% confidence level, after
	eliminating 2% outlier data with the highest standardized residuals117
5.21	Correlation of bioyield force measurements of the small-thick
	(SK) probe and the medium-thick (MK) probe118

LIST OF TABLES

Tat	<u>ole</u>	<u>Page</u>
5.1	Dimensions and abbreviations of the probes	89
5.2	The correlation coefficient (r) between the Magness-Taylor	
	firmness and force, deformation, slope or energy at the	
	bioyield point	102

Introduction

1.1 Introduction

Firmness is an important attribute for evaluating the quality of fruit; it is directly associated with fruit growth, maturity, the resistance for bruising, the potential for good storability, shelf life and the acceptability by the consumer. Therefore, it is of critical importance and interest for fruit growers, handlers, quality controllers and retailers. In general, firmness of climacteric fruit, including apples, decreases gradually with maturity and decreases rapidly after the onset of the climacteric rise where the respiration has a peak rate (Seymour et al., 1993).

Growers use the number of days after bloom as an estimator of fruit firmness, but this is a subjective measure, since fruit firmness varies within the same tree, and it might be influenced by a diversity of features. Among them are the environmental conditions during the growing season and the storage conditions after harvest, the cultural practices, the apple cultivar and variety, the use of plant growth regulators and calcium content (Watkins *et al.*, 1980).

The dependence of fruit quality preharvest factors is complex and not well understood (Shewfelt and Prussia, 1992). Fruit firmness in the postharvest stage is also influenced by several handling techniques and storage conditions.

Fruit growers, processors, and retailers compete to supply and maintain certain standards of quality to meet the consumer's demands, which is the ultimate objective of the fresh fruit industry. Therefore, it is advantageous to be able to pack the fruit at a stage of maturity that will ensure adequate maturity, satisfactory and consistent quality as the product reaches the terminal market.

Fresh apples must be handled properly to retain high quality so as to meet the high standards of the domestic and export markets. Postharvest sorting is of critical importance in the fruit industry. The consumers prefer a high quality fruit that is firm, has a smooth, clean skin and a good color. Human senses are commonly used to evaluate fruit quality. For example, consumer might inspect apple firmness by holding it in the palm of the hand and listening to the sound pitch generated from thumping the fruit. However, instrumental measurement of firmness is more objective than sensory evaluation, and is, therefore, preferred.

A novel approach is used in this study; the firmness of the fruit is estimated by measuring the bioyield strength. The test must not result in degrading of the fruit. The bruise allowance for Extra Fancy apple grade is 3.2 mm (1/8 inch) in depth and 15.9 mm (5/8 inch) in equivalent diameter (The USDA Shipping Point Instructions, 1976). Canadian standards for the Extra Fancy grade requires apples to be free from individual bruises that exceed 19 mm (3/4 inch) in diameter or an aggregate area of bruises per apple greater than 25 mm (1 inch) in diameter (Canada Extra Fancy Grade Standards, 2001).

1.2 The Standard Firmness Test

Instruments and techniques for evaluating the textural properties of fruits are important in grading, quality control, and in predicting the mechanical behavior of the product during certain handling and storage conditions.

The most widely used instrument for evaluating the firmness of fruits is the Magness-Taylor (MT) pressure tester, which was developed in 1925 and still is accepted as the standard measure of firmness in the fruit industry. The test is composed of a cylindrical steel probe with a rounded tip; the probe is pressed into the peel fruit flesh to a certain depth. The maximum force required to penetrate the probe is considered as the firmness index of the fruit. Because of its destructive nature, the use of MT test is limited to fruit sampling and is inappropriate for sorting each individual fruit.

There are variant forms of MT testers available, for example:

- 1. The hand-held Effe-gi instruments (Abbott et al., 1976).
- The foot pedal modification of the hand-held instrument (Shewfelt, et al., 1987).
- 3. The mechanized Instron test.

The MT pressure tester is simple, low cost, and portable. However, it has the following disadvantages:

- 1) The test is of destructive nature in that the fruit being peeled and penetrated.
- 2) Penetration into the fruit involves a complex loading process, which makes it virtually impossible to simulate analytically.
- 3) MT firmness measurements may vary significantly with operator, owing to the viscoelastic behavior of flesh material, which is sensitive to strain rate or loading speed.

Elastic parameters of the quasi-static force / deformation compression curve of fruit were often considered as satisfactory indicators of fruit firmness. These parameters are based on the quasi-static compression of fruit in the elastic range, and are therefore related to the modulus of elasticity rather than firmness. Our preliminary experiments confirmed the conclusions of Bourne (1966) that MT firmness is best correlated with the shear strength and the bioyield compression strength. However, the measurement of shear strength requires relative deformation, for example cutting of fruit flesh, which would cause fruit destruction. Thus, the hypothesis of this study was to use the bioyield compression strength as a parameter for apple firmness prediction.

The bioyield point of biological materials is analogous to the yield point of engineering materials (Mohsenin 1986). Bioyielding is due to cell rupture. However, the damage due to the bioyield point measurement is minimal and the bruise depth is less than 2 mm (1/16 inch) under the skin. Therefore, Mohsenin *et al.* (1965) considered the bioyield approach as a practicable nondestructive technique for fruit firmness evaluation.

Grading of apples based on this concept could be accomplished without requiring that each apple reach the bioyield point. As such, good, firm apples can be judged by their capacity to withstand a threshold value of load without demonstrating a bioyield point.

1.3 Objectives

The objective of this study was to develop a nondestructive or a minimally destructive mechanical probe to evaluate apple firmness. The probe is used to detect the bioyield strength, which is considered an important textural property that relates to fruit firmness.

The specific objectives of the research reported in this dissertation were:

- 1) To establish an experimental technique for determining the bioyield point nondestructively.
- 2) To apply the finite element method to investigate the effect of the various parameters on the evaluation of the bioyield strength of fruit material.
- To design an optimal mechanical probe for nondestructive or minimally destructive evaluation of firmness.
- 4) To examine different failure criteria in order to specify the most suitable criterion, this could predict apple tissue failure in the bioyield test by comparing with the criterion at failure of a uniaxial sample with the corresponding value, obtained by the finite element solution of the same apple.
- 5) To use the designed mechanical probes and experimentally evaluate their ability to measure the bioyield point and predict the standard MT firmness test measurements.

Literature Review

Nondestructive fruit firmness evaluation has been a subject of interest to researchers for many years. Several methods have been investigated for the nondestructive evaluation of apple firmness. These methods are based on quasistatic loading, sonic vibration, and impact response. Most of the nondestructive methods measure elastic properties and relate them to the firmness of the fruit. The modulus of elasticity is a measure of material capacity to store energy as it undergoes a given elastic deformation. The material will recover the original shape when the load is released. Firmness is a measure of produce resistance to puncture in which material undergoes permanent plastic deformation, and tissue failure takes place past the bioyield point.

2.1 Acoustic and Impact Tests

When an impulse strikes an apple, it displays a series of resonant frequencies. The stiffness index $f^2m^{2/3}$, where f and m are the second resonant frequency and mass of the fruit, respectively, was the best related to the Magness-Taylor firmness of the fruit (Abbott *et al.*, 1968, 1992, 1994, 1995; Armstrong *et al.*, 1990, 1997; and Chen *et al.*, 1993, 1996). On the other hand, the analysis of the fruit impact with a rigid surface produced the impact index F/t^2 , which was the best related to the firmness measurement. F and t are the peak impact force and time to reach that peak, respectively (Delwiche *et al.*,

1987, 1989, and 1996). Unfortunately, both of the sonic and impact indices were unsatisfactorily correlated with MT firmness. Conceptually, the sonic and impact indices are estimators of the fruit modulus of elasticity rather than firmness (Armstrong *et al.*, 1990).

In studying a probe-type impact sensor, Delwiche et al. (1996) had attributed the lack of agreement with the conventional penetrometer firmness to the reason that each instrument was measuring a distinct physical property. They concluded that the "nondestructive measurements of fruit tissue strength will never be highly correlated with the penetrometer measurements."

2.2 Quasi-Static Loading

Fruit material exhibits viscoelastic behavior under dynamic mechanical loading such that the response depends on the amount of load as well as on the rate of loading. Many nondestructive methods for firmness evaluation often assume that apple material has elastic behavior, which is independent of the loading rate.

For practical purposes, elasticity at small deformations was considered a reasonable indicator of fruit firmness. Abbott *et al.* (1995) used fruit stiffness rather than failure strength as a measure of fruit texture. Timm *et al.* (1993) built a portable data-acquisition instrument to evaluate firmness of cherries and berries in terms of the mean chord stiffness computed from a force-deformation curve. Perry (1977) applied air pressure on small areas on the opposite sides of peaches, the produced deformation was used to characterize fruit firmness.

A majority of the previous quasi-static applications were based on the force-deformation curve in the elastic range. They measure either the deformation of the intact fruit caused by a predetermined force or the force required to cause a predetermined deformation and relate the measurement to fruit firmness.

In an attempt to limit fruit destruction, Schomer and Olsen (1962) developed an instrument called the 'mechanical thumb'. They had replaced the probe of the MT tester with a cylindrical plunger of ½ inch (12.7 mm) diameter and a spherical head. The mechanical thumb was nondestructive in that the intact fruit could be tested without removing the skin. It resulted in a small bruise on fruit skin, since it created an indentation depth of 0.05-inch (1.4-mm). However, the nature of the contact area variations during loading was unknown, hence the measured force was not very informative. Mattus (1965) questioned the validity of this test for MT estimation and concluded that it had overrated large and soft fruit, underrated hard and small fruit, and was variety-dependent.

The measurement of the amount of deformation when the fruit is subjected to a known load is a second option for quasi-static firmness assessment. Fridley (1969) and Fridley et al. (1977) applied preset loads to a plunger and a ball, respectively. Mehlschau et al. (1981) had developed a nondestructive deformeter that detected the deformation created by two steel balls acting on opposite sides of pear fruit. In comparing several probe geometries, Wilkus (1980) concluded that the flat probe was more appropriate for apple firmness measurement than spherical or conical probes. Mizrach et al.

(1992) developed a mechanical thumb to sense the firmness of oranges and tomatoes. An adjustable, spring-loaded 3-mm (1/8-inch)-diameter pin was operated in a Go-No-Go mode to discriminate between firm and soft fruit. The pin was also applied on a continuous basis by measuring the deflection of the elastic cantilever beam to discriminate between hard-green, firm-red and soft-red tomatoes. Dobrzanski and Rybczynski (1999) used the same pin for strain measurement to assess slight changes in apple firmness. The 3-mm plunger was reported as too small and induced a bruise when the contact stress exceeds the bioyield strength. Also, the elastic modulus rather than the strain had better relationship with fruit firmness.

The soft touch sensor, HIT-Counter (stands for Hardness, Immaturity and Texture) was commercialized in Japan since 1989 (Takao and Ohmori 1994). The sensor integrates the time interval required for a plunger to pass across a specified load increment within the elastic range. The sensor was used for online fruit sorting; the correlation coefficient with the conventional firmness was as high as 0.927 for kiwifruit. Later, a small portable version called the Handy HIT was developed (Takao and Ohmori 1994). The sensor was able to evaluate the firmness of Japanese persimmon, a type of oranges (Yakushiji *et al.*, 1995).

Within a certain range of strain, the apple can be deformed without any permanent deformation. A small penetrometer for quasi-nondestructive measurement of apple firmness at a very slow compression rate had no significant distortion for deformations below the point of inflection, nearly 0.3 mm (0.01 inch) in the case of apples (Fekete, 1994).

2.3 The Behavior of Apple Material

The bioyield point is believed to be closely related to the MT firmness, which could also cause permanent deflection or damage to the fruit. At the bioyield point, cell rupture occurs so that browning and discoloration are initiated. However, the damage to the tissue is small, and the bruise depth is less than 2 mm (1/16 inch) under the skin. Mohsenin and co-workers (1965) had considered the bioyield point measurement a feasible nondestructive method for fruit firmness evaluation. A ¼ inch (6.4 mm) diameter flat-ended steel plunger was driven at a speed of 0.6 inch/min (15.2 mm/min) against the fruit skin until the bioyield point was detected at about 0.04 inch (1.0 mm) of deformation. The study was focused on the variations of the bioyield strength and the corresponding deformation with time during maturation and ripening. The decrease of the bioyield force with time was reported to represent the decrease of fruit firmness, but the relation between the bioyield strength and the firmness was not investigated.

The compression force at the bioyield point is predominant in the MT test. The primary step of the penetration process is bioyielding; however, the penetration physics is not well understood and a comprehensive analysis is not available to the best of the author's knowledge. During penetration the material is sheared and compressed simultaneously. Bourne (1966) considered the shear strength and the compressive strength as the major parameters that are involved in the penetration process, and hence in the MT test. The total force required for

penetration was expressed as a rectilinear combination of the compression and the shear coefficients, equation (2.1):

$$F = K_C A + K_S P + C \tag{2.1}$$

where F= measured force (kg), K_C = compression coefficient of the material being tested (kg/cm²), K_S = shear coefficient of the material being tested (kg/cm), A= area of punch (cm²), P= perimeter of the punch (cm), and C= constant (kg).

The coefficients K_C , K_S and the constant C are dependent on the nature of the tested material. The constant C that usually has a negative value was thought to account for the influenced zone around the puncture and other uncertain minor parameters. Tensile and pumping effects were introduced as minor parameters that counteract the MT puncture force (Jeong, 1997). A radial tensile force pulling the surrounding zone is implicated with the shearing process, and the curved tip of the puncture promotes the tensile force. The pumping effect, on the other hand, is due to the piston action of the puncture that expels the juice throughout the annular clearance around the puncture sides. The compression of a cylindrical sample was modeled by a series of Maxwell units with a fracture element; each unit represents a single layer of the apple sample. The layers were believed to bioyield sequentially with compression, which explained the saw-tooth force deformation relationship (Jeong, 1997).

According to the trend of the penetration force following the yield point, Bourne (1980) classified the curves into three possible groups: increasing, almost remaining constant and decreasing. Fresh apples exhibited a rapid increase of force with deformation after the bioyield point, whereas the cold stored apples had roughly constant force over a considerable deflection after the bioyield point, and the curve looked like a plateau. On the other hand, the apples stored at elevated temperatures exhibited a sharp drop of penetration force after the bioyield point. In the first two groups the penetration depth could be controlled but not in the group of decreasing force (Bourne, 1980). There was no physical reasoning reported behind these differences of the trends.

Air space makes up about 25% of the mature fruit volume; air is produced by cell separation that occurs during apple growth. The air spaces tend to form radial canals through the cortex and they continue to increase during storage and ripening (Seymour *et al.*, 1993). This increase in air space may contribute to the decline in flesh firmness during storage and ripening.

Chen et al. (1996) concluded that the MT test is more sensitive to viscous properties than elastic properties. The viscoelastic characteristics of fruit material are significantly divergent from those of engineering material in which Hooke's law holds for the elastic range. The contact problem of fruit material is, consequently, deviant from the classical Hertz contact theory. Fridley et al. (1968, 1977) reported that the forces required to deform whole pears and peaches with a cylindrical plunger or a flat plate were significantly below those predicted by Hertz contact theory. This difference was due to the relaxation of fruit material upon compression. Likewise, Hertz contact model overestimated the bruise diameter due to apple impact with a hard flat surface. Also, the plastic theory that considers the permanent deformation after the bioyield point,

generally, underestimates the bruise diameter. However, experimental adjustment of Hertz contact theory by considering the effect of loading rate of the viscoelastic apple material has given more accurate estimation of the bruise size (Siyami *et al.* 1988).

The applied compression force by a sensor on an elastic body is proportional to the local deformation raised to the power of 3/2 (Fridley *et al.*, 1968), as predicted by the classical Hertz contact theory. However, due to stress relaxation of fruit material the power is less than 3/2. A range of 0.9-1.4 was reported by Cherng (1999), which varies with fruit growth and storage period.

2.4 Failure Criteria

Many researchers have studied the failure criteria of fruits. The maximum shear stress was believed to cause failure of apple samples (Miles and Rehkugler, 1973). Experimental results of De Baerdemaeker (1975) supported the maximum shear stress theory. Failure was initiated at a depth of less than one third the contact diameter in flat plate compression for pears and peaches (Fridley *et al.*, 1968). The maximum shear stress in an elastic material is located at a depth of about one half the contact diameter. In contrast to the maximum shear stress theory, Segerlind and Fabbro (1978) reported that apples fail when the normal strain exceeds a critical value. This critical value was in the range of 0.10–0.15 strain.

2.5 Finite Element Studies

The contact problem of biomaterials has been studied using the finite element method. Sherif (1976) applied the finite element technique to investigate the stress distribution in diametrically loaded cylindrical samples of apples, peaches and potatoes. The material was assumed homogenous, isotropic and elastic, the apple samples failed at the maximum shear strength. Rumsey and Fridley (1977) analyzed the contact problem of a viscoelastic spherical body with an exponential decaying shear modulus and a constant elastic bulk modulus. They found that there was good agreement between the analytical and the finite element solutions. De Baerdemaeker (1975) considered apple material with time dependent bulk modulus and shear modulus in studying the creep and the contact problem of spherical samples of Red Delicious with a flat plate. He supported the theory of distortion energy over the maximum shear stress theory to account for the failure pattern. The relaxation functions were found to be sensitive to the loading rate. De Baerdemaeker and Segerlind (1976) developed a procedure to determine the viscoelastic properties - the coefficients and exponents of the exponential series - using the generalized Maxwell model for apple samples.

2.6 Finite Element Studies

The dynamic techniques were more sensitive to the elastic properties of the fruit material rather than the firmness. In attempting to achieve a nondestructive testing, the quasi-static studies were primarily restricted to the inspection of the force-deformation relationship in the linear range prior to the bioyield point. Therefore, the measurements could be considered as different approaches to estimate the elastic properties rather than the tissue strength. The later property is the dominant property in determining the maximum force, which the fruit tissue is able to withstand before failure under the MT probe. Therefore, creating a failure of fruit tissue is necessary to evaluate the apple material strength and eventually the firmness. However, minimizing the damage in the measurement of tissue strength is the challenge for developing a new successful firmness sensor.

Chapter3

Theory of Contact between Bodies

The proposed method for evaluating the apple firmness is based on contacting the apple fruit with a probe. The understanding of classical contact theory is necessary for designing a new probe that would be appropriate to detect the strength of apple material while causing minimum damage.

When two solid bodies are brought into contact, they touch each other at a single point or occasionally along a line. This general case of contact, where no perfect fit is accessible between the two surfaces prior to deformation, is known as a non-conforming contact. As load is applied on the bodies, the high stress concentration at the contact point causes deformation in the two surfaces at the neighborhood of the initial contact point. Therefore, it results in a small finite area of contact. The order of magnitude of the contact area and the deformation are very small compared to the dimensions of the bodies. This chapter looks into the classical Hertz contact theory, and investigates the Boussinesq die contact and the contact due to a uniform pressure, which is applied throughout this study. The divergence of the contact with viscoelastic material from contact with elastic material is presented. Finally, some criteria for the onset of material yield are stated.

3.1 Hertz Contact Theory

When two non-conforming bodies are pressed against each other, they touch at a single point, as the load is applied, the surfaces in the vicinity of the contact point start to deform and a finite area of contact is developed. The Hertz theory investigates the contact process of two elastic bodies to predict the shape, deformation of the contact region, the way in which bodies respond as load progresses, and specifies stress distribution that is generated at the interface.

The Hertz theory is based on the fact that the deformation and dimensions of the contact area are sufficiently small compared to the dimensions of the contact bodies, such that each body is considered a semi-infinite half space.

In analyzing the contact problem of axi-symmetric bodies, it is advantageous to use cylindrical polar coordinate systems. The origin "O" is chosen as the first point of contact (Fig. 3.1), and the axis Oz is the common

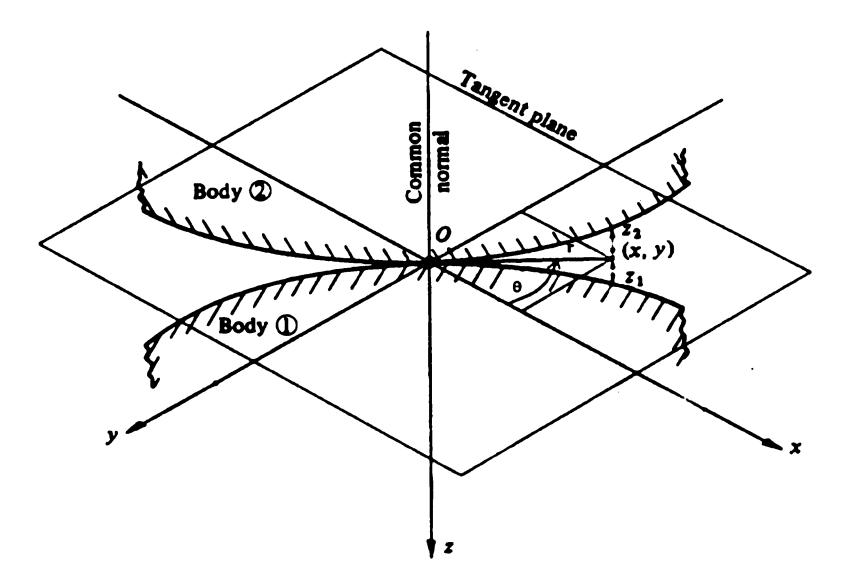


Fig. 3.1 Coordinate system for the contact problem

normal to the contact surfaces. The coordinate r is the radial distance from the axis Oz, and θ is the angle between r and a certain reference axis Ox.

3.2 Assumptions for Apple-Probe Contact

The intended apple firmness test used a cylindrical probe with a rubber tip contacting the apple. The probe is pressed against the fruit surface until the bioyield stress is achieved underneath the contact area. In developing his classical contact theory Hertz had made some assumptions. Before analyzing the contact problem, it is necessary to discuss the extent to which Hertz's assumptions are valid in the intended contact problem between the apple and the probe. Hertz assumptions include:

- 1. The materials of the contact bodies are homogeneous. This is valid for the probe material, which is made of steel and rubber, while for apple, as a biological material this condition does not hold.
- 2. The applied load is static. The rate of compression process (0.5 inch/min) is slow enough such that the inertia forces are insignificant and can be neglected.
- 3. The contacting bodies are elastic. Again this is not an exact condition for apple material, since the viscous behavior is anticipated to be more significant with time. However, the duration of the test is small compared with the smallest time constant of average apple relaxation function. The later was found experimentally to be 2.27 seconds (see Chapter 5).
- 4. The contacting bodies are semi-infinite. Apple bioyield stress is moderately small, and the test is conducted over a small area such that the stress vanishes at

the opposite side of the contact area, as found by the finite element simulation, (See Fig. 4.7). Hence an apple can be considered a semi-infinite body.

- 5. The radii of curvature of the contacting surfaces are very large compared to the radius of the contact area. For a cylindrical probe, the radius is small compared to the radii of curvature of the contact surfaces, the probe cross-sectional area is assumed to be the upper limit for the contact area (neglecting the radial expansion of the rubber tip). Hertz designated a threshold of 10 for the ratio of the radius of curvature of the contact surface to the contact radius for his equations to be applicable. This ratio is achieved for probe diameter less than 3/8 inch in contact with an average apple fruit.
- 6. The surfaces in contact are sufficiently smooth, such that no radial friction forces are encountered as the loading progresses. The rubber is expected to have a high friction coefficient with the skin, however, the relative radial movement is negligibly small.

3.3 Analysis

The contact situation of two bodies is shown in Fig. 3.2. Throughout the analysis we use the subscripts 1 and 2 to refer to the two contact bodies. The profile of the original surface can be described by:

$$z_1 = f_1(x, y) = A_1 x^2 + B_1 y^2 + C_1 xy + \cdots$$
 (3.1)

Due to the small order of magnitude of x and y within the contact area, the higher order terms are neglected. The third term (C_1xy) , on the other hand,

would vanish by choosing the orientation of the coordinate system to coincide with the principal axes. The principal axes x_1 and y_1 shown in Fig. 3.2 are in the direction of the projection of the planes that contain the principal radii on the common tangent plane of those planes, which contains the principal radii of curvature as below. Then equation 3.1 becomes:

$$z_1 = \frac{1}{2R_1'} x_1^2 + \frac{1}{2R_1''} y_1^2$$
 (3.1)

where R'_1 and R''_1 are the principal radii of curvature of body 1 at the origin. Similarly the surface profile of the second body may be described by:

$$z_2 = -\left(\frac{1}{2R_2'}x_2^2 + \frac{1}{2R_2''}y_2^2\right) \tag{3.3}$$

A similar approach can be used to express the separation between the surfaces

 $(h=z_1-z_2)$, such that:

$$h = Ax^2 + By^2 = \frac{1}{2R'}x^2 + \frac{1}{2R''}y^2$$
 (3.4)

where R' and R'' are the principal relative radii of curvature.

The requirement for eliminating the xy-term in Eq. 3.4 implies the following expressions for the constants **A** and **B** (refer to Johnson (1985) for more details).

$$(A+B) = \frac{1}{2} \left(\frac{1}{R'} + \frac{1}{R''} \right) = \frac{1}{2} \left(\frac{1}{R'_1} + \frac{1}{R''_1} + \frac{1}{R''_2} + \frac{1}{R''_2} \right)$$
and
$$|A-B| = \frac{1}{2} \left\{ \left(\frac{1}{R'_1} - \frac{1}{R''_1} \right)^2 + \left(\frac{1}{R'_2} - \frac{1}{R''_2} \right)^2 + 2 \left(\frac{1}{R'_1} - \frac{1}{R''_1} \right) \left(\frac{1}{R'_2} - \frac{1}{R''_2} \right) \cos 2\alpha \right\}^{1/2}$$
(3.5)

where α is the angle between the principal axis x_1 and x_2 (Fig. 3.2). The contour of points which has constant separation h in Eq. 3.4 is an ellipse with axis ratio equal to $(B/A)^{1/2} = (R /\!/R /\!/)^{1/2}$.

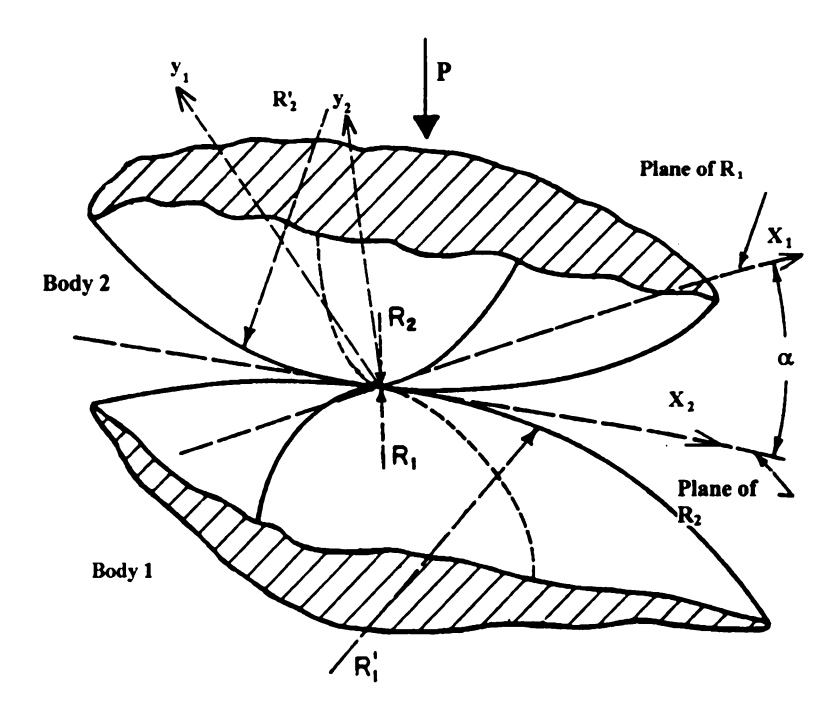


Fig. 3. 2 Hertz contact of two convex bodies, showing the principal axes.

If the two bodies are assumed solids of revolution (axi-symmetric), then, the angle $\alpha=0$, $R'_1=R''_1=R_1$, and $R'_2=R''_2=R_2$, hence $A=B=^1/_2(1/R_1+1/R_2)$. Therefore, the contours of constant separation are always circles.

When a normal load is applied, the boundary condition of no interference between the points on the two contact surfaces together with the linear elastic behavior of the materials, suggests that the mean contact pressure within the contact area (p_m) be:

$$p_m \propto \frac{a(1/R_1 + 1/R_2)}{1/E_1 + 1/E_2} \tag{3.6}$$

where E is the material modulus of elasticity.

Hertz proposed a pressure distribution that satisfies the above conditions as follows:

$$p = P_o \sqrt{1 - r^2/a^2} ag{3.7}$$

The expressions of the contact radius (a), the approach distance of two points far away on the two bodies (δ) and the maximum pressure at the center (p_0) are given by:

$$a = \left(\frac{3PR}{4E^*}\right)^{1/3}, \quad \delta = \frac{a^2}{R} = \left(\frac{9P^2}{16 RE^{*2}}\right)^{1/3}, \quad p_o = \frac{3P}{2\pi a^2} = \left(\frac{9P^2E^{*2}}{\pi^3R^2}\right)^{1/3}$$
 (3.8)

where $1/R=1/R_1+1/R_2$ is the relative curvature, P: is the applied force, a: is the contact radius and E^* is given by:

$$\frac{1}{E^*} = \frac{1 - \nu_1^2}{E_1} + \frac{1 - \nu_2^2}{E_2}$$

Although the Hertz stress distribution has no stress concentration at the boundary of the contact area, it has a peak at the center. Thus, if a spherical probe were used in apple testing to determine the bioyield strength, the failure of apple tissue would initiate at the center and extend outwards gradually in the radial direction. Furthermore, the continuous variations of the contact radius, the approach distance, and stress with loading make it unfeasible to detect a certain value that is clearly indicative of bioyield strength.

Finney (1963) suggested a rigid cylindrical probe for testing fruits and vegetables to determine their mechanical properties. Prior to the full contact, a cylindrical probe has to pass through a preparatory stage that is initiated from the onset of contact, and terminated as the entire probe end area becomes in contact with the fruit. Throughout the preparatory stage, the contact area is increasing continuously, in a way similar to Hertz contact, in which the probe end is seen as a flat plate. Once full contact is achieved, the contact area almost remains constant. As load increases in this stage, the stress concentrates at the outer edge. If the cylindrical probe is rigid, the trend of stress distribution shifts from Hertz distribution (elliptic concave down), to Boussinesq distribution of rigid dies (concave up) as shown in Fig. 3.4. The infinite stress at the outer edge would be of destructive nature and should be eliminated. Introducing a rubber tip at the end of the probe would not only eliminate this stress concentration, but also distribute the stress over the entire contact area, resulting in quasi-uniform stress distribution.

A thorough understanding of the contact situation would be achieved when the components of stress and deformation due to the applied load at the contact area can be recognized. Since most of the material behavior can be approximated by linear functions at small deformations, the superposition principle is applicable. For elastic materials, this technique can be used when the components of displacement and stress produced by a concentrated force are known, and then integrated over the entire loading area.

3.3.1 Concentrated Normal Force

The classical approach, which is based on the theory of potential, developed by Boussinesq and Cerruti, enabled the finding of the stresses and displacements due to load at the surface. Using that approach, Timoshenko and Goodier (1951) introduced a stress function to deduce the components of stress and displacements due to a concentrated force *P* acting on an axi-symmetric elastic half-space (Fig. 3.3).

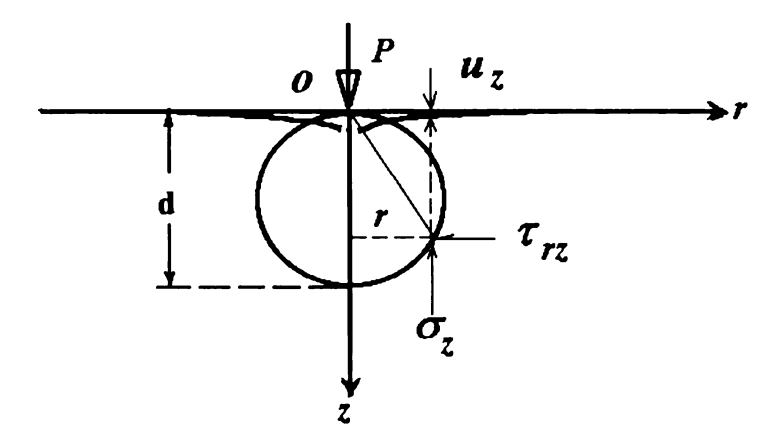


Fig. 3.3 Concentrated force acting at the surface of a half-space

The problem is axi-symmetric, using cylindrical coordinates (r, θ, z) , the solution is independent of θ , and the $\tau_{r\theta}$ and τ_{dz} are zero, the remaining stress components are:

$$\sigma_{r} = \frac{P}{2\pi} \left\{ (1 - 2\nu) \left(\frac{1}{r^{2}} - \frac{z}{r^{2} \sqrt{r^{2} + z^{2}}} \right) - \frac{3zr^{2}}{\left(r^{2} + z^{2}\right)^{5/2}} \right\}$$

$$\sigma_{\theta} = -\frac{P}{2\pi} (1 - 2\nu) \left(\frac{1}{r^{2}} - \frac{z}{r^{2} \sqrt{r^{2} + z^{2}}} - \frac{z}{\left(r^{2} + z^{2}\right)^{3/2}} \right)$$

$$\sigma_{z} = -\frac{3P}{2\pi} \frac{z^{3}}{\left(r^{2} + z^{2}\right)^{5/2}} , \qquad \tau_{rz} = -\frac{3P}{2\pi} \frac{rz^{2}}{\left(r^{2} + z^{2}\right)^{5/2}}$$
(3.9)

Since at any point $\sigma_r/\tau_{rz}=z/r$ in the above equations, therefore, they concluded that the horizontal component of the resultant stress at any point on the surface of the sphere of diameter d is constant and equal to $3P/2 \pi d^2$.

The components of displacement in the vertical and radial directions are:

$$u_{z} = \frac{P}{2\pi E} \left[\frac{(1+\nu)z^{2}}{(r^{2}+z^{2})^{3/2}} + \frac{2(1-\nu^{2})}{\sqrt{r^{2}+z^{2}}} \right]$$

$$u_{r} = \frac{(1-2\nu)(1+\nu)P}{2\pi E r} \left\{ \frac{z}{\sqrt{r^{2}+z^{2}}} - 1 + \frac{1}{1-2\nu} \frac{zr^{2}}{(r^{2}+z^{2})^{3/2}} \right\}$$
(3.10)

3.3.2 General Axi-Symmetric Pressure Distribution

An axi-symmetrical pressure distribution applied by a probe over a circular interface area with elastic half-space is to be analyzed in this section. The pressure distribution takes the general form:

$$p = P_o \left(1 - \frac{r^2}{a^2} \right)^n {(3.11)}$$

where P_o is the pressure at the center of the contact area, and the exponent n is any real number. Fig. 3.4 shows pressure distributions for selected values of the parameter n.

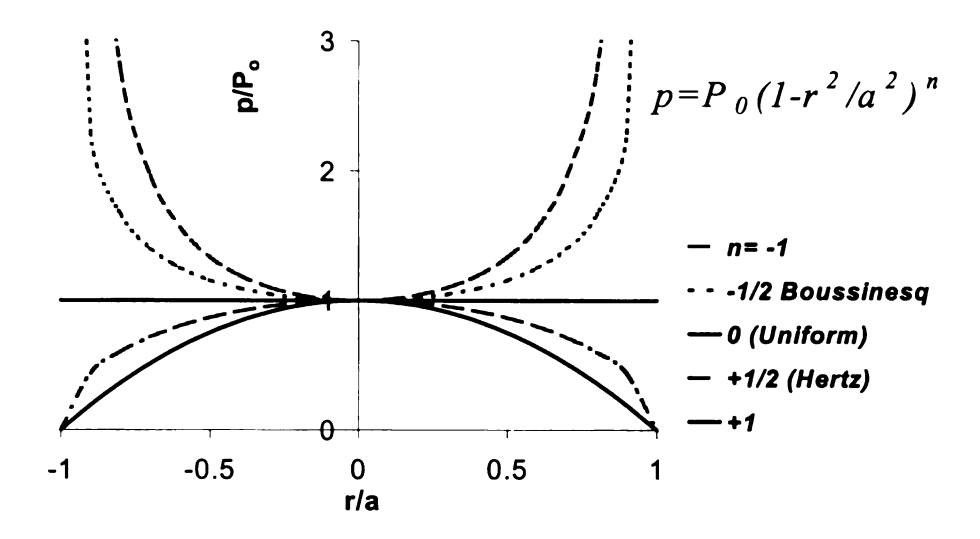


Fig. 3.4 General axi-symmetric pressure distribution

Three particular values of the parameter n are of classical importance and will be discussed in detail. These are n=0, -1/2, and +1/2. For n=0 the pressure distribution is uniform; at n=-1/2 the distribution corresponds to the case of loading by absolutely rigid die which is known as Boussinesq problem. The pressure distribution is elliptical when n=+1/2, which is associated with the Hertz contact.

3.3.2.1 Uniform Pressure (n=0)

When a uniform load is applied over a circular area of radius a at the apple surface, the displacements in the vertical and radial directions are found by integrating equations 3.10 over the circle as shown in Fig. 3.5 (Johnson 1985).

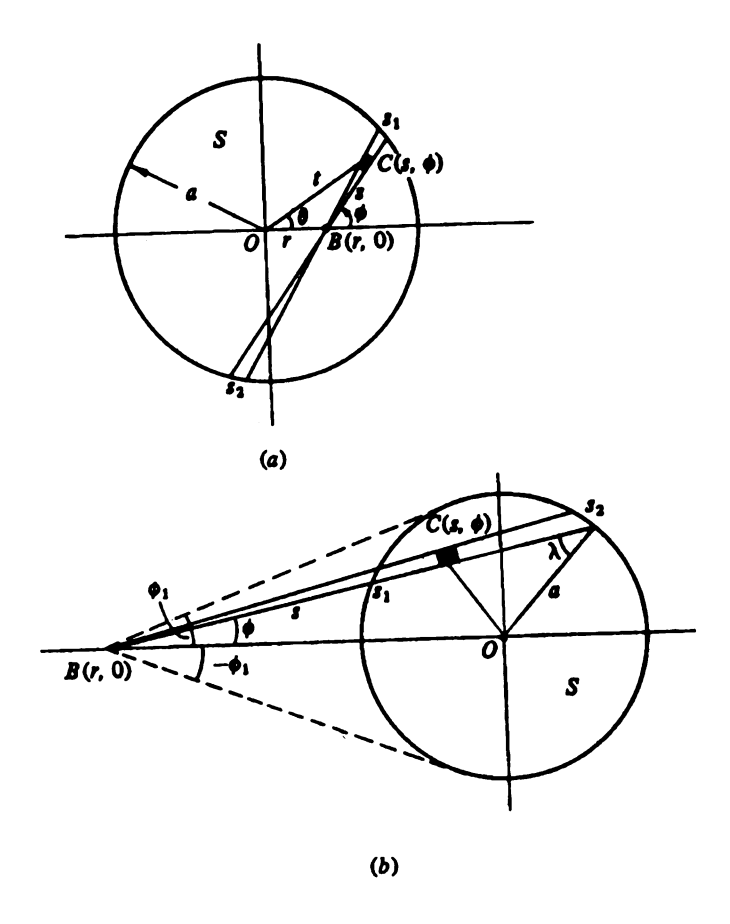


Fig. 3.5 Integration of the effect of pressure applied over a circular area at point B(r, 0) located: (a) Inside the circle [r < a] (b) Outside the circle [r > a]

The displacement in the vertical direction is:

$$u_{z} = \begin{cases} \frac{2a^{2}(1-\nu^{2})P_{o}}{\pi E}E(r/a) & r < a \\ \frac{2a^{2}(1-\nu^{2})}{\pi E}P_{o}r\{E(a/r)-(1-a^{2}/r^{2})K(a/r)\} & r > a \end{cases}$$
(3.12)

where E(m) is the complete elliptic integral of the second kind of modulus m, and K(m) is the complete elliptic integral of the first kind, defined as:

$$E(m) = \int_{0}^{\pi/2} (1 - m^{2} \sin^{2} \phi)^{1/2} d\phi$$

$$K(m) = \int_{0}^{\pi/2} (1 - m^{2} \sin^{2} \phi)^{-1/2} d\phi$$
(3.13)

The maximum vertical displacement occurs at the center $[E(0)=\pi/2]$, and drops gradually with radial distance to a minimum value at the boundary edge [E(1)=1]. Outside the contact area, it continues to drop asymptotically with distance.

The radial displacement at the solid surface is:

$$u_{r} = \begin{cases} -(1-2\nu)(1+\nu)P_{o}r/2E & r \leq a \\ -(1-2\nu)(1+\nu)P_{o}a^{2}/2rE & r > a \end{cases}$$
 (3.14)

Since the total load is $P = P_o ma^2$, the radial displacement in Eq. 3.14 is identical to that generated by an equivalent concentrated force applied at the center (Eq. 3.10 for z=0). Using the superposition principle, Johnson (1985) concluded that the radial displacement depends only on the total load, and is independent of the nature of stress distribution as long as it is axi-symmetric.

As far as the components of stress are concerned, they can be found by integrating Eq. 3.9 over the entire circle, the final forms of stress components along the Oz-axis (Timoshenko & Goodier, 1951) are:

$$\sigma_z = P_o \left\{ -1 + \frac{z^3}{(a^2 + z^2)^{3/2}} \right\}$$

$$\sigma_{r} = \sigma_{\theta} = \frac{P_{o}}{2} \left[-(1+2v) + \frac{2(1+v)z}{\sqrt{a^{2}+z^{2}}} - \frac{z^{3}}{(a^{2}+z^{2})^{3/2}} \right]$$
 (3.15)

Then by using the Mohr's circle, the principal shearing stress at any point along the z-axis occurs at 45 degrees to the z-axis, and its magnitude is $^{1}/_{2}|\sigma_{\theta}-\sigma_{z}|$ given by:

$$\tau_1 = \frac{P_o}{2} \left[\frac{1 - 2\nu}{2} + (1 + \nu) \frac{z}{\sqrt{a^2 + z^2}} - \frac{3}{2} \left(\frac{z}{\sqrt{a^2 + z^2}} \right)^3 \right]$$
 (3.16)

The maximum value of the principal shear stress is:

$$\tau_{\text{max}} = \frac{P_o}{2} \left[\frac{1 - 2v}{2} + \frac{2}{9} (1 + v) \sqrt{2(1 + v)} \right]$$
at
$$z = a \sqrt{\frac{2(1 + v)}{7 - 2v}}$$

3.3.2.2 Uniform Normal Displacement (n=-1/2)

When an absolutely rigid, frictionless cylindrical probe is pressed against an elastic half space, this case is known as the flat die Boussinesq problem (Fig. 3.6). The vertical displacement u_z is uniform inside the contact circle, and the contact stress can be found by substituting n=-1/2 in Eq. 3.10.

$$p = \frac{P_o}{\sqrt{1 - r^2/a^2}} \tag{3.17}$$

where a is the radius of the probe, and P_o is the stress at the center, which is equal to half the average contact stress.

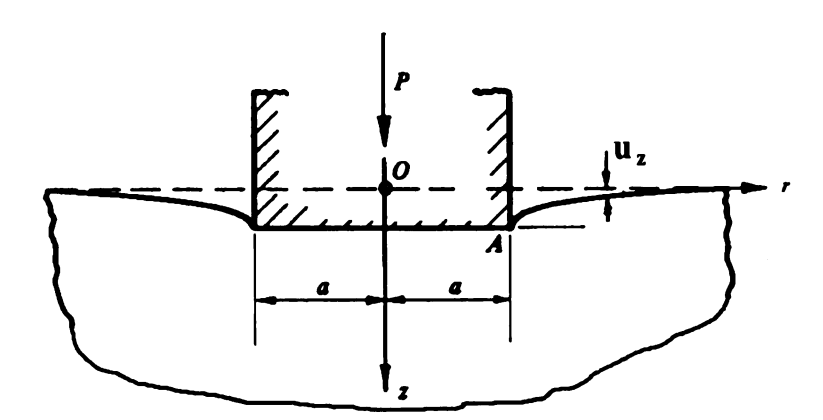


Fig. 3.6 Rigid cylindrical die loaded against half-space (Boussinesq problem)

The vertical displacement at the surface is constant within the contact area. However, it decreases with distance from the origin outside, such that:

$$u_{z} = \begin{cases} \pi(1-v^{2})P_{o}a/E & r \leq a \\ \\ \frac{2(1-v^{2})}{E}P_{o}a \sin^{-1}(a/r) & r > a \end{cases}$$
 (3.18)

Note that for a given value of P_o , the deflection at the contact area increases linearly with the probe radius (a). On the other hand, the normal stress has theoretically an infinite value at any point on the boundary (r=a), and drops to zero outside, resulting in an infinite stress gradient. If used for apple testing, this probe would cause damage to apple tissue, therefore, hard probes should be excluded.

3.3.2.3 Hertz Pressure (n=+1/2)

The case of n=1/2 corresponds to contact between two axi-symmetric frictionless bodies, where the pressure distribution is elliptical as stated in Eq. 3.7 earlier as:

$$p = P_o \sqrt{1 - r^2/a^2}$$

The displacement and stress components in the vertical and radial directions, again, can be obtained by integrating the load over the circular contact area. The final form of the vertical displacement at the surface (z=0) as stated by Johnson (1985) is:

$$u_{z} = \begin{cases} \frac{1 - v^{2}}{E} \frac{P_{o}}{4a} (2a^{2} - r^{2}) & r \leq a \\ \frac{1 - v^{2}}{E} \frac{P_{o}}{2a} \left\{ (2a^{2} - r^{2}) \sin^{-1}(a/r) + r^{2} (a/r) (1 - a^{2}/r^{2})^{1/2} \right\} & r > a \end{cases}$$
(3.19)

The radial displacement u_r is given by:

$$u_{r} = \begin{cases} -\frac{(1-2v)(1+v)}{3E} \frac{a^{2}P_{o}}{r} \left\{ 1 - \left(1 - r^{2}/a^{2}\right)^{3/2} \right\} & r \leq a \\ -\frac{(1-2v)(1+v)}{3E} \frac{a^{2}P_{o}}{r} & r > a \end{cases}$$
(3.20)

The radial displacement outside the contact circle is related to the total force, in this case $P = 2P_o \pi a^2/3$. Thus u_r is 2/3 that of the uniform pressure (P_o) .

The stress components at the surface (z=0) are:

$$\sigma_{r}/P_{o} = \begin{cases} \frac{1-2v}{3} \frac{a^{2}}{r^{2}} \left\{ l - \left(1-r^{2}/a^{2}\right)^{3/2} \right\} - \left(1-r^{2}/a^{2}\right)^{1/2} r \leq a \\ (1-2v)a^{2}/3r^{2} & r > a \end{cases}$$
 (3.21)

$$\sigma_{\theta}/P_{o} = \begin{cases} -\frac{1-2\nu}{3} \frac{a^{2}}{r^{2}} \left\{ l - \left(l - r^{2}/a^{2}\right)^{3/2} \right\} - 2\nu \left(l - r^{2}/a^{2}\right)^{1/2} r \le a \\ -(l-2\nu)a^{2}/3r^{2} & r > a \end{cases}$$
(3.22)

At any point on the surface outside the contact area, the radial stress (σ_r) and the circumferential stress (σ_θ) have the same magnitude. However, the former is tensile and the later is compression. The maximum tensile stress of a value $\sigma_{max} = P_o (1-2\nu)/3$, occurs at r=a. This stress is the absolute maximum

tensile stress throughout the whole body, which may cause failure when the body material is brittle.

Along the axis Oz, the stress components σ_z , σ_θ , and σ_r are principal stresses, thus the principal shear is $\tau_1 = \frac{1}{2} |\sigma_z - \sigma_\theta|$, thus:

$$\begin{split} &\sigma_{z}/P_{o} = -\left(1+z^{2}/a^{2}\right)^{-1} \\ &\sigma_{r}/P_{o} = \sigma_{\theta}/P_{o} = -\left(1+\nu\right)\left\{1-\left(z/a\right)\tan^{-1}\left(a/z\right)\right\} + \frac{1}{2}\left(1+z^{2}/a^{2}\right)^{-1} \\ &\tau_{1}/P_{o} = \frac{1+\nu}{2}\left\{1-\left(z/a\right)\tan^{-1}\left(a/z\right)\right\} - \frac{3}{4}\left(1+z^{2}/a^{2}\right)^{-1} \end{split}$$
(3. 23)

The stress components at the solid surface and along the symmetrical axis are illustrated for the case of uniform pressure and compared with Hertz pressure distribution acting on a circular area of a half space elastic material with v=0.3. The maximum shear stresses are:

$$(\tau_l)_{max}=0.33P_O$$
 at $z=0.64a$ (Uniform)
 $(\tau_l)_{max}=0.31P_O$ at $z=0.57a$ (Hertz)

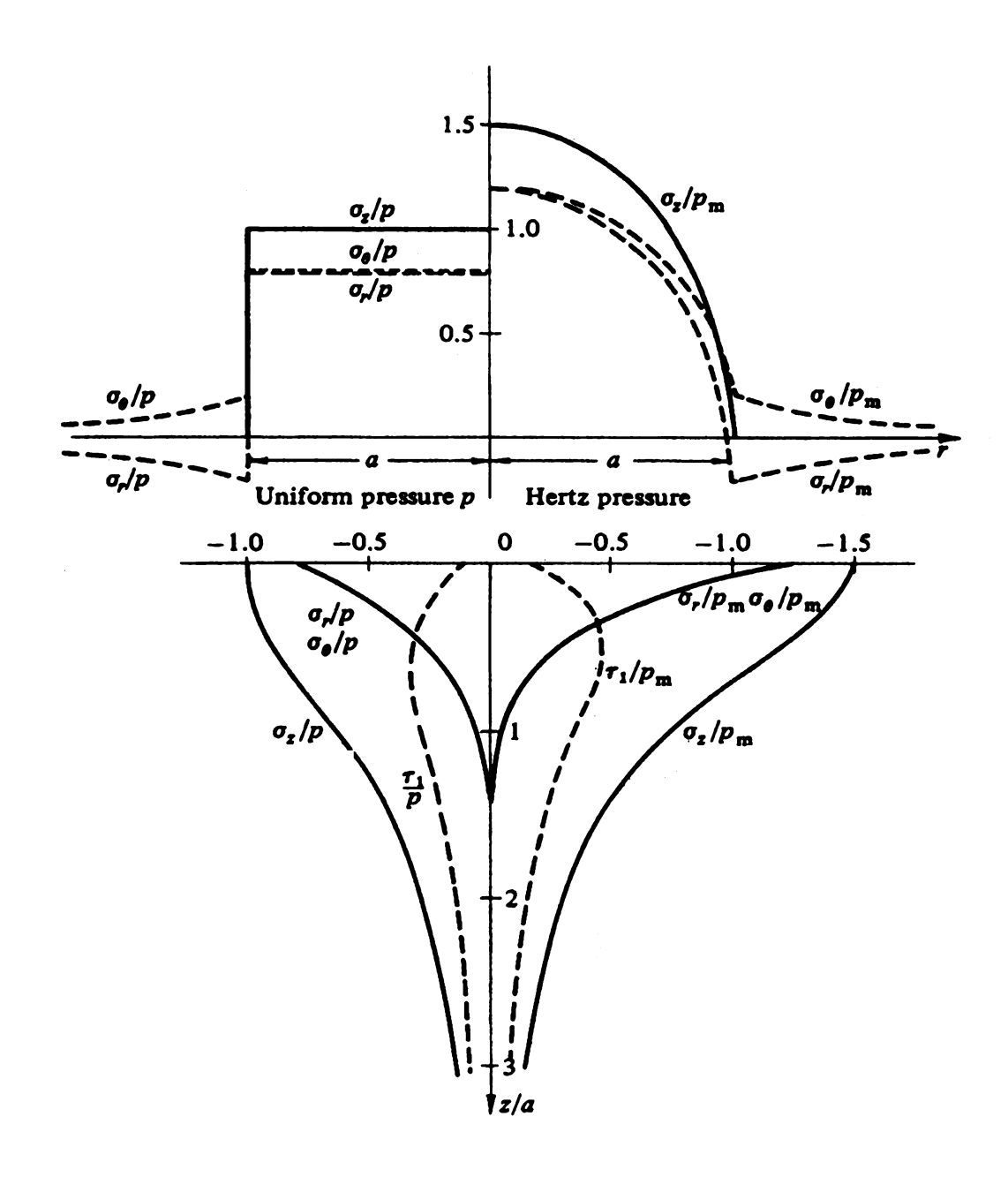


Fig. 3.7 Comparison of stress distributions at the surface and along the axis of symmetry due to (left) uniform pressure and (right) Hertz pressure on a circular area of radius a (Johnson 1985)

3.3.3 Normal Stress at Any Point

The formulas in the previous discussion are restricted to a point located either on the surface of a solid or along the axis of symmetry (z-axis). The stress at an interior point B(r, z) throughout the solid can be treated similarly by superimposing the solution due to the concentrated force over the entire circular area shown in Fig. 3.5. The final result for the normal stress is:

$$\sigma_{z} = \begin{cases} -\frac{3}{2\pi} \int_{0}^{\pi} \int_{s_{I}}^{s_{2}} \frac{p(\phi, s)}{(s^{2} + z^{2})^{5/2}} & s & ds & d\phi & r \leq a \\ -\frac{3}{\pi} \int_{0}^{\pi\pi/2} \int_{s_{I}}^{s_{2}} \frac{p(\phi, s)}{(s^{2} + z^{2})^{5/2}} & s & ds & d\phi & r > a \end{cases}$$
(3.24)

where:

$$s_{1,2} = \begin{bmatrix} -r & \cos & \phi \pm \sqrt{r^2 \cos^2 \phi + (a^2 - r^2)} & r \le a \\ r & \cos & \phi \pm \sqrt{a^2 - r^2 \sin^2 \phi} & r > a \end{bmatrix}$$

This reduces the problem to the solution of an integral equation involving the contact circle generally it has no closed form solution and can be evaluated by numerical integration. The same procedure could be used to formulate the solution involving any other stress component or displacement.

3.3.4 The Viscoelastic Contact

Viscoelastic materials exhibit time-dependent behavior in their stressstrain relationships. At the instant of contact, viscoelastic material would respond in a way similar to elastic material. However, the viscoelastic characteristics, progressively lead to a gradual divergence from the elastic classical contact due to viscous properties.

The compression of an intact fruit exhibits three consecutive and indefinite stages of deformation, namely, the elastic stage, the viscoelastic prefailure stage, and the viscoelastic post-failure stage (Peleg *et al.*, 1976). In the elastic stage no permanent physical changes take place and the deformation is independent of the strain rate. Irreversible physical changes due to failure in the microstructure may occur as the deformation passes the bioyield point. This produces a permanent deformation and triggers the enzymatic actions that induce bruising.

The behavior in this stage is still viscoelastic, but it is considerably different from that of the pre-failure stage. Consequently, different rheological models are necessary to represent the same material in each stage. Hence, in this study we are concerned with the attributes in the pre-failure stage prior to the bioyield.

Lee and Radok (1960) deduced the viscoelastic counterpart solution of the Hertz contact problem between a rigid sphere and the viscoelastic half space using the Maxwell model. The dimensionless pressure distribution is plotted versus the dimensionless contact radius in Fig. 3.8. Initially, the pressure distribution corresponds to the Hertz elastic solution. As time progresses, the contact area grow and a gradual departure from Hertz distribution is observed. The recently contacted area at the periphery of the circle continues to follow Hertz solution, while at the central region; the stress relaxes such that the pressure distribution is flattened, eventually resulting in a dip.

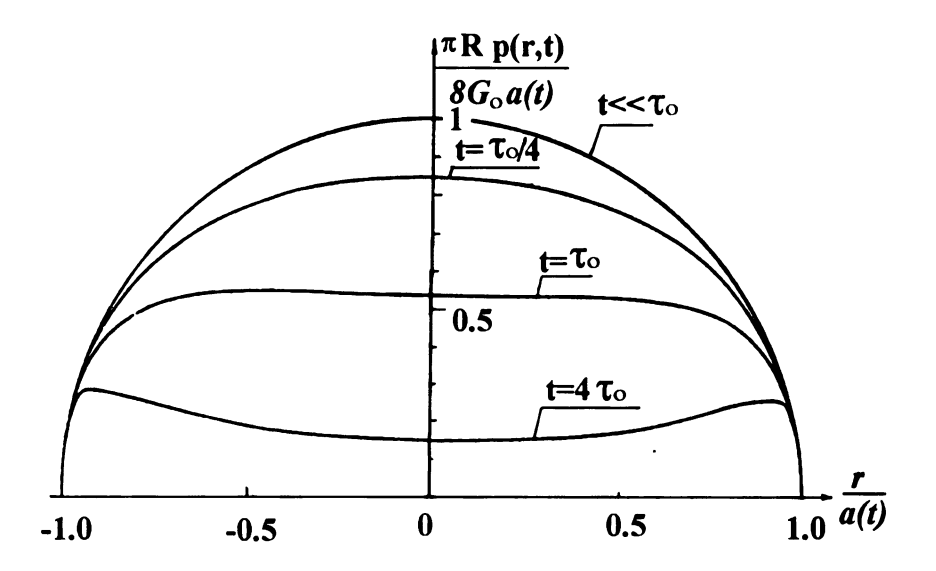


Fig. 3.8 Variation of the pressure distribution against dimensionless radius at particular times (Lee and Radok, 1960)

3.3.5 Onset of Bioyield

Yielding of a material is initiated at regions of high stress that become high strain regions. Failure of brittle material occurs abruptly without considerable distortion, while yielding of ductile materials begins by the formation of a neck and significant change in shape occurs at the yielding zone before failure.

When brittle material fails in tension or compression, the maximum stress criterion can be applied, this simply states that the material break down when a principal stress component reaches the ultimate tensile strength of the material. In the case of ductile materials the most satisfactory failure criteria are the von Mises criterion and the Tresca yield criterion. To present these criteria a few definitions should be understood.

The state of stress at any point can be split into a hydrostatic stress component and a deviatoric stress component, such that:

$$\begin{bmatrix} \sigma_{x} & \tau_{xy} & \tau_{xz} \\ \tau_{xy} & \sigma_{y} & \tau_{yz} \\ \tau_{xz} & \tau_{yz} & \sigma_{z} \end{bmatrix} = \begin{bmatrix} \sigma_{x} - \sigma_{av} & \tau_{xy} & \tau_{xz} \\ \tau_{xy} & \sigma_{y} - \sigma_{av} & \tau_{yz} \\ \tau_{xz} & \tau_{yz} & \sigma_{z} - \sigma_{av} \end{bmatrix} + \begin{bmatrix} \sigma_{av} & 0 & 0 \\ 0 & \sigma_{av} & 0 \\ 0 & 0 & \sigma_{av} \end{bmatrix}$$
(3.25)

Where $\sigma_{av} = \frac{1}{3}(\sigma_1 + \sigma_2 + \sigma_3)$ is the average of the principal stresses, which represents the hydrostatic component of stress and only affects the size by producing material dilatation, but does not affect the shape or produce material distortion. On the other hand, the average of the deviatoric stresses is zero, thus, it only affects the angle(s) between surfaces due to shear deformation and causes material distortion.

The onset of yielding is independent of the orientation of the coordinate system; thus it can be expressed in terms of the so-called invariants. The type and orientation of the coordinate axis, as the name suggests, are functions of the stress that do not affect the invariants. Krishnamachari (1993) defined the first, second, and third invariants of stress in terms the principal stresses as:

$$J_{1} = \sigma_{1} + \sigma_{2} + \sigma_{3}$$

$$J_{2} = \sigma_{1}\sigma_{2} + \sigma_{2}\sigma_{3} + \sigma_{3}\sigma_{1}$$

$$J_{3} = \sigma_{1}\sigma_{3}\sigma_{3}, \qquad (3.26)$$

The von Mises criterion states that the onset of plasticity takes place when a function of the deviatoric of the invariants $f(J'_1, J'_2, J'_3)=0$; the prime is referred to the deviatoric stresses. Since $J'_1=0$ and J'_3 can be dropped off for material

that doesn't exhibit strain-hardening or strain-softening (i.e. Bauschinger Effect), the von Mises criterion simply states that the onset of plastic yielding is initiated when the distortion strain energy exceeds a constant value:

$$J_{2}' = \sigma_{1}'\sigma_{2}' + \sigma_{2}'\sigma_{3}' + \sigma_{3}'\sigma_{1}' \ge -K^{2}$$
(3.27)

The value of K can be estimated from the uniaxial loading test such that $3K^2 = \sigma_Y^2$ thus:

$$(\sigma_1 - \sigma_2)^2 + (\sigma_2 - \sigma_3)^2 + (\sigma_3 - \sigma_1)^2 \ge 2\sigma_Y^2$$
 (3.28)

In two-dimensional problems (σ_3 =0), the von Mises criterion can be represented, geometrically, by an ellipse whose axis is tilted 45 degrees from the horizontal direction on the $\sigma_1\sigma_2$ plane as indicated in Fig. 3.9.

When the point (σ_1, σ_2) lies inside the ellipse, the material does not yield. Yielding begins as the point passes the elliptic contour. Note that in the shaded regions the material doesn't yield based on von Mises criterion, even though the principal stress is higher than the yield strength (σ_Y) .

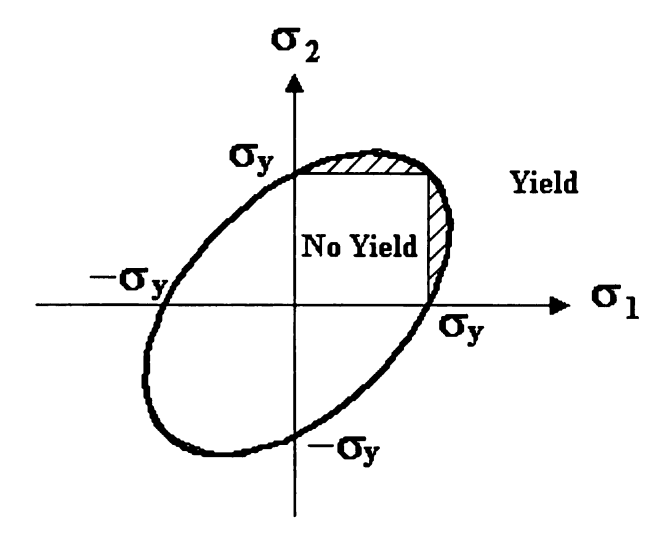


Fig. 3.9 von Mises failure criterion in two-dimensional body

The Tresca yield criterion is based on considering the maximum shear stress as the dominant factor for creating distortion instead of the maximum shear strain energy, therefore yielding occurs whenever any of the shear components exceed the yield strength:

$$Max (/\sigma_1 - \sigma_2 /, /\sigma_2 - \sigma_3 /, /\sigma_3 - \sigma_1 /) \ge \sigma_Y$$
 (3.29)

3.4 Summary

The classical contact problems in the elastic domain provided an understanding of the contact between the probe and apple. Hertz contact of concaved bodies, and the Boussinesq contact with a rigid cylindrical plunger are two extreme cases that could not be used in apple firmness estimation. Both of them are characterized by non-uniform contact stress distributions that if applied in apple firmness testing would cause excessive damage and the failure of the fruit tissue would take place gradually. Thus, an ill-defined bioyield point would

result that could not be measured. The variability of the contact area in Hertz problem further complicates the objective of estimating the bioyield strength of the fruit tissue. A probe that applies a uniform contact stress distribution with constant contact area should be used. A uniform stress is necessary to inspire the bioyield failure of the entire contact area simultaneously that produces a well-defined bioyield point, and can be measured easily and reliably.

For the contact of elastic material, the component of displacement in the axial direction (indentation) is given by Eq. 3.12, and the components of contact stress are given by Eqs 3.15 and 3.16. The contact stress distribution is expected to decrease with time in a way similar to that shown in Fig. 3.8 due to the relaxation behavior of the viscoelastic apple material. Finally, failure criteria that might be able to explain apple tissue failure in the bioyield test were considered.

Chapter 4

Finite Element Simulation of the Contact Problem

A numerical solution of the probe contact with apple can be obtained using the Finite Element Method (FEM). A close form analytical solution is unattainable due to the complexities of apple geometry and viscoelastic behavior of its material, which would be evaluated experimentally. The FE scheme would be used to investigate the effect of several probe design parameters and fruit parameters on the contact stress distribution. Accordingly, a number of probe designs would be built and evaluated experimentally in the next chapter (Chapter 6) for nondestructive apple firmness evaluation.

At the bioyield point the deformation increases without an increase in the applied load, computer simulation of the contact problem with apple is promising in gaining a thorough understanding of the mechanism of bioyield phenomenon. Sherif (1976) applied the finite element technique to investigate the stress distribution in cylindrical samples of apples, peaches and potatoes. The material was assumed homogenous, isotropic and elastic, the apple samples failed by the maximum shear strength. Rumsey and Fridley (1977) used a two-dimensional, viscoelastic FE computer program to analyze the internal stress distribution of the contact-loading situation. De Baerdemaeker (1975) used the finite element technique to solve the viscoelastic boundary value problem of contact with a rigid flat plate. Chowdhury (1995) studied stress distribution due to contact with a sphere to explore bruise susceptibility of potatoes. Wu et al. (1994) developed

a three-dimensional finite element model to predict apple behavior between two parallel plates.

An axisymmetric finite element model of apple-probe contact will be used to investigate the effects of different parameters on the contact stress distribution. Apple material is non-homogeneous and anisotropic. Sample's orientation and location in the fruit significantly affect the mechanical properties of apples (Abbott and Lu 1996). For simplicity, apple material is assumed to be an isotropic viscoelastic material, while the rubber is assumed to be elastic material in the moderately low range of stresses required for apple tissue bioyielding.

4.1 The Concept of the Finite Element Method

The finite element method is a general technique for structural analysis; it is based on the distinctive feature of dividing the complex geometrical domains into a set of simple subdomains called *finite elements*. The procedure involved in the finite element technique to analyze a typical problem are summarized by Reddy (1993) in the following steps:

- 1. Discretization: the given problem domain is represented by a mesh of simple finite elements interconnected at points called nodes.
- 2. Derivation of the elemental equations: the governing constitutive equations are approximated in a variational form evaluated at selective points in the element.

3. Assembly: the equations of the elements are assembled using the continuity of the solution and the balance of the internal fluxes, to obtain the equations of the whole problem. The force-displacement relation for a linear static problem takes the form:

$$Ku = f (4.1)$$

Where K is the system stiffness matrix, which is symmetric banded matrix, u is the displacement vector of the nodes, and f is the force vector.

- 4. The boundary conditions are imposed at selected nodes.
- 5. Solution of the assembled algebraic equations.
- 6. Postprocessing of the solution to present the results of concern in a tabular or a graphical form.

A commercial finite element program called MARC was used to simulate the apple-probe contact problem. The analysis of the apple contact behavior requires the ability to model the contact phenomena by tracking the displacements of the elements at the interface of the contacted bodies to avoid penetration. The non-penetration constraint can be applied by several techniques using the Lagrange multiplier, penalty functions, or solver constraint. The later technique is used to analyze the contact problem (MARC, 2000).

4.2 Probe Design Considerations

Probe designs based on either Hertz theory or Boussinesq contact, which use a spherical or a rigid cylindrical plunger, respectively, are inappropriate for nondestructive bioyield point evaluation.

The classical Hertz contact is characterized by variable contact area and the stress distribution is elliptic. Hence the bioyield of apple tissue originates at the center of the contact area, and gradually, expands outward; a severe penetration is produced, which degrades the fruit due to bruising. A spherical probe causes the gradual failure of the flesh over a period of time, which makes it undesirable and inefficient for the bioyield point measurement. Chowdhury (1995) was not able to assess the yield point of potato tuber by compression with a spherical indenter. However, the sudden drop of the load was observed when excessive failure of the entire contact area occurred which was accompanied with skin separation, while the onset of flesh bioyielding has taken place at the center of contact area and continued gradually in the linear range of force-deformation curve but could not been detected.

On the other hand, the contact area with a rigid cylindrical die "Boussinesq contact" is constant. But the stress concentration at the sharp edge has excessive destructive effects. A uniform stress distribution induces simultaneous bioyielding of the tissue (gross failure) beneath the contact area, such that the bioyield failure stress is integrated into a measurable force associated with a hook in the force-deformation curve.

Since rubber material exhibits a high degree of elastic deformability under the action of comparatively small stresses, the use of rubber at the end of the cylindrical steel probe (Fig. 4.1) will assist in the following improvements of the contact situation:

- 1. The full contact with skin is achieved at lower load, after that the contact area remains constant.
- 2. The stress concentration is eliminated, which enhances the uniformity of the contact stress distribution.
- 3. Eliminate gradual failure that accompanies the variable contact area.
- 4. Enhance bioyield point measurement through simultaneous bioyielding of the entire flesh tissue within the contact area.
- 5. Reduce tissue bruising.
- 6. Provide an average value of the bioyield stress.

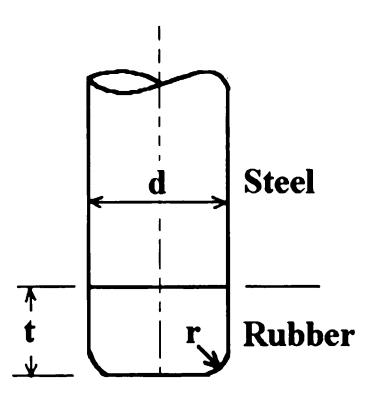


Fig. 4.1 Probe geometry

Comparison of the force-deformation curve of apple contact with cylindrical probe indicates that the use of a rubber tip tends to produce a smooth curve and the bioyield tissue failure is observed obviously at a single point. While in the case of rigid steel probe a series of micro failures occur over a wide range of deformation (Fig. 4.2). Note that the force value at the bioyield point doesn't change and the change in the slope is due to the elasticity of the rubber.

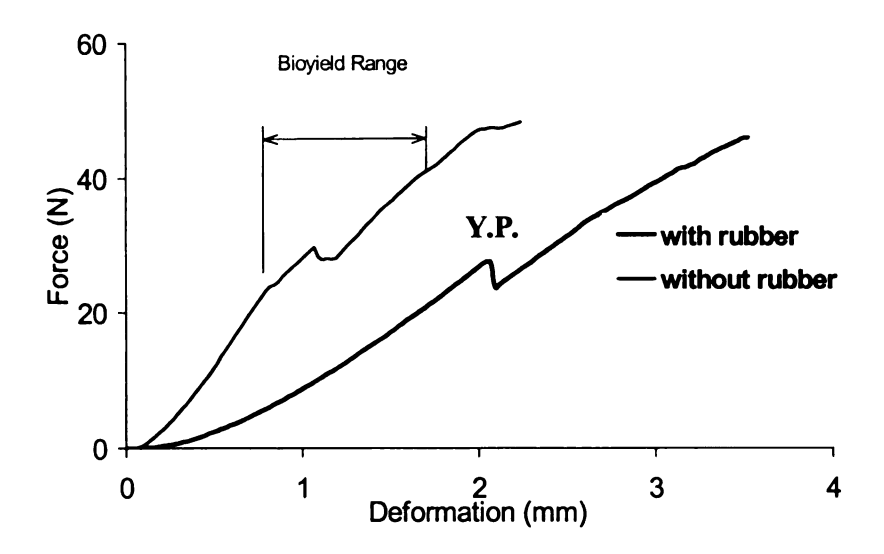


Fig. 4.2 Comparison of apple bioyield test by a cylindrical steel probe with and without rubber tip

4.3 Objectives

The primary objective of the finite element simulation was to design a probe that would produce the most uniform stress distribution over the entire contact area. This probe was considered to be optimal in accomplishing nondestructive or minimally destructive detection of the bioyield point. In addition, the displacement of the contact area (indentation) would be evaluated

by the finite element method since it is associated with apple bruise susceptibility.

The specific objectives were to:

- Investigate the distributions of stresses and deformation in the vicinity of the contact area.
- 2. Study the effects of *probe parameters*, such as the rubber modulus of elasticity (E_R), thickness (t), probe diameter (d), and fillet radius (r) at the outer edge of the rubber tip.
- 3. Study the effects of apple *fruit parameters* including fruit size (D), skin modulus of elasticity (E_S), and skin thickness (t_S).
- 4. Study the effect of the contact *friction* between the fruit's skin and the probe.

4.4 The Finite Element Model

The basic finite element model is described in this section. Investigation of the effect of a parameter was carried out by altering that parameter, while the rest of the parameters were held constant. The findings were considered in the construction of a few of probes that would be evaluated experimentally in Chapter 5.

The apple-probe contact problem was assumed to be axisymmetric in the neighborhood of the contact point where the variation with the transverse angular coordinate about the probe axis was neglected. Therefore, the contact problem was reduced to a two-dimensional problem, resulting in a significant saving in

the required computational memory. This saving is primarily due to two factors:

1) the finite elements of revolution are simple and require a lesser number of nodes per element; and 2) the total number of the elements which constitute the axisymmetric mesh is much less than that used to construct the complex three-dimensional mesh. Furthermore, since the other half of the fruit on the opposite side of the contacted region doesn't contribute significantly to the contact solution, only one quarter of the fruit cross-section needs to be considered (De Baerdemaeker 1975, Rumsey and Fridley, 1977, and Chowdhury 1995). A zero displacement boundary condition was imposed at the nodes of symmetry (see Fig. 4.3).

The profile of the longitudinal cross-section of an average "Beauty Rome" apple sample was traced and used as the basis of the model. The apple sample was 92 mm in diameter and 73 mm in height. The fruit flesh is divided into 793 triangular elements, taking into consideration that the mesh is refined in the locality of the contact region. The Poisson's ratio was taken as 0.3 (Clevenger and Humann, 1968). The material is isotropic and viscoelastic. The material properties of the flesh were obtained as the average of 15 cylindrical samples of three apple varieties tested experimentally. The flesh modulus of elasticity was about 5.0 MPa, and the relaxation function, corresponding to a two-element generalized Maxwell model, is given by:

$$\sigma(t) = \varepsilon_{o} \left(E_{1} e^{-t/\tau_{1}} + E_{2} e^{-t/\tau_{2}} + E_{3} \right)$$
 (4.2)

where

 σ = Compression stress.

 $\varepsilon_0 = 0.1 \equiv \text{initial strain}.$

t = time (second).

 $E_1 = 0.488$, $E_2 = 0.590$, and $E_3 = 1.13$ MPa = stiffness of the springs.

 $\tau_1 = 2.27 \text{sec}$, $\tau_2 = 45.6 \text{ sec} = \text{the first and the second time constants}$.

The material properties of the core carpel are different from the apple flesh, but it is located far away from the contact region and their effect can be neglected.

A thin layer enclosing the apple flesh was used to model apple skin. Skin thickness of 0.5 mm and a modulus of elasticity of 10 MPa were used in the model (Clevenger and Humann, 1968). The layer is divided into 46 quadratic elements.

A rigid flat plate models the steel end of the probe, and the diameter of the probe was d=7/16 inch, similar to the Magness-Taylor pressure tester. The tip was divided into 284 triangular elements. The rubber modulus of elasticity (E_R=3.27 MPa) was taken from the stress-strain relationship of rubber samples (Fig. 4.4). The linear relationship in the range of compression stress, which is below the bioyield strength of apple fruit, suggested that an elastic model of rubber would be satisfactory. A Poisson's ratio of 0.48 of nearly incompressible material was used for rubber.

The contact process originated when the flat plate was moved against the rubber part at a constant speed (i.e. constant strain rate) of 0.5 mm/sec (1.18

inch/min) downward in the negative x-direction. The apple and the rubber tip are deformable bodies that respond to the applied load and the nodes at the axis of symmetry were not allowed to separate. The skin was assumed to be glued to the apple flesh and the plate glued to the upper surface of the rubber tip. The glue option implied that there was no relative tangential motion. The plate moved a total of 4 mm displacement. This displacement was divided into 100 equal steps. At each step the distances between each node and the surfaces of other bodies were checked and compared with a preset small contact tolerance. If the distance was below the tolerance, the no-penetration constraint was applied; an iterative procedure was continued until both the equilibrium of the element was achieved, such that the node was held in contact with the surface.

The degree of uniformity of the contact stress distribution was considered the measure of the suitability of the probe design for bioyield point detection. The uniformity was estimated by computing the standard deviation of the normal stress at the nodes located within the contact area; the lower the standard deviation the more uniform the stress.

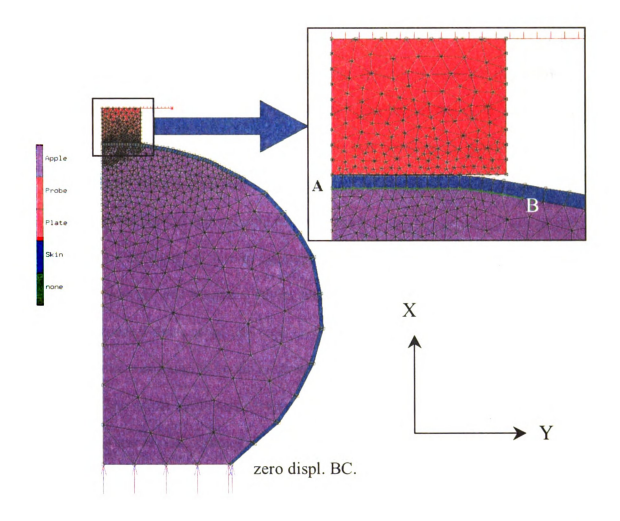


Fig. 4.3 The finite element model showing the model components, the boundary condition, and the path AB in the zoomed view of the contact area

4.5 Results and Discussion

4.5.1 Validation of the Finite Element Solution

The validity of the finite element solution was established in comparison with experimental data. The measured force-deformation relationship of the bioyield point evaluation test of a particular apple was used for this purpose. The finite element model represents only the upper half of the apple, as shown in Fig. 4.3. Although the compression strain was small away from the contact point, strain at the plastic seat was expected to be significant, and deformation of the lower half of the apple should be considered.

A Fuji apple, 81 mm in equatorial diameter, and 70 mm in height, with a 231 gram mass, and Magness-Taylor firmness measured to be 49.4 N was tested with the small-thick probe (1/4 inch in diameter with 1/8 inch rubber thickness). This probe was found to be the most suitable for firmness assessment.

The whole apple was compressed by the probe and the force-deformation (F_W-D_W) curve was obtained experimentally, where the subscript W stands for "Whole apple". The bioyield point occurred at 27.2 N load, which corresponded, to a total deformation of 2.02 mm (Fig. 4.5).

The material properties of the same apple were obtained by testing two cylindrical samples (20 mm in diameter and 12.4 mm height). The samples are taken from the locality of the tested point. One sample is tested in compression. The average slope of the stress-strain diagram in the linear range between 0.037 and 0.27 MPa stress (Fig. 4.4) was used to determine the modulus of elasticity (E_A =4.01 MPa). The other sample was tested in relaxation from the initial

compression strain of ε_0 =0.1; the stress-time relationship was fitted to the twoelement generalized Maxwell model given in Eq. 4.2. The constants are: E_1 =1.51 MPa, E_2 = 0.50 MPa, E_3 = 0.53 MPa, τ_1 = 1.14sec, and τ_2 =13.87 sec. The above tests of the whole apple, including the MT firmness test, were all conducted on the upper half of the apple. After testing the whole apple, the upper half was cut and removed, and the lower half was compressed with a rigid flat plate against the seat. The force-deformation curve (F_L - D_L) of the lower half apple was obtained, where L stands for "Lower half".

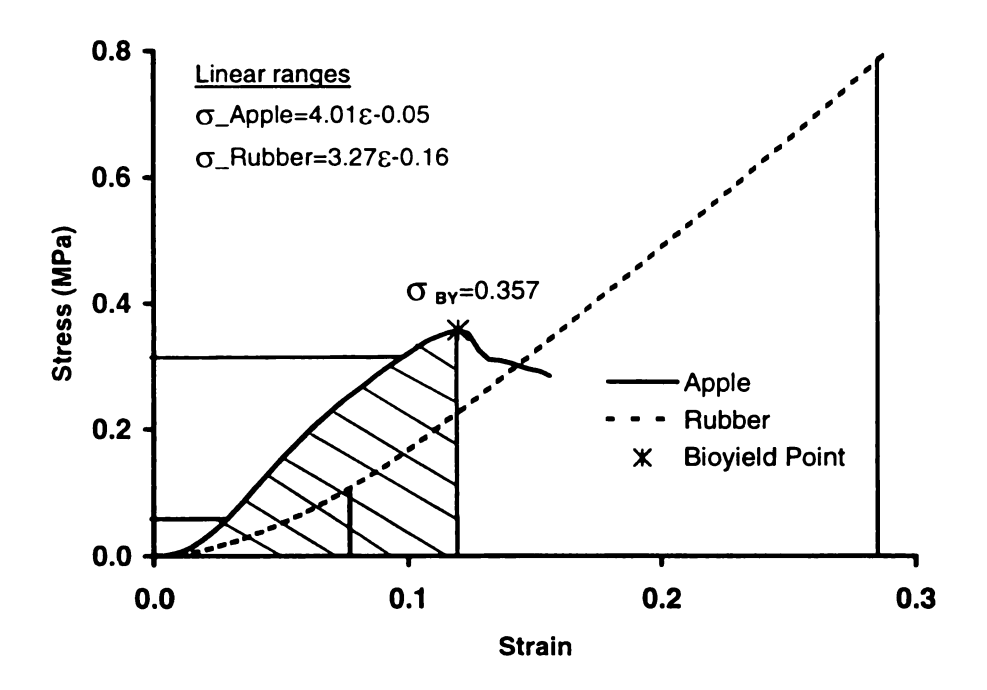


Fig. 4.4 Uniaxial compression of cylindrical samples of apple and rubber, the horizontal and vertical lines identify the linear ranges

The superposition principle was applied to compute the force deformation curve of the upper half of the apple that was used in the FE model. The net deformation of the modeled half is the difference between the deformation of the whole apple and the deformation of the lower half of the apple $D_N=D_W-D_L$, where the deformations were evaluated at common force measurements, such that $F_W=F_L=F_N$.

The simulated force and deformation of the probe from the FE model correspond to the Force and Position of the plate, where the rigid plate resembled the steel part of the probe. The time variations of any variable can be tracked using the history option in MARC and the data was collected at a specified increment.

A comparison of the force-deformation curve from the FE model using the elastic modulus for the same apple that computed from Fig. 4.4 with that of the net curve F_N - D_N computed from the experiments is shown in Fig. 4.5. The curves are in good agreement; the high correlation between the measured and simulated force (r = 0.99) indicates that the finite element model is adequate in simulating the actual apple-probe interaction. The deviation beyond 0.8-mm deformation might be explained by the strain hardening (slope increase at higher strains) of the rubber material and the nonlinear behavior of apple tissue at larger deformations (Fig. 4.4).

The finite element model computed that, at the bioyield point, the average rubber deformation was 0.6 mm, whereas the apple deformation was 0.8 mm. This deformation can be divided into elastic deformation, and a permanent

plastic deformation in the form of a bruise. However, the bruise volume was too small to be observed.

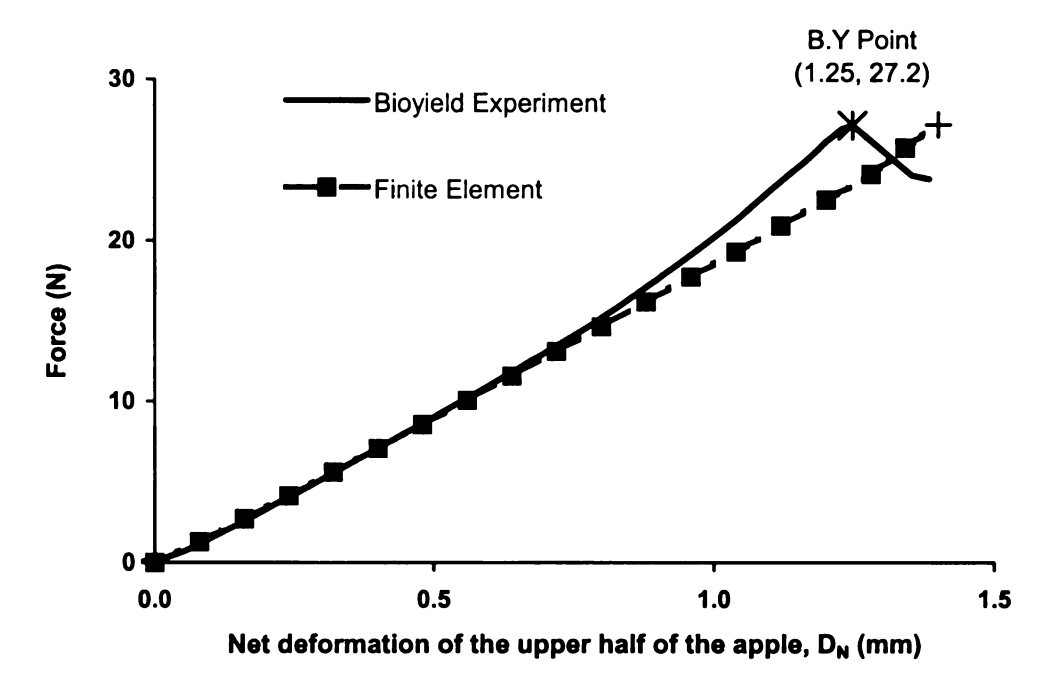


Fig. 4.5 Comparison of the FD-curve of experimental and FE simulation results of a particular apple

4.5.2 Development of Bioyield Failure Criterion

It is conventionally believed that either shear or normal stress causes the fruit tissue failure, depending on the loading condition. Segerlind and Fabbro (1978) proposed the normal strain as a criterion for apple failure, such that apple flesh fails when the strain exceeds a critical value. Because of discrepancies in the data, which were attributed to the effect of loading rate, the strain failure criterion was questioned by Chen and Sun (1984).

Several failure criteria were examined to recognize which one could accurately explain the failure of tissue at the bioyield point. It was done by comparing the value of the proposed criterion for the uniaxial loading with that of the tri-axial loading condition. The former was obtained from the compression of a cylindrical sample between parallel plates, while the later were estimated by the finite element model for the probe-apple contact at the bioyield point.

The bioyield of the whole apple occurred at a force of 27.2 N, corresponding to 1.25-mm net displacement. The bioyield force rather than displacement was used as the basis of comparison between the model and the experiment. This was due to two reasons: 1) The stress was thought to be more important than strain in causing the bioyield failure. 2) The inaccuracy involved in estimating the net displacement at the bioyield point. The plus sign in Fig. 4.5 indicates the point at which the apple material bioyielded. This point was associated with the increment number 35 of the FE model, where the probe displacement was 1.4 mm.

The images of the FE solution in this chapter were presented in colors, each color corresponds to a range of results as indicated in the associated scale bar (Fig.s 4.6-4.11). Examination of Fig. 4.6 indicated that the gradient of the axial displacement was greatest near the contact area. Only about 10% of the probe displacement (0.14mm) was recorded at about 2 cm away from the contact area. Most of the effects due to contact with the probe were mainly confined to a small region in the neighborhood of the contact area as shown in Figs. 4.7-11.

Therefore, the contact with probe is expected to be insensitive to the variation of apples geometry of different apple varieties. In this study, the actual surface of a particular apple profile was used in the FE model, the model was assumed to be axisymmetric about the stem-calyx axis. A sphere was used to model the apple and potato geometry by some researchers (Rumsey and Fridley, 1977, De Baerdemaeker 1975, and Chowdhury, 1995).

The component of compression stress in the x-direction (σ_x : component 11 of stress) is shown in Fig. 4.7 at the bioyield load, which occurs at increment 35. The maximum compression stress of about 0.51 MPa took place directly under the contacted skin; the stress was uniformly distributed at the skin in accordance with our goal. The value of compression stress at failure in tri-axial FE model was significantly higher than that measured in the uni-axial loading condition (σ_{BY} =0.36 MPa, Fig. 4.4). Therefore, the maximum stress failure criterion was unable to predict the onset of tissue failure in the bioyield test. This might be explained by the influence of the hydrostatic pressure inside the apple fruit as compressed by the probe on the maximum axial stress that apple material could withstand without failure. Such that the compressive and the total axial stresses were excluded as parameters that predict tissue failure (Miles and Rehkugler, 1973)

The shear stress (component 12 of stress) was concentrated under the outer edge of the probe (Fig. 4.8). The maximum value of shear was about 0.15 MPa, which was very small compared with the compression stress. The failure surface was observed to be, approximately, of a paraboloid shape pointing

downward with a circular base at the contact area, while the shear stress was maximum along a circular ring located directly under the probe sharp edge. Thus the maximum shear failure criterion was not a suitable criterion to explain the bioyield failure. This appears to be out of perspective of Fridley *et al.*, (1968), that tissue failure under a rigid flat plate was due to the maximum shear stress.

The strain failure criterion states that apple tissue fails when the normal strain exceeds a critical value. For the uniaxial loading of the cylindrical sample, the bioyield point occurred at about 11.9% normal strain, whereas in the tri-axial loading of a whole apple, the maximum compression strain at failure was predicted by the FE model to be 10% strain. Both the experimental and the FE prediction of the critical strain were within the range of 0.10–0.15 that was specified by Segerlind and Fabbro (1978). The locus of the nodes of maximum strain was also very close to the actual failure location. Therefore, the critical strain failure is a possible criterion for the bioyield failure prediction.

The strain energy density of the uniaxially compressed cylindrical sample can be obtained by integrating the shaded area under the stress-strain curve of Fig. 4.4 and divide it by the sample volume. It was estimated as 0.0224 MJ/m³ [J/cm³], in comparison with the maximum value of the strain energy density that was predicted by the FE solution (Fig. 4.10). The maximum energy density occurred at a circular disc adjacent to the internal skin surface of 0.0255 MJ/m³ value, with 0.00159 J/cm³ standard deviation, which was slightly greater than that of a uniaxial sample. The location of the actual failure was far away from

the zone of maximum strain energy density. Therefore, the strain energy density was not able to predict the failure of apple tissue when tested by the probe.

The von Mises stress is the distortion component of strain energy, which is function of the three components of principal stress. The von Mises failure expects tissue failure to occur wherever Eq. 3.28 is satisfied. A numerical output (not shown) indicated that the locus of the nodes of local maximum von Mises stress was along the green line indicated in Fig. 4.11. The value of the von Mises stress directly under the probe edge (at the arc beginning) was 0.41 MPa, and at 1.3 mm below the center of contact (at the arc end), it was 0.36 MPa in comparison with the bioyield stress for the uniaxially loaded cylindrical sample, which was taken from the same apple of 0.357 MPa (Fig. 4.4). The high value of the von Mises stress under the probe edge was due to the high shear stress concentration, which is a major parameter of distortion effect. Therefore, the onset of tissue fracture is believed to originate at the point below the probe edge and propagates along the locus of maximum Von Mises stress towards the central end of the locus. The actual failure surface in three dimensions was observed as a circular paraboloid. The failure of cylindrical samples took place along a conical surface (Miles and Rehkugler 1973). The locus of maximum von Mises stress as obtained by the finite element model was approximately coincident with the cross section of the actual failure zone, and the numerical values were comparable with the bioyield strength. Therefore, the von Mises stress was a possible failure criterion that enabled to predict apple tissue failure. The von Mises stress was also considered satisfactory criterion to explain tissue

failure of potato tuber as contacted with a spherical probe (Chowdhury, 1995), its value was exceeded the bioyield strength in the actual failure zone below the surface of contact.

In summary, the FE model of apple-probe contact at the onset of bioyielding was compared with the uniaxial compression of cylindrical sample taken from the same apple. The critical normal strain and the von Mises equivalent stress were able to predict the failure of apple tissue whereas the normal stress, shear stress and the strain energy density were not able to predict the failure of apple tissue. They were rejected as possible failure criteria because either their values were different from the corresponding uniaxial compression, and/or the loci of their maximum values were located far away from the actual failure zone.

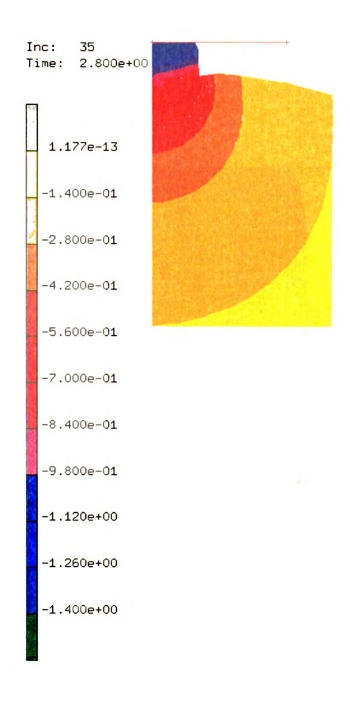


Fig. 4.6 Displacement in the axial direction (mm)

Inc: 35 Time: 2.800e+00

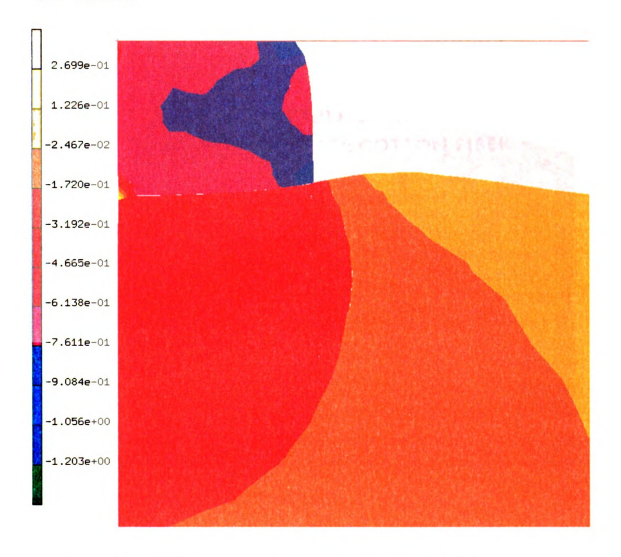


Fig. 4.7 Component of stress in the axial direction, σ_X (MPa)

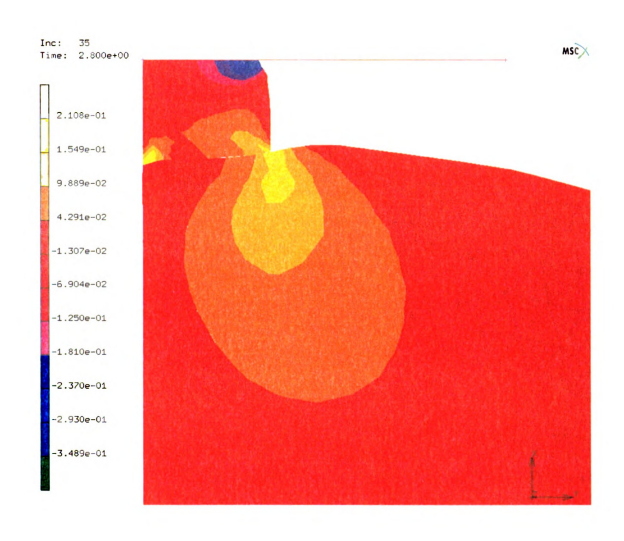


Fig. 4.8 Shear stress concentration under the outer edge (MPa)

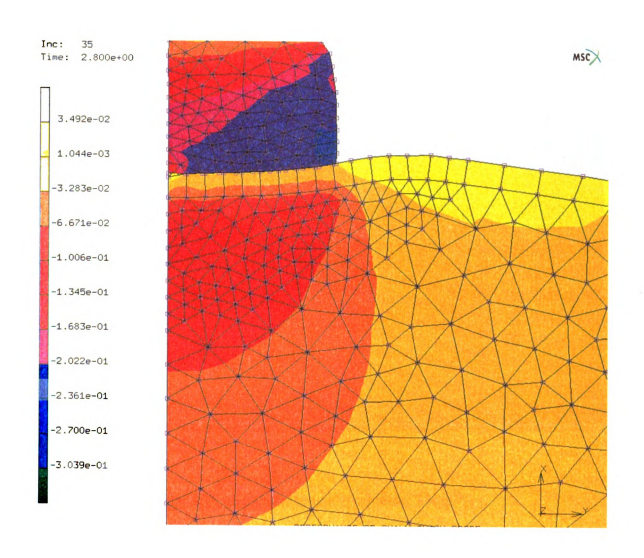


Fig. 4.9 Axial component of total strain (ϵ_{11})

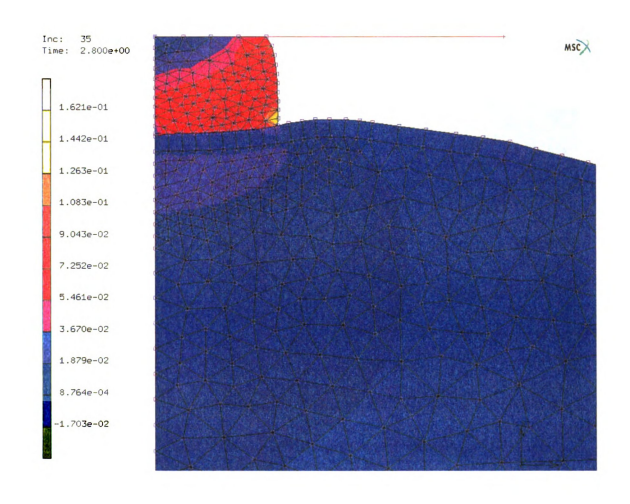


Fig. 4.10 Total strain energy density (J/cm³)

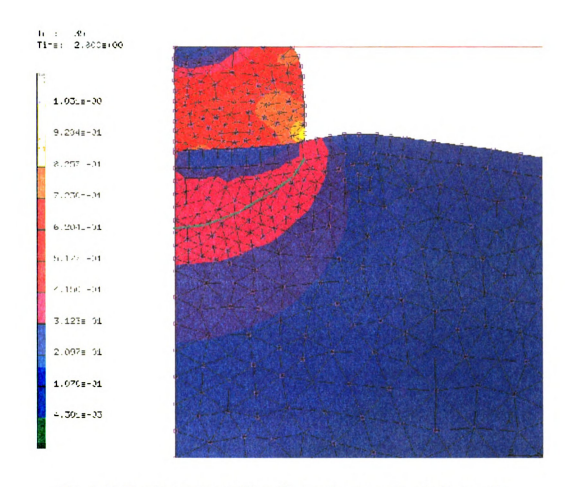


Fig. 4.11 Equivalent von Mises Stress, the green line indicates the locus of local maximum stress

4.5.3 Effects of Probe and Fruit Parameters

The objective of this study was to develop a mechanical probe that would apply a quasi-uniform stress over the contact area. The uniform compression stress distribution over the contact area would enable accurate estimation of the bioyield point. In order to achieve this objective, it is crucial to examine different probe design parameters and fruit parameters that might alter the uniformity of the contact stress distribution.

The displacement and the normal stress values at the nodes along the path AB (Fig. 4.3) were estimated as the stress approaches a threshold value of bioyield strength. Note that the path AB is located at the apple flesh-skin interface right underneath the contact area. A threshold value of 0.64 MPa was assigned to the bioyield point strength, which corresponds to an average apple with Magness-Taylor firmness of 14 lb. (Ababneh *et al.*, 2000). When a stress concentration occurred at the probe outer edge, the threshold value was only applied to a few central nodes for comparison purposes. However, stress concentration is a serious problem, which tends to occur at the outer edge of the contact area that causes apple bruise; hence it should be eliminated.

4.5.3.1 Rubber Elastic Modulus

The solution of the contact problem is compared for different values of rubber elastic modulus (E_R); a low value corresponds to soft rubber, while a large value to rigid rubber. The normal stress distribution is shown in Fig. 4.12, for E_R = 2.5, 4, 5, 7.5, 10,15, 25, 100, and 1000 MPa. A rubber with elastic modulus

of less than 10MPa or two times that of the apple $(E_R < 2E_A)$, generated a satisfactory degree of uniformity, such that the standard deviation was less than 12% of the bioyield strength. A very soft rubber was not practical because it bulges at a pressure corresponding to the bioyield strength of apple.

The stress concentration factor at the outer edge was 1.14 for $E_R = E_A = 5$ MPa, and increases to 1.28 for $E_R = 2E_A = 10$ MPa. As the rubber modulus increases further, the stress converges to the Boussinesq solution of the rigid cylindrical die in contact with a semi-infinite elastic body as given by equation 3.17 as shown in Fig. 4.12. However, due to the apple curvature, a slight deviation was discerned as the radial distance was increased. The stress concentration at the outer edge increased the applied load required to reach the bioyield strength, enhanced skin deformation and consequently would produce larger bruise volume.

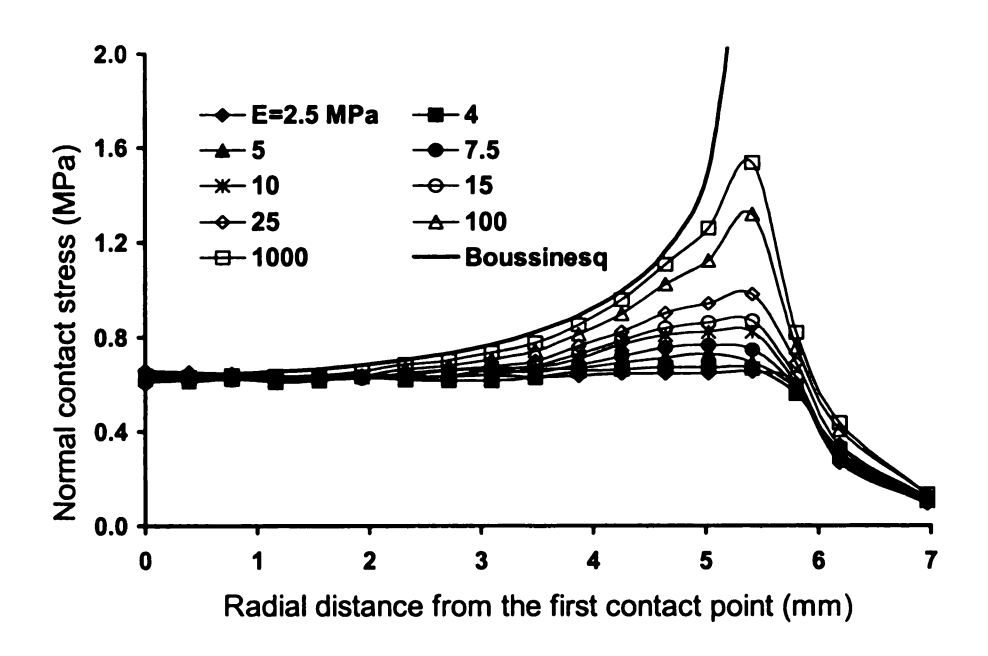


Fig. 4.12 Effect of rubber modulus of elasticity on the normal stress distribution

4.5.3.2 Probe Diameter

The diameter of the probe (d) is a crucial factor in bruise volume consideration. The finite element solution indicated that the maximum deformation at the center or the bruise depth has a linear relationship with the diameter of the probe. The volume of the bruise would be proportional to the cubic power of the diameter (d^3). The uniformity of the stress distribution, on the other hand, was not influenced by probe diameter for $d \le 7/16$ inch (Fig. 4.13). Hence, a small probe diameter is recommended for a nondestructive measurement of apple firmness.

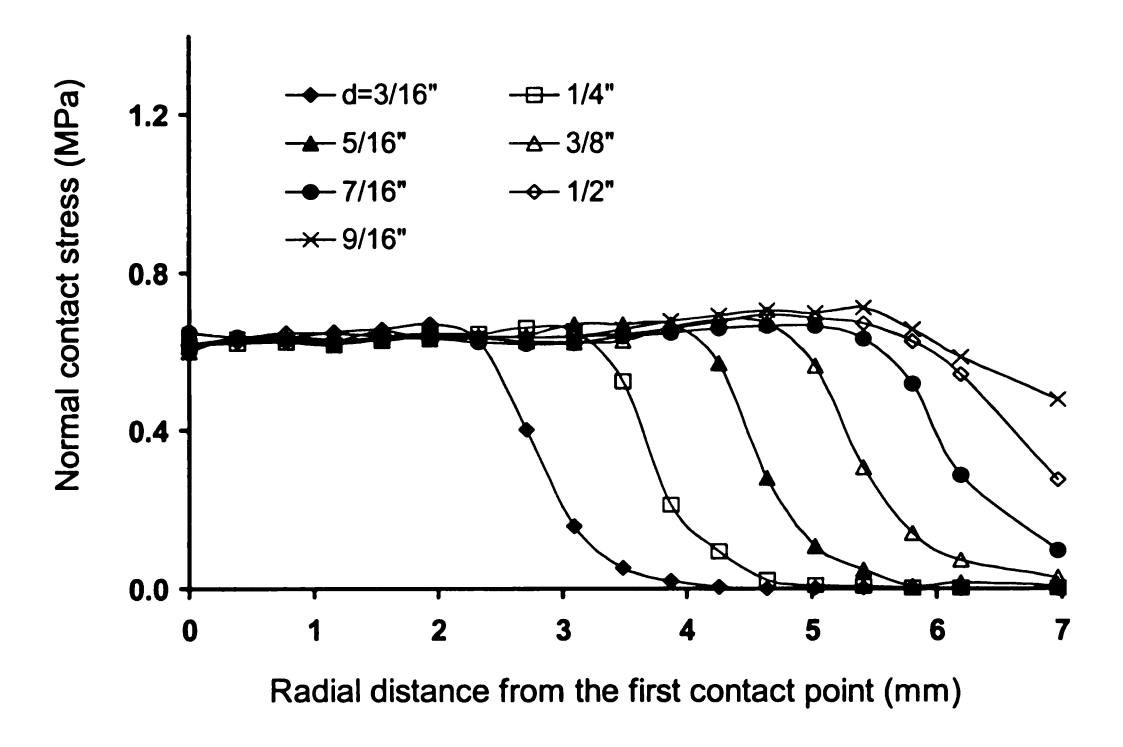


Fig. 4.13 Effect of probe diameter on the normal contact stress distribution

4.5.3.3 Rubber Tip Thickness

The use of a rubber piece at the end of the steel tends to lower the effective stiffness of the probe, the effect of increasing the tip thickness (t) would be equivalent to that of using softer rubber material. Fig. 4.14 indicates the normal contact stress distribution for t=0,1,2 ...5 mm. A thickness of 2 mm or greater should be used to produce a quasi-uniform contact stress. For t=2 mm, the maximum deformation was less than 1.25 mm, and the standard deviation was below 4.2% of the normal stress. The standard deviation was a decaying function of the thickness (t), such that the uniformity of stress distribution was increased for increasing thickness. However, when large thickness was used in a preliminary study, which was equal to the probe diameter or greater, testing instability was observed in the laboratory. A thin rubber produces stress concentration and would prevent the simultaneous failure of the tissue under the contact so as to detect the bioyield point. Again, the state of t=0 approaches the Boussinesq rigid die stress distribution, but the apple curvature would mitigate the stress concentration.

4.5.3.4 Probe Edge Fillet Radius

Stress concentration occurs at sharp corners. In this study, for a rigid probe with sharp edge, stress concentration was a serious problem in as discussed earlier in Section 3.3.2.2. A gradual variation of the cross section, by introducing a round fillet at the sharp edges, is a common practice to alleviate the

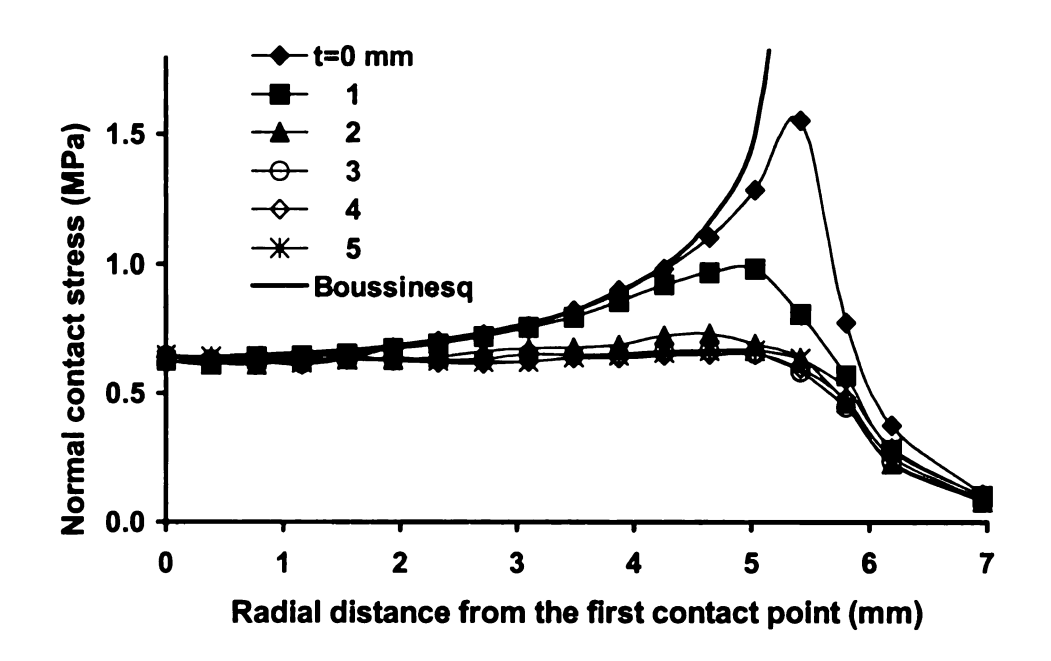


Fig. 4.14 Effect of rubber tip thickness on the normal contact stress distribution

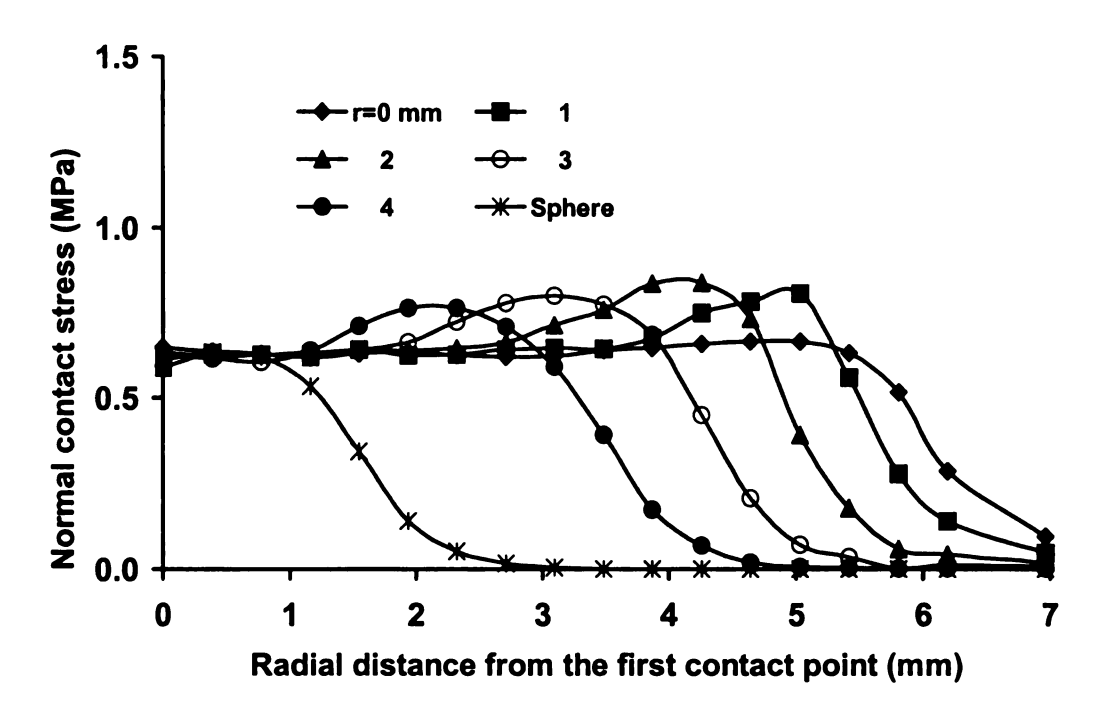


Fig. 4.15 Effect of fillet radius on the normal contact stress distribution

stress concentration. In the finite element model, values of radius of the fillet of r=0,1...4 and 5.6 mm (Fig. 4.1) were examined. The last value represents a hemispherical tip. The normal stress distribution for these values is plotted in Fig. 4.15. The fillet has altered the contact stress distribution when the contact area changed with load, the stress distribution got a sort of Hertz profile, and a peak stress outgrew in the outer part of the contact area. The outgrowth of the stress distribution can be explained as increased load that should be supported by the outer portion of the contact area after the contact with the flat portion is established. On the other hand, the newly contacted part at the outmost of the contact area would provide lower support.

The probe with the sharp edge (r=0) had the most uniform normal contact stress; the flexibility of rubber eliminates the stress concentration associated with a rigid probe. Therefore, the fillet technique was not recommended, and sharp edge probes were used in the experimental study of the bioyield point determination.

4.5.3.5 Apple Size

A suitable design of the firmness sensor that would be practical for online apple sorting should be independent of fruit size. The proposed bioyield test is based on contacting a small area of the fruit by the probe. Although apple size is related to the magnitude of the radius of curvature at the contacted region, the geometric irregularity of the real fruit may offset the effect of fruit size. The flexibility of the rubber would make up for slight variation of the radius of curvature and take care of the small clearance that exists between the probe end

and fruit skin at zero load. Small apple size affects only in delaying the achievement of full contact with the probe.

The use of a small probe compared with the apple diameter, would ensure a quick developing of full contact with the apple at a relatively low normal stress. After full contact, the primary duty of compression is carried out; the effect of stress distribution required for full contact is comparatively insignificant on the stress distribution at the onset of tissue bioyield.

The effect of fruit size was investigated by the FE method through three apple sizes; small, medium and large. The size of the original model was considered as the medium one with an equatorial diameter $D_M=3$ 11/16 inch (93.7 mm). The small size was obtained by scaling down the original apple by a factor of 20%, the small diameter was $D_S=2$ 15/16 inch (74.9 mm), whereas the large size by scaling up by a factor of 20%, the large diameter was $D_L=4$ 7/16 inch (112.4 mm).

Even for the largest probe that was used (d=7/16 inch) the normal stress distribution was not affected significantly by apple size (Fig. 4.16). Note the small range of probe to apple diameter ratio, which was between 0.10 and 0.15 for large sized and small sized apples respectively.

The delayed contact of the outer edge of the probe with the small apple reduced the stress at that area and increased the stress at an intermediate area (about 4 mm from the contact center). Therefore the total load was not affected and the measured bioyield strength would be independent of apple size, especially when a smaller probe is used.

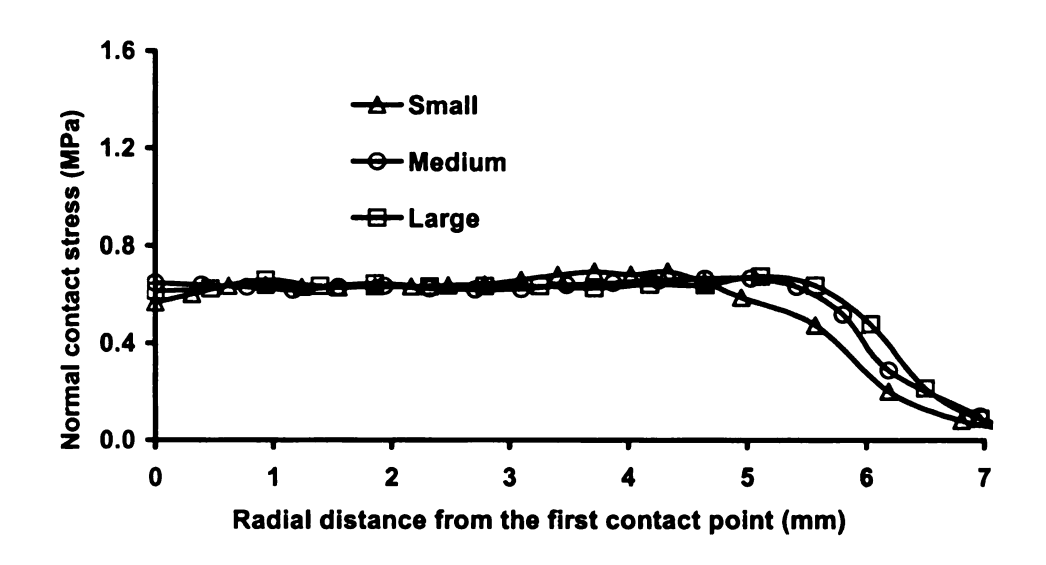


Fig. 4.16 Effect of fruit size on the normal contact stress distribution

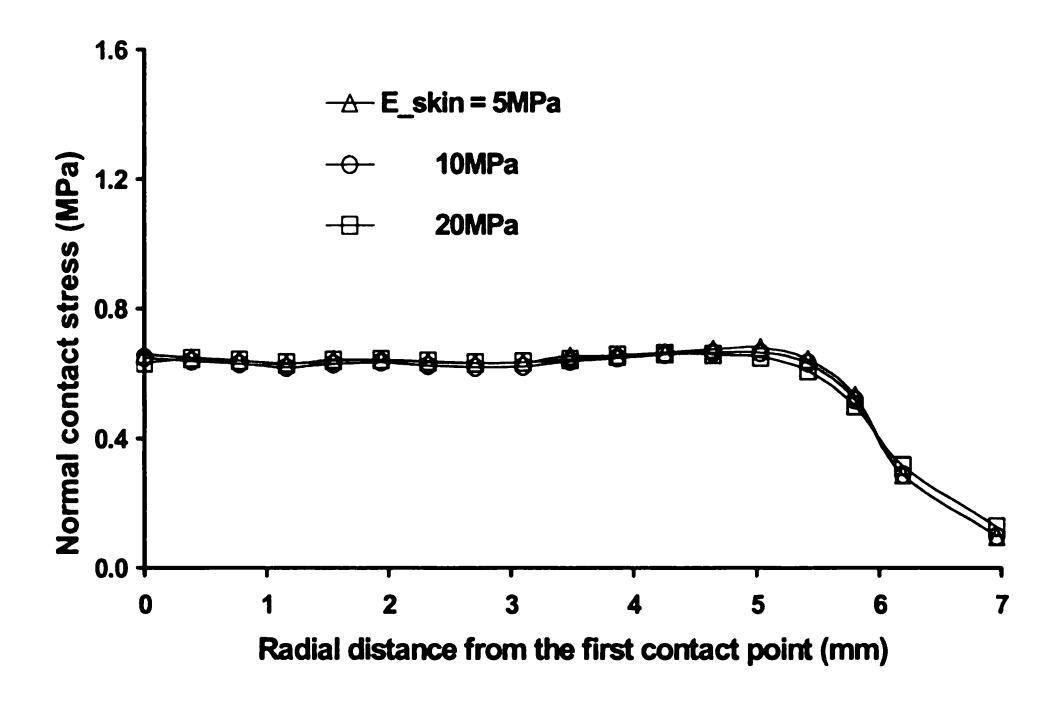


Fig. 4.17 Effect of skin modulus of elasticity on the normal contact stress distribution

5.3.6 Apple Skin

Skin thickness and modulus of elasticity varies with and within apple variety. The possible effects of their variations were investigated in this section. Apple skin does not only protect the fruit from environmental conditions, but also protects from mechanical damage. A stiffer, thicker skin layer would withstand mechanical load and reduce the fruit susceptibility to injury. However, apple skin is comparatively thin and flexible, which is expected to provide an extremely low bending resistance; therefore, flesh integrity or firmness would be the dominant factor, which specifies the bioyield point measurement. Yet, skin can withstand shear and tensile loading so it can resist cut and injury.

The tensile secant modulus of elasticity for Golden and Red Delicious apple skins ranged from 1450 psi to 1930 psi (10-13.3 MPa) and thickness ranged from 0.015-0.022 inch (0.38-0.56 mm) (Clevenger *et al.*, 1968). Note that the measurement of the compression modulus of elasticity of the skin is not feasible.

Values of skin modulus $E_S = 5$, 10 and 20 MPa that cover an extended range were used in the FE model, but no significant effect on the stress distribution was indicated (Fig. 4.17). Skin thickness of $t_S = 0.3$, 0.5 and 0.8 mm was considered in the finite element model; again the effect on stress distribution was negligibly small (Fig. 4.18). Hence the skin modulus of elasticity is an unimportant factor in bioyield point measurement.

A stiffer skin (high elastic modulus and/or large thickness retards the response of the internal flesh in the same way that the small radius of curvature of small apple reduced the stress at the outer edge.

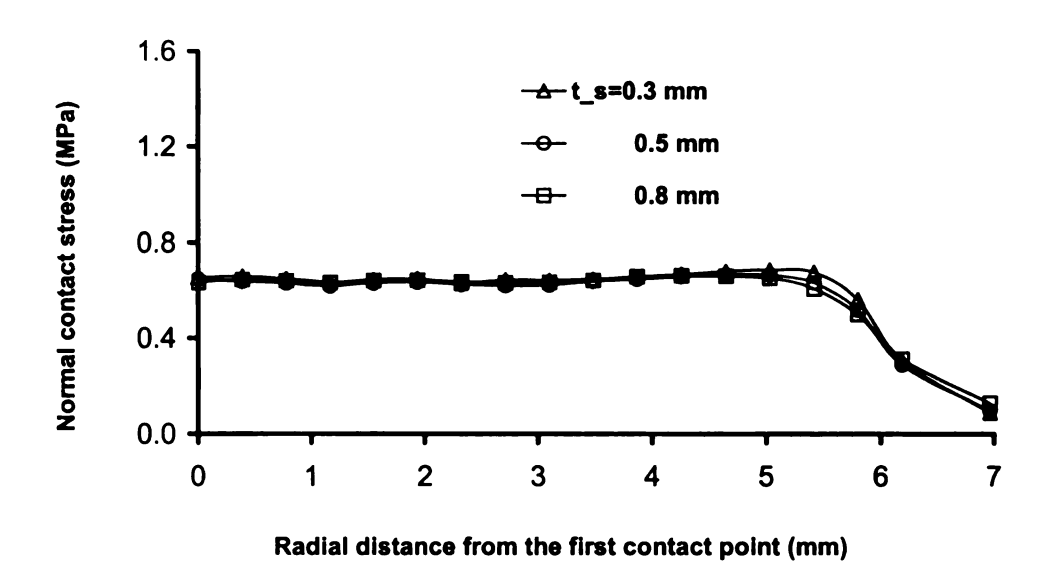


Fig. 4.18 Effect of skin thickness on the normal contact stress distribution

4.5.3.7 Friction

The effect of friction between the probe and the fruit skin was investigated using the FE model. Two limiting cases were considered: the case of no friction and the case of maximum friction in which the apple skin was glued to the probe, such that there was no relative tangential motion. Friction increased the shearing stress significantly (Fig. 4.19), especially at the outer zone of the contact area, whereas, the friction effect on the contact stress was insignificant. Thus, friction would be ignored in analyzing failure at the bioyield point.

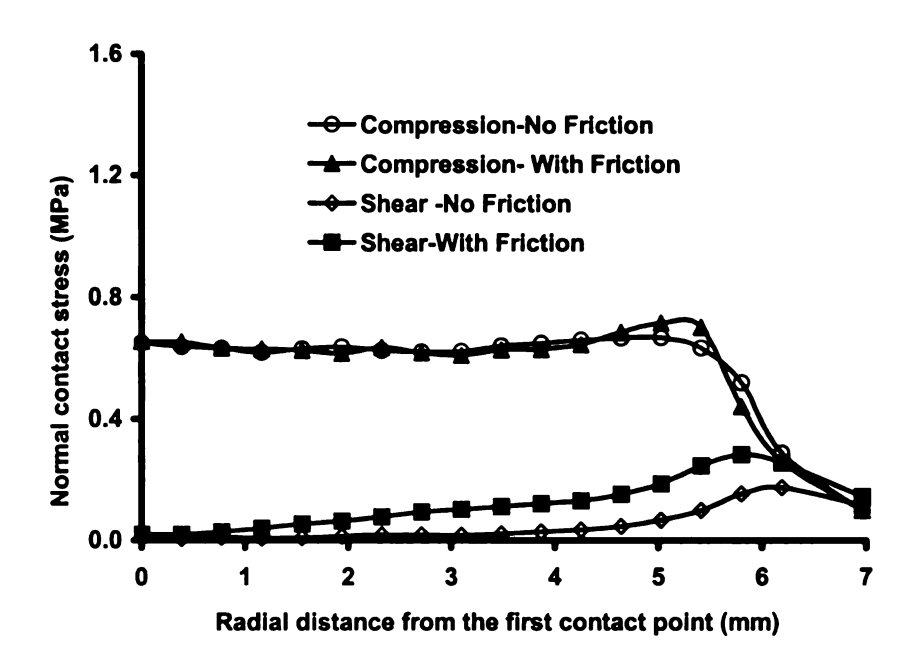


Fig.4.19 Effect of friction on the compression and shear stress distributions

4.6 Summary and Conclusions

The finite element model has described the quasi-static compression of the viscoelastic apple fruit effectively. The prediction of the FE model for the force-deformation curve of testing a particular apple for bioyield point was in good agreement with the experimental curve. The numerical results of the FE model indicated that the critical strain and the von Mises stress were two possible failure criteria for predicting the onset of tissue bioyielding. This was in part due to the magnitudes of their maximum values that were approximately matching those found experimentally from the compression of the cylindrical sample taken from the same apple. Also, the locations of these maximum values were approximately coincident with the actual failure location. The shape of the tissue failure could be approximated by a three-dimensional circular paraboloid

pointing downward with a height of 1.3 mm, and a base coinciding at the contact area.

The application of a quasi-uniform contact stress to detect the bioyield point could be facilitated by using a mechanical probe with the following features:

- 1. The rubber modulus of elasticity should be less than two times that of apple flesh.
- 2. A smaller size should be used to reduce the bruise volume and eliminate the curvature effect.
- 3. The rubber thickness should be at least 2 mm, but not greater than, roughly, the probe diameter, because it would cause test instability.
- 4. Sharp rubber edge (r = 0) should be used to maintain a constant contact area and a quasi-uniform stress distribution.

Apple size, skin elasticity, skin thickness and friction have negligible effects on the normal contact stress distribution.

Chapter 5

Experimental Evaluation

5.1 Introduction

This chapter is primarily devoted to the experimental evaluation of a few mechanical probes. The force, deformation at bioyield point, slope of the force-deformation curve and the energy of compression will be investigated for each probe to determine the most appropriate measurement parameters that are related to the firmness of the fruit. An optimal probe would be selected based on the ability to predict the MT firmness while causing minimal damage.

Apple material properties were measured and used for the FE study in the previous chapter. The properties included the modulus of elasticity and the relaxation parameters. The FE study has provided general guidelines for probe design that would be able to measure the bioyield point with minimal damage. The performance of six probes (3 diameters × 2 thickness to diameter ratios) will be investigated experimentally. Five of six probes were designed according to the FE guidelines, whereas the other design differed with the guidelines, in that its rubber thickness was below 2 mm in order to examine the validity of the FE findings.

5.2 Objectives

The primary objective of the experimental study was to estimate the material properties of the average apple and evaluate the performance of a few

probe designs in apple firmness prediction based on the assessment of bioyield point detection.

The specific objectives were to:

- 1. Estimate the average modulus of elasticity of apple flesh.
- 2. Determine the viscoelastic characteristics of apples and develop a suitable rheologic model to describe the relaxation behavior of apple flesh.
- Explore the relationships of the measured bioyield deformation, force, slope of the F-D curve, and the compression energy required to achieve the bioyield point with the standard Magness-Taylor firmness.
- 4. Investigate the performance of the probes to assess their suitability as nondestructive firmness sensors.
- 5. Compare the bioyield point measurement with the standard MT firmness measurement.

5.3 Materials and Methodology

The Universal Testing Machine, model 4202 (Instron Corporation, Canton, MA.) was used throughout the entire experimental study. The probe was attached to the load cell, which was mounted to the crosshead of the Instron machine (Fig. 5.1). The loading rate is "apparently a less important factor than might be supposed" Magness and Taylor (1925). A large increase in the loading

rate would cause a small increase in the MT firmness and the yield point. (Bourne, 1965).



Fig. 5.1 The bioyield point test setup using the Instron Universal Testing Machine.

The force measurement of the load cell and the extension (deflection) of the crosshead assembly, can be sampled at any desired rate. The software series XII was used to control the Instron machine, record the data and perform preliminary analysis, subsequent analyses were performed using MS Excel.

5.3.1 Measuring Apple Material Properties

Compression and relaxation tests were conducted to measure the modulus of elasticity and the relaxation behavior of apple material for use in the FE simulation. Typical values reported in the literature were used for the Poisson's ratio, and apple skin properties.

Apple cylindrical specimens of 20 mm (25/32-inch) in diameter were taken from the equatorial zone by driving a sample borer radially into the apple. Then each specimen was cut to 12.4-mm (1/2 inch) thickness with a parallel blade tool Fig. 5.2. The sample was tested using two parallel flat plates Fig. 5.3.

Four apple varieties were used in the experiment: Golden Delicious, Red Delicious, Fuji and Gala. A total of 20 apples (4 varieties × 5 apples / variety) were tested to evaluate the average material properties of apple flesh.

5.3.1.1 The Compression Test

Compression test was conducted by loading the cylindrical sample between two parallel flat plates (Fig. 5.3) at a rate of 0.5 mm/sec (1.18 inch/min). This rate was the same that was used in the MT firmness measurement. The specimen was compressed until failure occurred. Complete force-deformation curve was recorded; a typical curve is indicated in Fig. 4.4.



Fig. 5.2 Preparation of the cylindrical sample



Fig. 5.3 Compression test or relaxation test of the sample between two parallel plates

A stress relaxation test was executed by compressing the specimen between two parallel flat plates and letting it relax for a certain period. Theoretically, compression should occur suddenly in order to depict the relaxation behavior (Mohsenin, 1986). However, infinite loading rate is unfeasible, hence a loading rate as high as 500 mm/sec was used. The crosshead of the testing machine was stopped at 10% strain, which is just below the bioyield strain. The specimen was then allowed to relax for 120 seconds. The relaxation test code is included in Appendix (A.1). Load variation with time was recorded and analyzed later in the section of results and discussions.

5.3.2 The MT Firmness Test and The Bioyield Test

The bioyield test was developed to measure the bioyield point of apple tissue with minimum destruction. This test was designed to assess fruit flesh strength underneath the skin. Based on a preliminary study the Magness-Taylor firmness was presumed to correlate to the bioyield point.

5.3.2.1 The Magness-Taylor Firmness Test

Fruit firmness is an assessment of quality, which is influenced by cell turgor pressure, cell wall strength, and intercellular cohesion.

Magness-Taylor firmness was measured by an 11.1 mm (7/16 inch) puncture probe (Ballauff Manufacturing Co., Laurel, MD.) as shown in Fig. 5.4. The probe was penetrated into a peeled apple to a 7.9 mm (5/16 inch) depth at a rate of 30 mm/min. The peak force during penetration was considered as the MT

firmness measurement of the fruit. This force was recorded in the computer connected to the Instron machine.



Fig. 5.4 The Magness-Taylor firmness test

5.3.2.2 The Bioyield Point Test

The bioyield point was detected by applying a specially designed probe against the intact fruit until a sudden drop of the load took place due to tissue failure under the contact area. The interaction of the probe with the fruit was comparable with that of the first stage of the Magness-Taylor test prior to flesh penetration, but it produced significantly less damage. The test must not result in fruit degrading, and bruise size must be within the allowance for Extra Fancy that stated in page 2.

The test was conducted at the apple equator. A doughnut shaped hard plastic seat was used to support the intact apple. The stem-calyx axis was positioned horizontally as shown in Fig. 5.1. The contact area with the seat was comparatively large such that the contact stresses were insignificant compared to that at the test point, which would eliminate any susceptible injury or bruise at the contact with the seat. The probe was programmed to move at constant rate of 30 mm/sec against the intact fruit until a sudden drop in load was detected (Fig. 5.7). As can be seen in the programming code for the test (Appendix A.2) the test was terminated as the instantaneous load dropped by 0.01%, at this instant the probe was stopped and no further penetration is allowed as shown in the case of Fig. 4.2. The load drop was due to tissue failure at the bioyield point, which is the peak point on the F-D curve. An audible crunchy signal was detected due to tissue micro-failure. The program recorded the peak load, the displacement at the peak load, the compression energy to peak load and the least square modulus

in a preset loading range. The test of every fruit was repeated for each of the six probes.

5.3.2.3 The Mechanical Probes

The FE modeling of the probe-apple contact has designated certain features that should be considered so as to produce a quasi-uniform contact stress distribution. The probe consisted of cylindrical steel rod with elastic rubber tip glued at the flat end. The finite element study indicated that the rubber elastic modulus should be less than two times that of apple material. The rubber tip should be greater than 2 mm (0.08 inch) in thickness, and the outer edge of the rubber should be sharp. Concerning the uniformity of the contact stress, the diameter of the probe was not a parameter, but it has crucial influence on the volume of the generated bruise. A larger probe diameter and small size fruit enhance the flat plate effect prior to the developing of full contact with the skin. Smaller probe reduces the effect of apple curvature. It has a higher perimeter to area ratio, which tends to increase the effect of skin strength. The volume of the bruise can express the degree of destructiveness.

Six probes were constructed using rubber pieces of two thickness to diameter ratios (t/d) on the tip of three probe sizes (d=1/4, 3/8 and 7/16 inch). These sizes were referred to as *small*, *medium* and *large* respectively. Rubber pieces were cut into cylindrical shapes and bonded firmly with a glue to the steel probe-end. Based on the t/d ratio the probes were classified into two groups, the group with t/d=1/2 was termed as *thick*, whereas the *thin* group had t/d=1/4. The

names of the probes were abbreviated by using the initial letter of the size name and the last letter of the group (since the two groups start with the same initials). For example, the SK-probe stands for the *small-thick* probe. The dimensions and abbreviations of the probes are shown in table 5.1 and Fig. 5.5.

Table 5.1 Dimensions and abbreviations of the probes. The 3rd and 4th columns contain the thick and thin groups, respectively. The probe abbreviation is indicated under the thickness

Size	Probe Diameter d (inch)	t/d=1/2 Thickness t (mm)	t/d=1/4 Thickness t (mm)
Small	1/4	3.18 SK	1.59 SN
Medium	3/8	4.76 MK	2.38 MN
Large	7/16	5.56 LK	2.78 LN

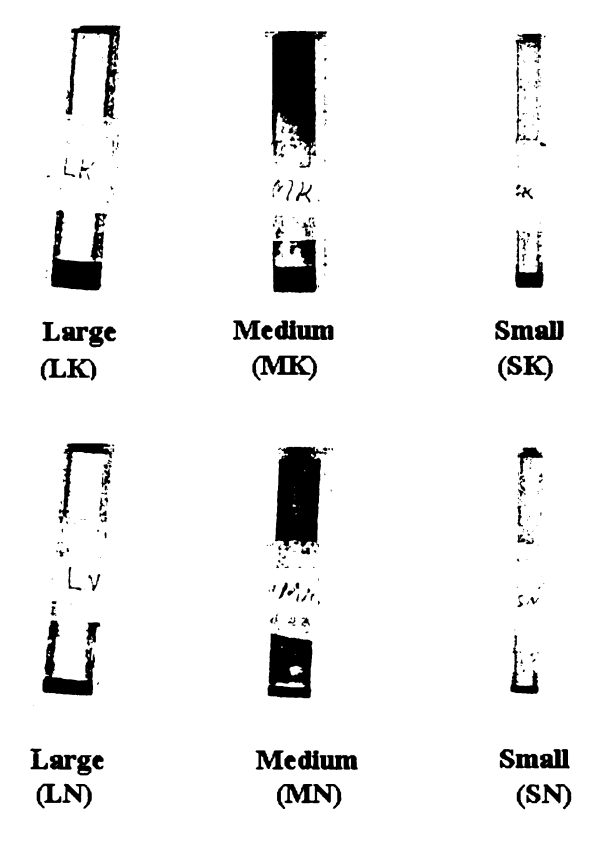
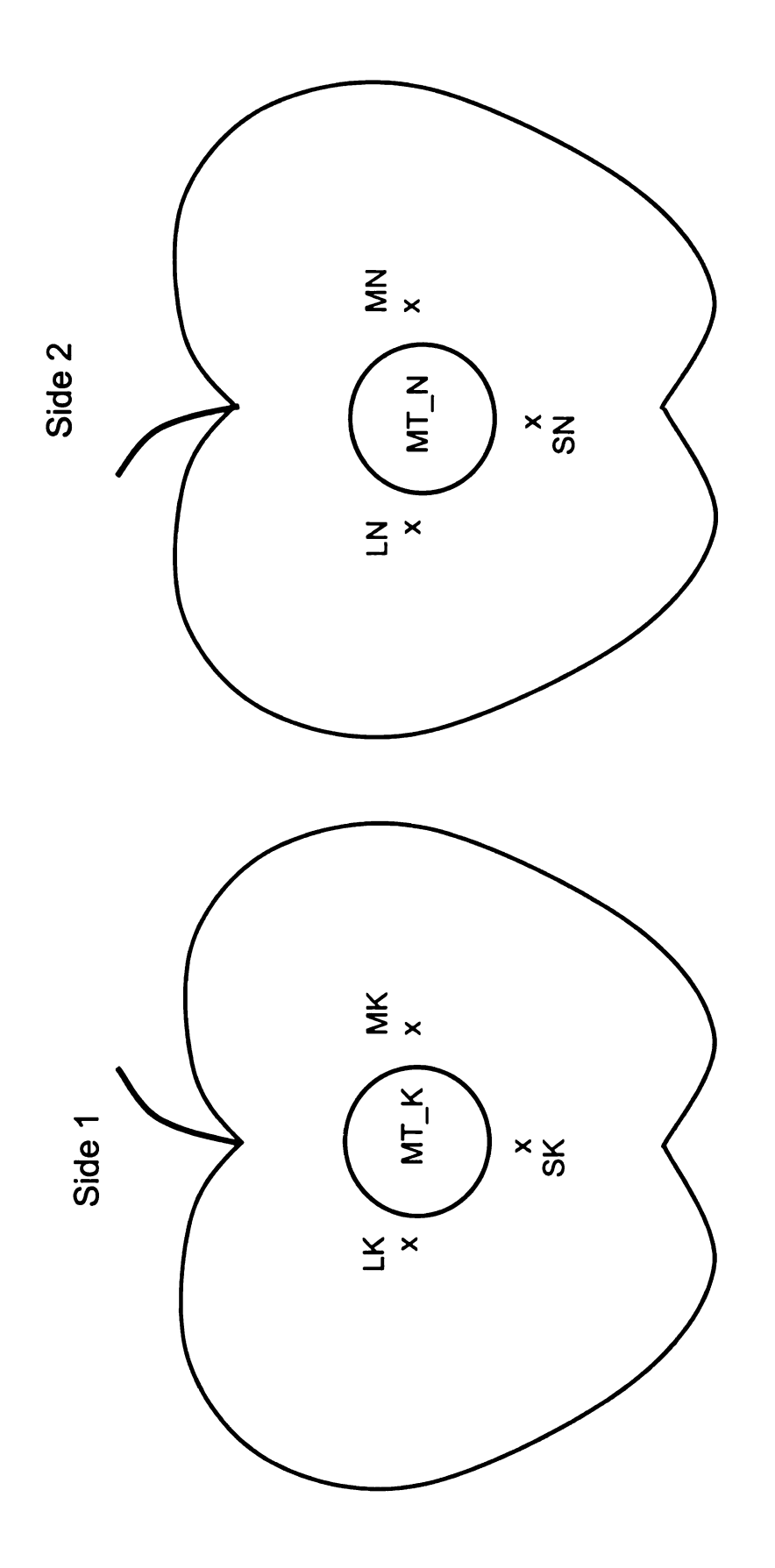


Fig. 5.5 The mechanical probes used in the bioyield test; the thick group is shown in the top row and the thin group in the bottom row

5.3.3 Testing Procedure

Each of the six probes was used to detect the bioyield point of every individual fruit successively. Two opposite sites on the equator of the fruit were selected for the MT puncture test. Adjacent to each MT site, three spots marked by (x) signs - about ½ inch apart - were assigned for the bioyield tests of a set of three probes as shown in Fig. 5.6. The MT firmness was measured twice for two reasons. Firstly, to estimate the variation of firmness measurements within the individual fruits. And secondly, to eliminate the effect of this variation by comparing the bioyield measurement and the firmness measurement that were conducted at the same side. All the bioyield tests were made prior to firmness measurement so as to eliminate the peeling and puncture effects on the bioyield point measurement.

A total of 640 apple samples of four varieties (160 Golden Delicious, 160 Red Delicious, 160 Gala, and 160 Fuji) were tested. A set of 40 apples was examined per day in February and March 2001. These apples were harvested in late September or early October from Michigan State University Clarksville Horticultural Experiment Station in Clarksville, MI, and were stored in controlled atmosphere conditions. Prior to testing, the fruits were left about 24 hours to equilibrate to room temperature, except one set of each Red Delicious and Fuji varieties that had been kept at room conditions for four days to allow for fruit softening.



the MT tests, and the bioyield tests are conducted at the spots marked by (x) using the probe abbreviated next to the mark Fig. 5.6 Locations of the MT firmness and bioyield tests at opposite sides of the fruit. The circular areas are reserved for

5.4 Results and Discussion

5.4.1 Typical Bioyield Test

Fig. 5.7 shows a typical force-deformation curve of a Golden Delicious apple tested with the small-thick (SK) probe. At the beginning of contact, the curve is concave upward due to the increasing contact area prior to full contact with the skin. Once the full contact was achieved, in this case, at about 0.2 mm probe deformation, a linear relationship proceeded up to a well-defined bioyield point (B.Y.). The coordinates of the bioyield point are (Xy, Fy), where Xy and Fy are the probe displacement and load, respectively. As the applied load reaches the bioyield point, a sharp drop in the applied force can be observed, accompanied by an audible crunchy sound due to bulk failure of the tissue beneath the contact area.

Since the force-deformation curve is highly linear with a correlation coefficient of r>0.99, the slope and the energy of compression can be approximated by the quotient and half the product of the force and deformation at the bioyield, respectively. The slope of the curve (Sy = Fy/Xy) is related to the combined elastic modulus of the fruit and the probe materials. The nominal bioyield strength was estimated by dividing the force at the bioyield point (Fy) by the cross-sectional area of the probe. The bioyield energy (toughness) on the other hand, is the work required to cause tissue failure. The bioyield energy can be integrated using the bioyield test code or approximated by the area under the force-deformation curve $(Ey=Fy\times Xy/2)$. Note that only a small fraction of this energy was stored in the rubber tip. In view of rubber as linear elastic material,

for the test shown in Fig. 5.7, the fraction of energy stored in the rubber tip constitutes about 23% of the total loading energy. The remaining energy was irreversibly consumed in apple tissue failure depicted as a permanent plastic distortion of the bruise.

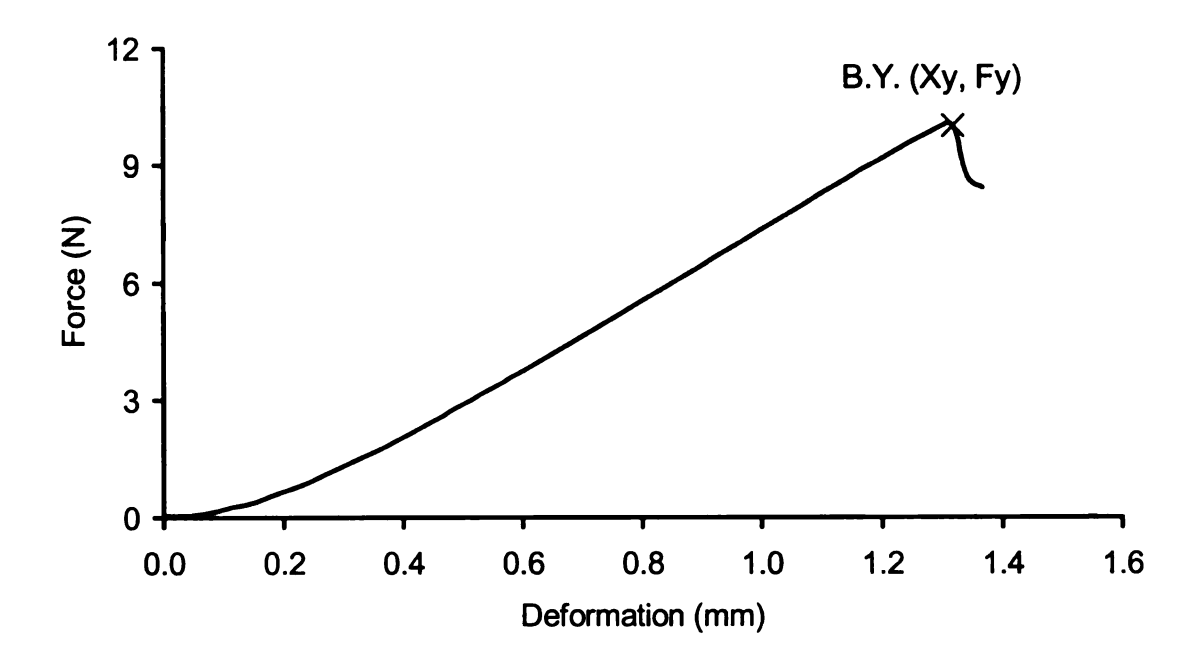


Fig. 5.7 Typical force-deformation relationship of the bioyield test generated by the small-thick probe

5.4.2 The Modulus of Elasticity

The slope of the stress-strain relationship in the linear elastic range estimates the apparent modulus of elasticity. A typical curve is plotted in Fig. 4.4 for the validation of the FE model against the experiment. The average value of the modulus of elasticity of apple flesh was 5.05 MPa (729.8 psi) with a standard deviation of 0.94 MPa (136 psi). This is comparable to 5.94 MPa (859 psi), the average of 16 values of the apparent elastic modulus as tabulated by Mohsenin (1986) from several studies for six apple varieties including: Delicious, Golden Delicious, McIntosh, Melba, Rome Beauty and Stayman, whose MT firmness ranges from 8-21 lb. In this study, a modulus of elasticity of 5.0 MPa was used for apple flesh material in the FE model.

5.4.3 The Stress Relaxation Function

The stress relaxation function describes the viscoelastic behavior of apple material. Due to the distinctive nature of the biological material, it couldn't be simulated by a specific model with fixed number of elements throughout the entire compression procedure (Peleg and Calzada, 1976). Therefore, the material characteristics in the neighborhood of the bioyield point were of major concern for simulating the bioyield process. The sample was strained to an extent just prior to the bioyield point where the viscoelastic pattern, which the material underwent would be as close as possible to that exhibited during the bioyield test.

Nevertheless, previous studies had shown that the generalized Maxwell model, which consists of a few simple Maxwell elements connected in parallel, could satisfactorily simulate the viscoelastic behavior of apple material.

The basic Maxwell element consists of a spring in series with a dashpot. Since the dashpot is unlimited in flow, the simple Maxwell element is characterized by a decaying stress that eventually converges to zero. However, in the real case, the stress in apple sample does not vanish completely. Therefore, a linear spring was introduced in parallel with the Maxwell model. This spring is manifested by a constant term in the relaxation function, which represents the stress at equilibrium. Fig. 5.8 shows the generalized Maxwell model composed of two simple Maxwell elements and the parallel spring that was used to represent the rheological behavior of apple flesh.

When a constant stress is applied, the model exhibits an instantaneous elastic response due to the three springs. The material shows limited creep when the stresses carried by the Maxwell elements vanish due to the flow of the viscous dashpots, but the parallel spring (E₃) limits the ultimate strain.

When the model is subjected to constant strain ε_0 , the stress relaxes with time. The spring E_3 maintains the equilibrium stress at value greater than zero. The stress relaxation function can be written as:

$$\sigma(t) = \varepsilon_0 \left(E_1 e^{-t/\tau_1} + E_2 e^{-t/\tau_2} + E_2 \right)$$
 (5.1)

Where:

 $\varepsilon_o \equiv$ the initial strain (mm/mm).

 $t \equiv time (sec).$

 E_1 , E_2 and $E_3 =$ the stiffness of springs.

 η_1 , $\eta_2 =$ the viscosity coefficients of the dashpots.

and $\tau_1=\eta_1/E_1,\,\tau_2=\eta_2/E_2\equiv$ the first and the second time constants.

The average stress for experimental data of the relaxation test of 20 apple specimens was computed at each time step. The data were best fitted to a two-term exponential function according to Eq. 5.1.

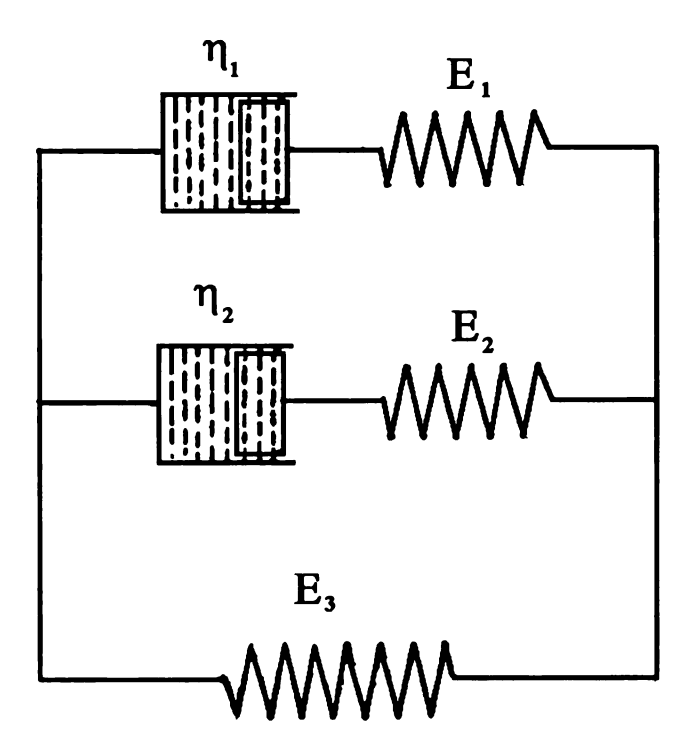


Fig. 5.8 The generalized Maxwell model of two simple elements

The constants of relaxation function for average apple material was approximated by:

$$\epsilon_0$$
=0.10
$$E_1$$
 = 0.488, E_2 = 0.590, and E_3 = 1.13 MPa.
$$\tau_1 = \eta_1/E_1$$
 = 2.27 sec, $\tau_2 = \eta_2/E_2$ = 45.6 sec.
$$\eta_1$$
=1.108, and η_2 =26.9 MPa.sec.

The uniaxial stress relaxation curve is shown in Fig. 5.9 for a time interval of 70 seconds. However, the bioyield test is accomplished within less than a 4 second interval. The high correlation coefficient between the model and experimental data (r=0.992) shows the accuracy of the generalized Maxwell model in representing the relaxation characteristics of apple material.

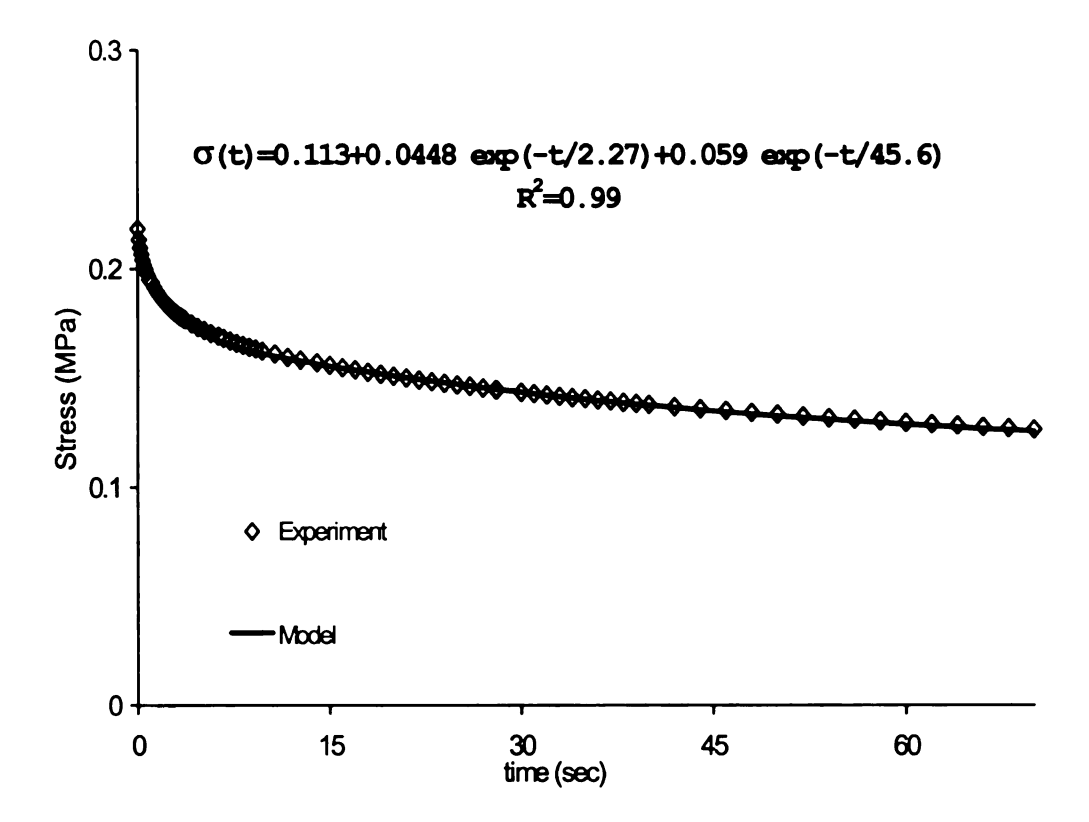


Fig. 5.9 The stress relaxation curve of apple material

5.4.4 The Bioyield Point Test and Firmness Prediction

The bioyield test resulted in a well-defined bioyield point for most of the test fruits. For probes with rubber tip thickness greater than 2 mm (all probes except the SN-probe), the percentage of samples that demonstrated a well-defined bioyield point from the first trial was 98%. Whereas, in the case of the SN-probe with rubber thickness of t=1.59mm (i.e. < 2 mm), the percentage decreased to 87%, the bioyield point was not measurable in 13% of the samples. In this case, the bioyielding of tissue had taken place, but the absence of a load drop was due to the gradual failure of the tissue cells within the contact area as a result of the non-uniform contact stress distribution. It can be deduced that the increase in force due to the progressive compression exceeded the decline in force due to cell failure.

The finite element investigation of the SN-probe indicated stress concentration at the probe outer edge; the thin rubber was inadequate to diminish the effect of the rigid die and generation of the quasi-uniform stress distribution. Therefore, the injury of fruit skin was observed in some samples when tested by the SN-probe. Concerning the completeness of data, when the bioyield point was not obtained from the first trial, the experiment was repeated at a spot of small radius of curvature so as to enhance the stress uniformity, which increase the tendency of bulk failure associated with a measurable bioyield point.

The load drop at the bioyield point was sharper for firm fruits, especially when a large cross-sectional probe was used.

Apple fruit is sensitive to the environmental conditions during storage. Some apple varieties may become mealy after a period of cool storage. Fruit mealiness is physiologically associated with low bonding between neighboring cells and a high resistance to cell rupture (Harker and Hallett, 1992). In the bioyield experiment of the Red Delicious group that was exposed to room temperature for about 4 days, 12 samples out of 40 did not exhibit a well-defined bioyield point regardless of the testing probe. The apples had mealy texture, with a brownish color and off flavor. The force in the F-D curve of the mealy apples was increasing continuously without a noticeable drop because the cells under the contact area did not break, as no crunchy sound was detected. This can be explained by the increased air space and the loose intercellular pectin bonds that permit the glide of the individual cells alongside each other without cell wall rupture (Mohsenin, 1986).

Tu and De Baerdemaeker (1995) analyzed the mealiness in fruit texture using the texture profile analysis (TPA) in which a food piece is compressed twice to resemble the mouth mastication process. The raw apples showed no adhesion (peak negative force during the upper stroke of the first cycle). For ripe apples, stored for 7 days at room conditions, the adhesion and the internal air space increased, while the cohesion (ratio of compressive energy of the second cycle to that of the first cycle) was decreased.

On the contrary, the apples group from Fuji variety –well known for its high firmness range – that were exposed for four days to room conditions did not become mealy in texture nor underwent significant firmness decline.

Nevertheless, the cell turgor pressure was brought down due to water loss, causing the bioyield point to occur at a larger deformation. In fact, the increase in the interstitial air space enlarged the required strain necessary to raise the cell turgor pressure to the value that causes cell wall breakage. A similar turgor effect was observed also in potato tubers, such that "increasing turgor resulted in significantly decreasing failure strain and tissue toughness, increasing secant modulus, and a slight decrease in failure stress" according to Bajema et al. (1998). The decrease in turgidity also explains why fruit are more susceptible to bruising at harvest than after storage (Garcia et al., 1995).

5.4.4.1 Regression Analysis

Linear regression analysis was carried out between the measured Magness-Taylor firmness and four different variables evaluated at the bioyield point. Each variable was investigated as a potential parameter to predict the MT firmness. The variables were the force at the bioyield point (Fy), the deformation (Xy), the slope of the force-deformation curve (Sy), and the bioyield energy (Ey).

The experimental data corresponding to samples from the four apple varieties and the linear regression line are plotted on scatter diagrams against the MT firmness measurement. Regression analysis was repeated for each of the four variables as measured by each of the six probes. Each variable measurement was plotted against the MT firmness, which was measured on the same side (see Fig. 5.6).

In the regression model, the MT firmness was the effect or the response variable and the measurement at the bioyield point (Fy, Xy, Ey, or Sy) was the independent variable or predictor, with the bioyield force (Fy) as the independent variable, a simple linear regression model can be written as:

$$MT = a + b Fy ag{5.2}$$

The constant a indicates the intercept with the MT-axis and b is the slope of the straight line, which represents the predicted change of the MT firmness associated with a unit change of the force measurement (Fy). The least square method was used to find the estimates of the regression parameters of the best-fit regression line.

The coefficient of correlation between the MT firmness and the variable in concern is a measure of the closeness of the relationship to a straight-line model. It can be used as an index to express the accuracy of predicting the fruit firmness by measuring the bioyield point. The values of the correlation coefficient are tabulated in Table 5.2 for the six probes.

The force at the bioyield point (Fy) was well correlated with the MT firmness. The correlation coefficient was equal to or greater than 0.792 for any probe, which is relatively high compared to the other variables. The deformation at bioyield point (Xy) did not correlate well with the MT firmness measurement (r≤0.571). The lack of fit to a linear model was due to the deficiency of an obvious pattern, in such a way the data were highly scattered. Indeed, firmness is not the only parameter that specifies the deformation at bioyield point. Other unknown

causal parameters such as apple variety, irrigation schedule, date of harvest, and storage conditions may affect this value.

The slope of the F-D curve (Sy) and the compression energy (Ey) have somewhat lower correlation coefficients with the MT firmness. These correlation coefficients were less than that of the bioyield force (Fy) itself because of the inclusion of the modestly correlated variable "the deformation" in their expressions. The scatter diagrams and the best-fit trendlines for MT firmness measurement versus Fy are shown for the six probes in Fig.'s 5.10- 5.15, the figures includes the Mean Square of the Residual (MSR) from the regression line.

From Tables 5.1 and 5.2, it can be concluded that decreasing the diameter of the mechanical probe generally enhances the correlation between the MT firmness and the force (Fy). In addition, probes with large rubber thickness to diameter ratio (t/d=0.5) produced higher correlation than those with small ratio (t/d=0.25), which have identical diameters.

Table 5.2: The correlation coefficient (r) between the Magness-Taylor firmness and force, deformation, slope or energy at the bioyield point.

Probe	Force (Fy)	Deformation (Xy)	Slope (Sy)	Energy (Ey)
LK	0.803	0.526	0.753	0.708
MK	0.819	0.560	0.744	0.726
SK	0.828	0.571	0.733	0.740
LN	0.792	0.333	0.749	0.604
MN	0.801	0.309	0.746	0.610
SN	0.806	0.249	0.712	0.615

Experimental results indicated that the average value of deformation necessary to reach the bioyield point (Xy) increases by increasing the diameter of the probe or the thickness of the rubber (Fig. 5.19). This finding was also observed in the finite element study (Chapter 4). Furthermore, since failure originates at the entire area of contact, then regardless of the geometrical shape of the bruise, its volume (V) is proportional to the probe area as well. Consequently, bruise volume is related to the cubic power of the probe diameter $(V \propto d^3)$. The proportionality of rubber deformation at a given stress with its thickness explains the increase of the gross deformation of the probe for the thick set of probes. In addition, applying a small probe for bioyield point detection reduces the curvature effect; therefore, a small diameter probe was highly suggested and seemed more promising for subsequent studies. Accordingly, the small-thick (SK)-probe was the optimal probe among the six probes evaluated. Detailed regression statistics of this probe are presented in the next section.

The slope of the MT-Fy relationship (Figs. 5.10-5.15) is proportional to the cross-sectional area of the probe. Hence, the bioyield stress rather than the bioyield force itself is the dominant factor in tissue bioyielding. Data points from the probes with three different diameters are clustered around a straight line on the scatter diagrams (Figs. 5.17 and 5.18) for the probes with thick and thin rubber, respectively. The slopes of the best-fit trendlines are 65.9 and 71.4 mm², and are significantly below the cross-sectional area of the standard MT puncture probe (96.9 mm²). This inconsistency between the values is a consequence of the deviations between the physics of MT firmness test from that of the bioyield

test in terms of the fruit-probe interaction. The following are some aspects of comparison between the bioyield test and the MT test that might explain the inconsistency of the two measurements:

- In the bioyield test the failure of the tissue under the skin is mostly
 caused by the normal compression stress, while in the firmness
 puncture test, failure is due to a combined effect of shear and
 compression stresses.
- 2. The MT firmness is defined as the maximum resistive force during the entire penetration course, whereas the bioyield measurement corresponds to the rupture of the first layer when the test is terminated.
- 3. The blunt end of the MT probe tends to lower the penetration resistance, while the lateral expansion of the rubber tip of the developed probe increases the effective contact area with fruit skin.
- 4. The anisotropy of apple material properties might contribute to this deviation. The cells immediately under the skin are of smaller size (<50μm), rounded shape, and randomly oriented. The cellular size gradually increases towards the fruit center, becoming radially elongated, and stacked in radial columns with radial air space channels in between the cells (Khan and Vincent, 1991). The local flesh firmness has a maximum value immediately under the skin, where the bioyield point test is conducted. This part is disregarded

in the MT puncture test since "peeled flesh" is considered, such that the MT test measures the firmness of the interior softer part.

5.4.4.2 The Small-Thick Probe

The small-thick probe (SK) has the highest potential for nondestructive firmness sensor because of its correlation with the MT firmness. Additionally, it was the least destructive and the most reliable probe for detecting the bioyield point.

The correlation coefficient of the measured bioyield force with the MT firmness was 0.828 (Fig. 5.9). When 2% outlier data points were neglected, the correlation coefficient was improved to 0.853 (Fig. 5.20). The neglected outlier data points with maximum standardized residuals have the highest attenuation on the correlation coefficient. The standardized residuals of the neglected outlier data were greater than 2.56. This correlation was considerably satisfactory in comparison with the ultimate limit that can be anticipated. The ultimate limit corresponds to the correlation of the MT firmness with itself as measured on opposite sides of the fruit. Experimental estimation of this limit was r=0.919 (Fig. 5.16).

The upper limit for the 99% confidence interval for probe displacement at the bioyield point was 1.8 mm, hence using the loading rate of 0.5 mm/s, the bioyield testing can be completed within 3.6 seconds. this is relatively slow compared with the required grading speed in the fruit industry.

The regression analysis resulted in a very small p-value (p \approx 0). The 95% confidence intervals for the slope and the intercept were 2.007<b<2.209 and

4.621<a<9.289, respectively. Fig. 5.20 indicates the 95% confidence and prediction intervals. The confidence interval (CI) is the narrow band about the fitted regression line which specifies the range of the population *mean* of all firmness values corresponding to a given value of the bioyield force measurement. The prediction interval (PI), on the other hand, is the wide band about the fitted regression line, which determines the range of firmness corresponding to an *individual* measurement of the bioyield force (MINITAB, 1994).

The repeatability of the bioyield test is tested by relating the measurements of the two probes that have the highest correlation with the MT firmness, because two measurements of the same probe are not available. Fig. 5.21 shows the correlation of the bioyield point measurements by the small-thick and the medium-thick probes, the correlation coefficient (r=0.889) is very close to that of the MT firmness correlation with itself shown in Fig. 5.16 (r=0.919). However, the value of the mean square of residual (MSR=8.0 N) which measures the scattering of the data points around the straight line was significantly less than that of the MT firmness measurements (MSR=38.1 N).



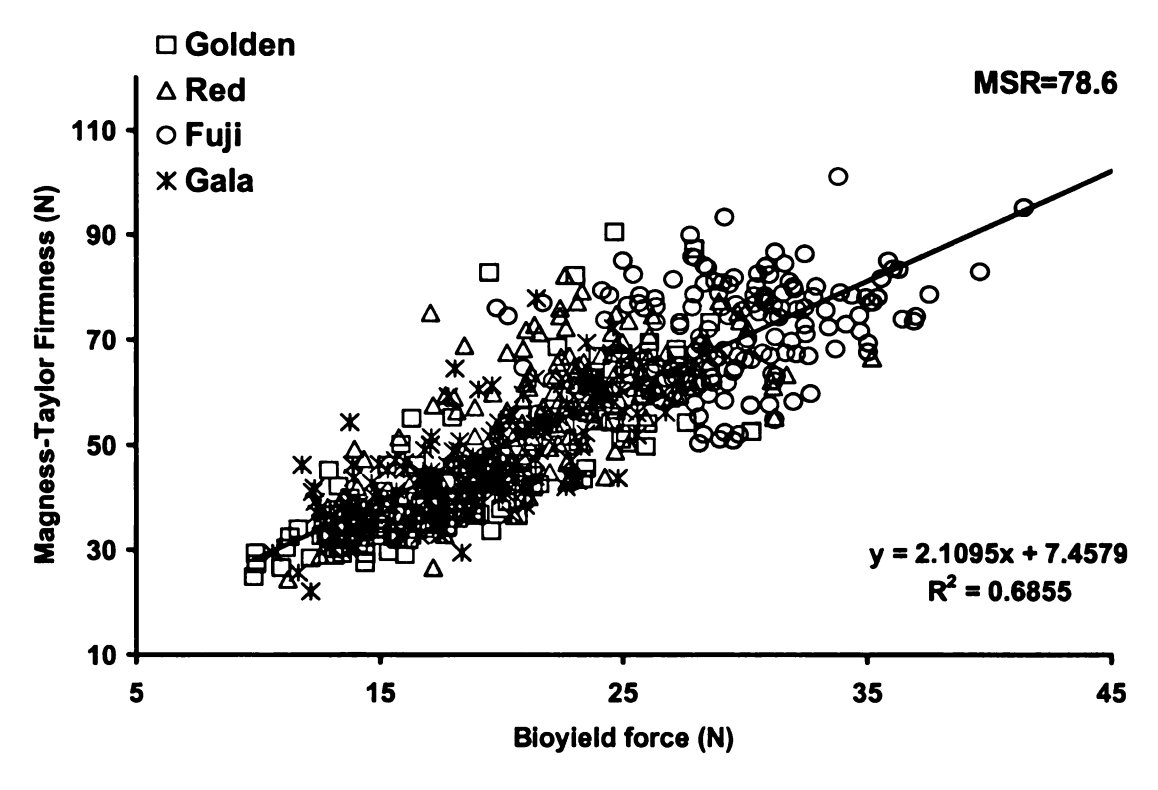


Fig. 5.10 Correlation of the Magness-Taylor firmness of four apple varieties with the force at the bioyield point measured by the small-thick probe (SK): diameter = 1/4", with rubber thickness to diameter ratio of ½

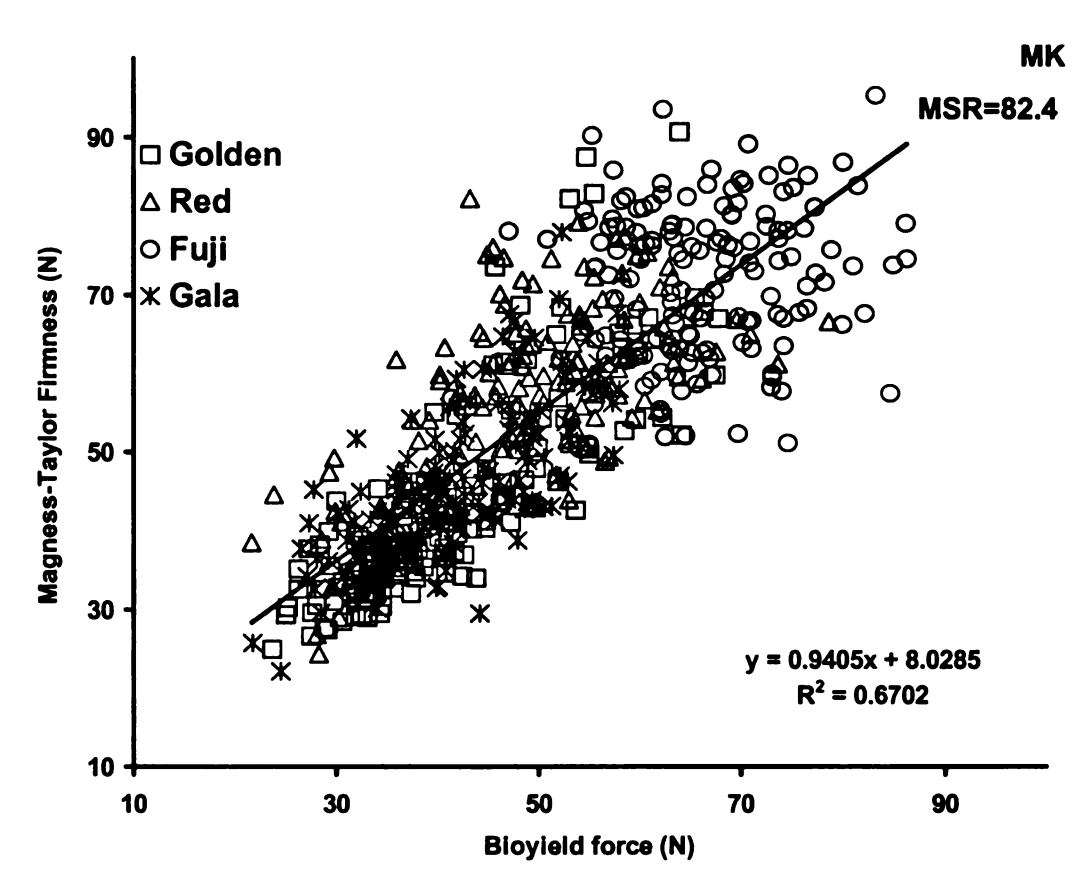
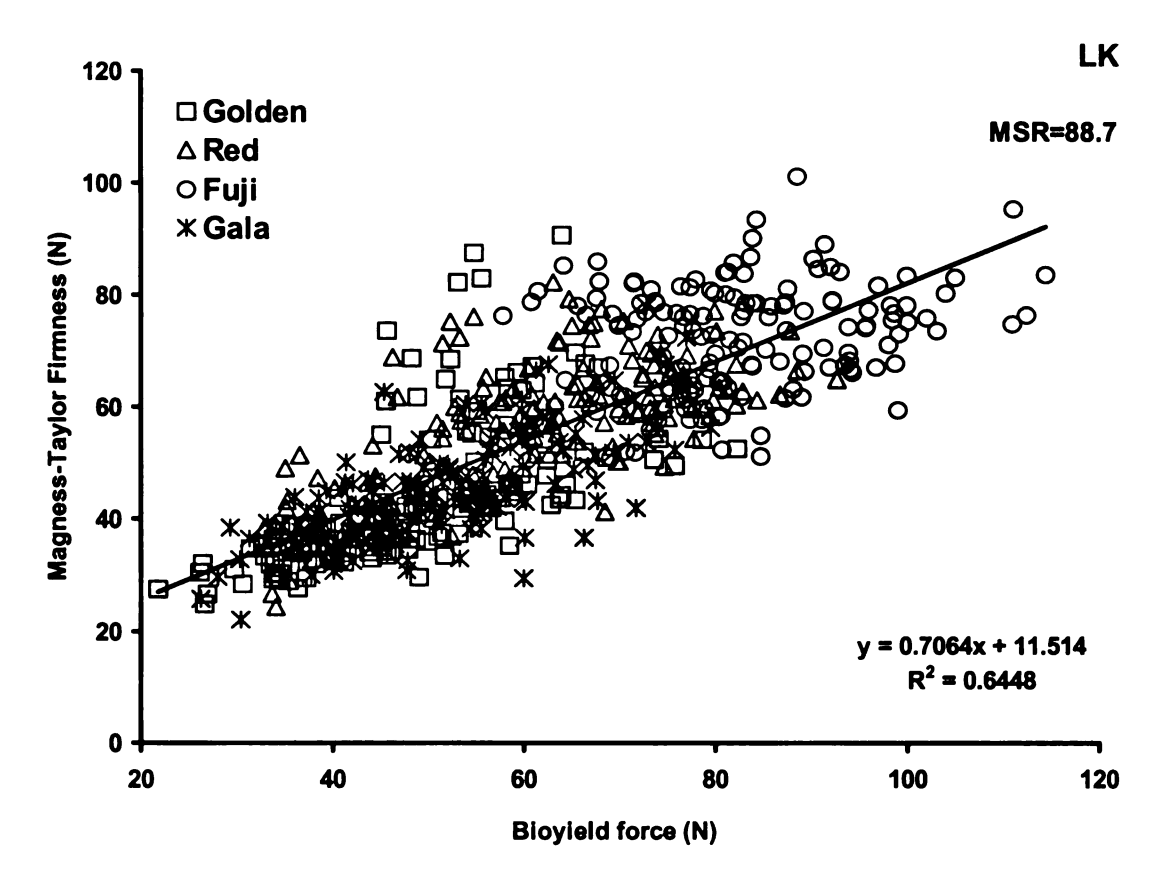


Fig. 5.11 Correlation of the Magness-Taylor firmness of four apple varieties with the force at the bioyield point measured by the medium-thick probe (MK): diameter = 3/8", with rubber thickness to diameter ratio of ½



A DECIMAL AND SECTION OF THE SECTION

Fig. 5.12 Correlation of the Magness-Taylor firmness of four apple varieties with the force at the bioyield point measured by the large-thick probe (LK): diameter = 7/16", with rubber thickness to diameter ratio of $\frac{1}{2}$



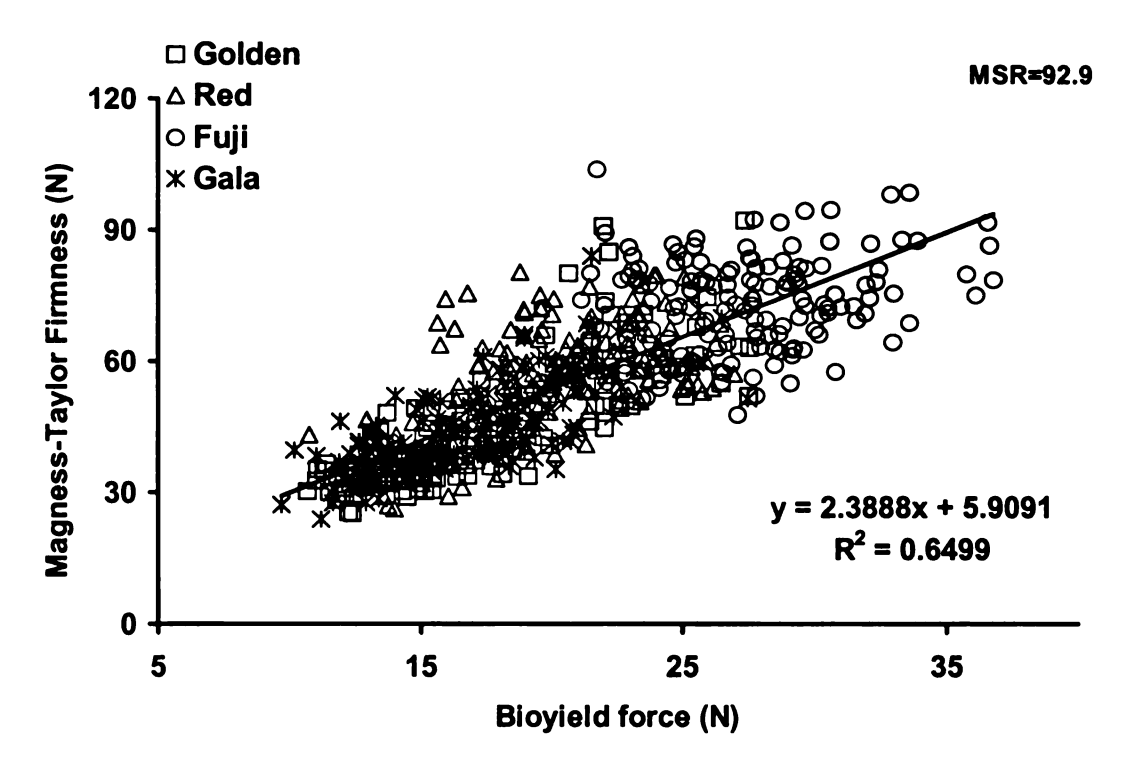


Fig. 5.13 Correlation of the Magness-Taylor firmness of four apple varieties with the force at the bioyield point measured by the small thin probe (SN): diameter = 1/4", with rubber thickness to diameter ratio of 1/4



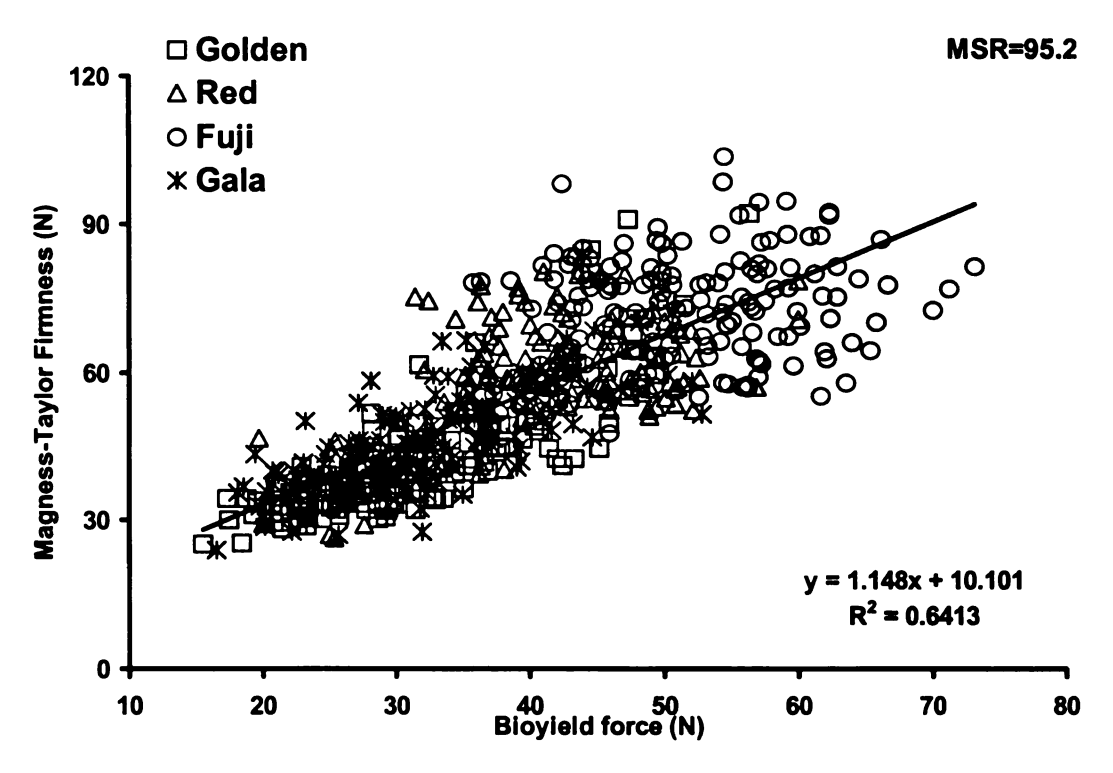


Fig. 5.14 Correlation of the Magness-Taylor firmness of four apple varieties with the force at the bioyield point measured by the medium-thin probe (MN): diameter = 3/8°, with rubber thickness to diameter ratio of $\frac{1}{4}$

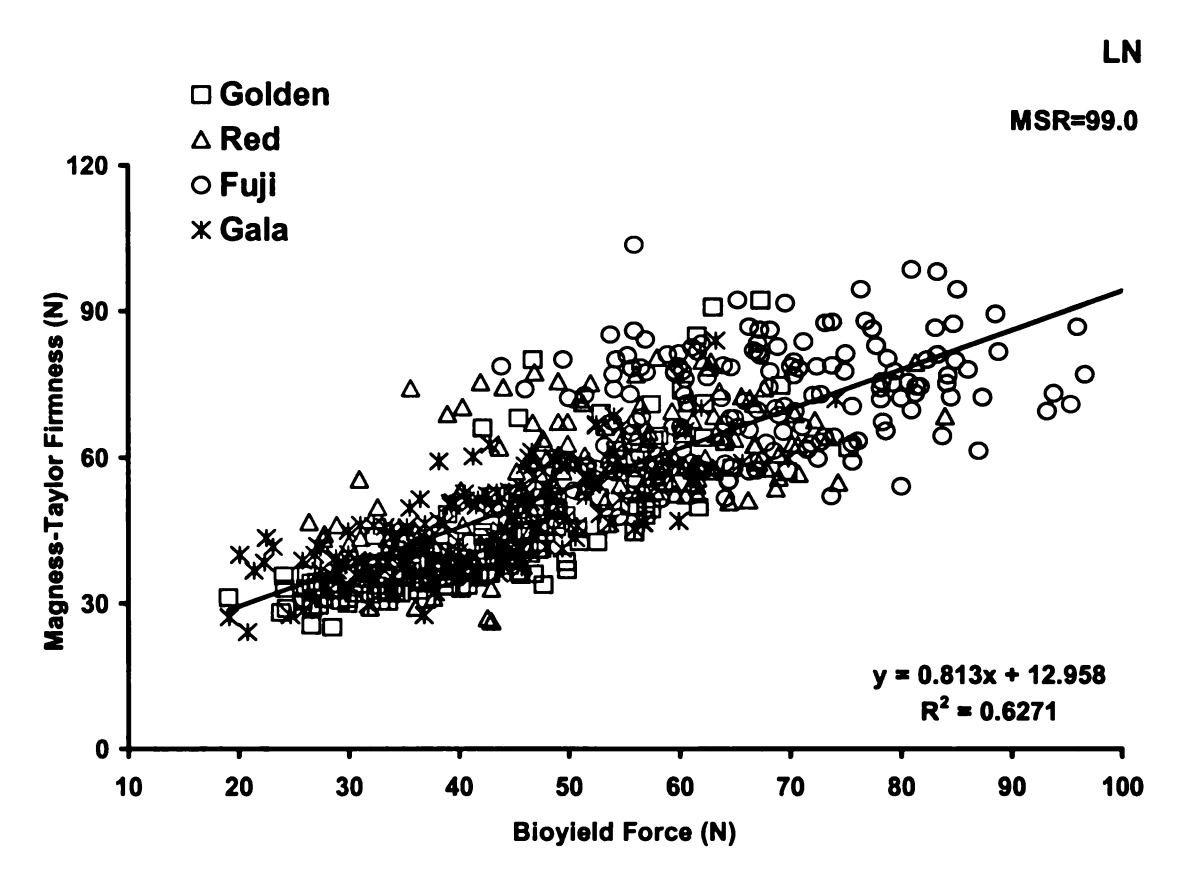


Fig. 5.15 Correlation of the Magness-Taylor firmness of four apple varieties with the force at the bioyield point measured by large-thin probe (LN): diameter = 7/16", with rubber thickness to diameter ratio of \(^1/4\)

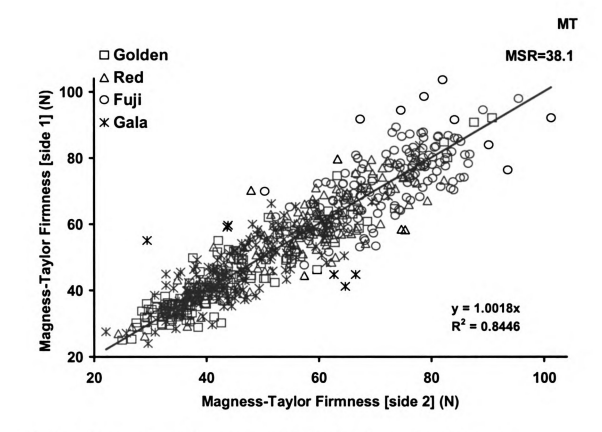


Fig. 5.16 Comparison of the Magness-Taylor firmness measurements at opposite sides of the fruit of four apple varieties

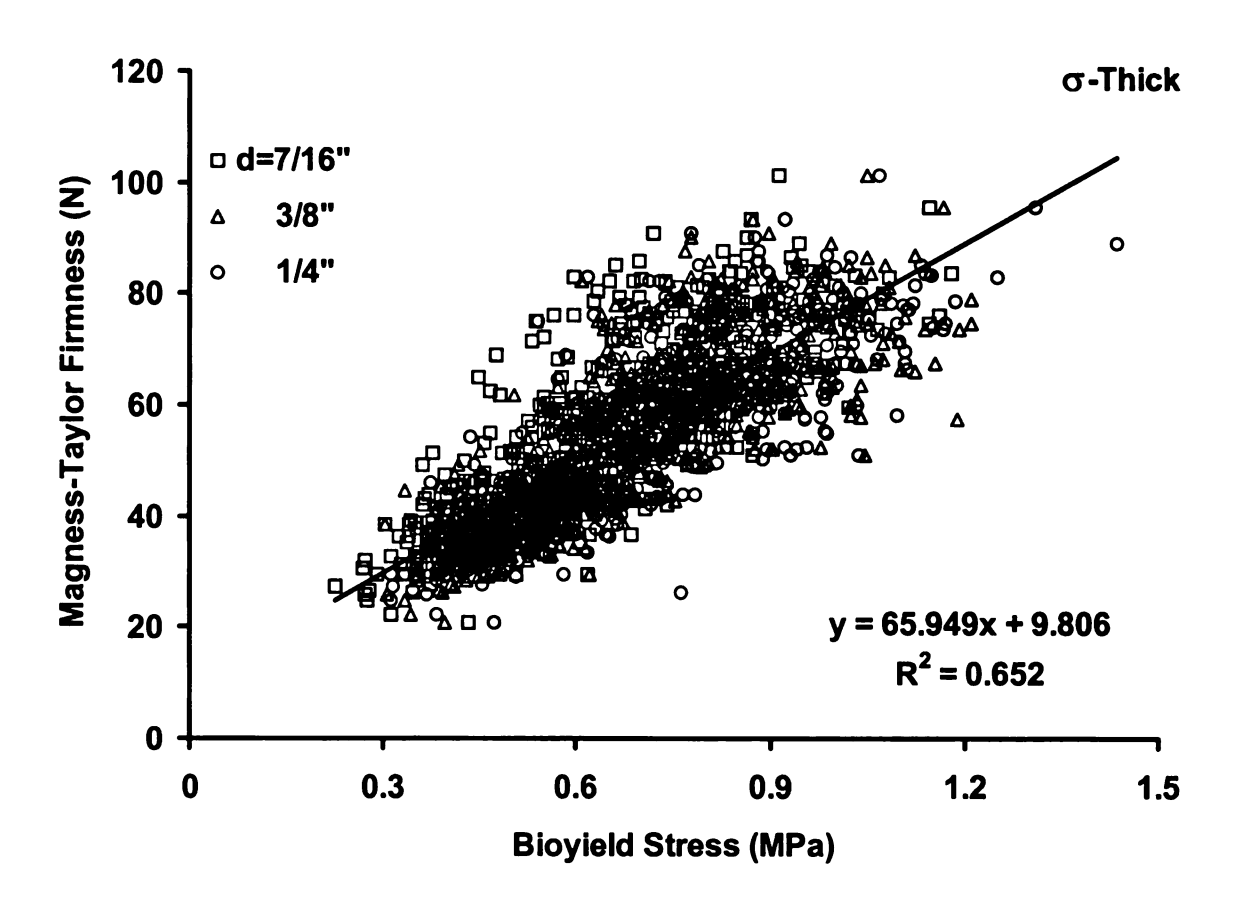


Fig. 5.17 Correlation of the Magness-Taylor firmness of four apple varieties with the stress at the bioyield point measured by three probe diameters (1/4, 3/8, and 7/16 inch), with the constant rubber thickness to diameter ratio of ½

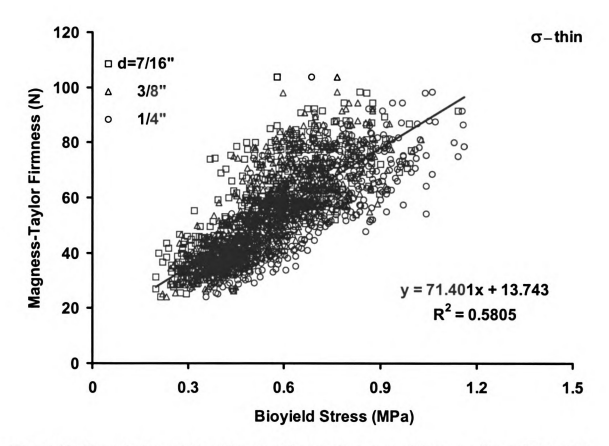


Fig. 5.18: Correlation of the Magness-Taylor firmness of four apple varieties with the stress at the bioyield point measured by three probe diameters (1/4, 3/8, and 7/16 inch), with constant rubber thickness to diameter ratio of 1/4

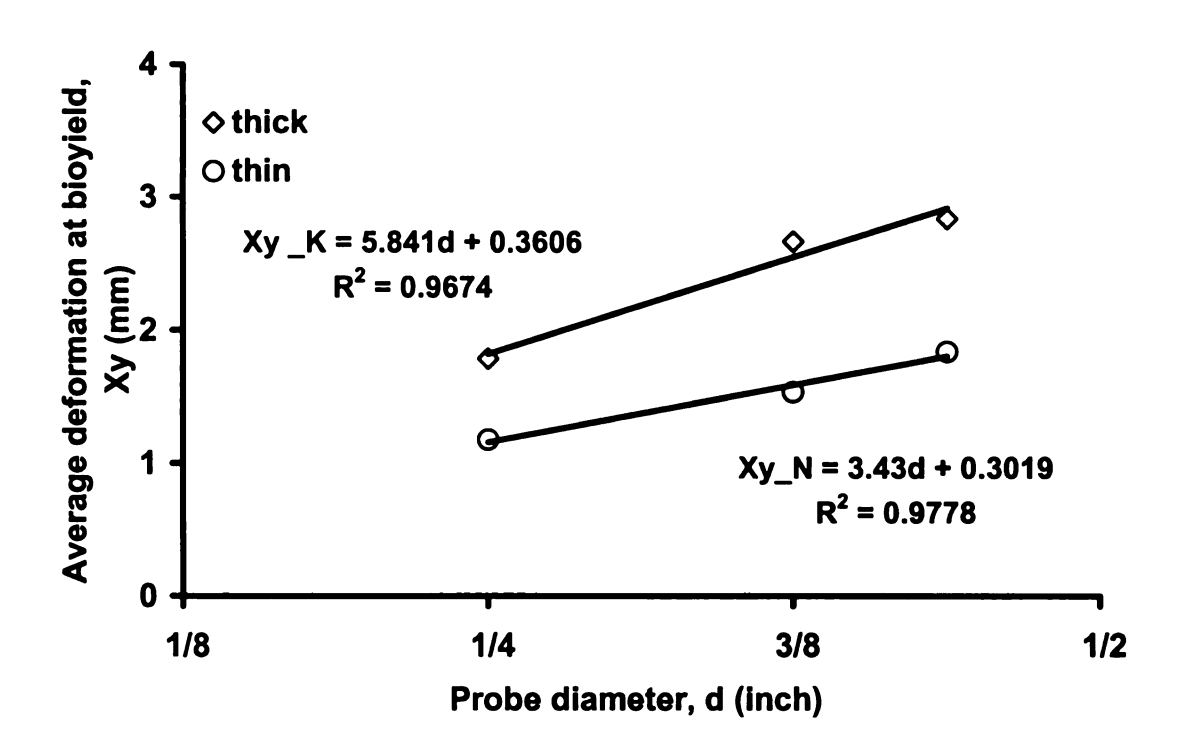


Fig. 5.19 Variation of the deformation required for tissue bioyield with the diameter of the probe for thin and thick rubber tips, t/d= 1/4 and 1/2, respectively

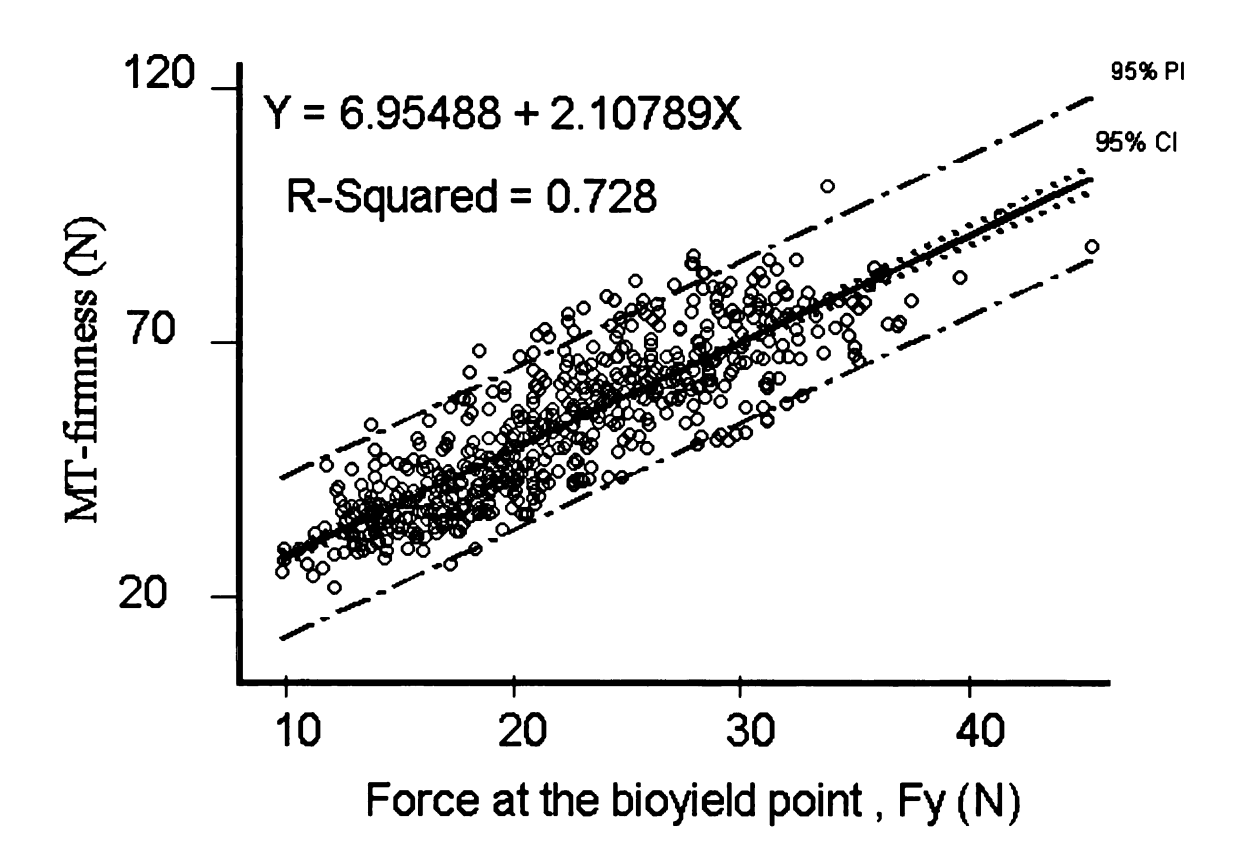


Fig. 5.20 Scatter plot of MT firmness versus the bioyield force measured by the small-thick SK-probe, showing the prediction interval (PI) and confidence interval (CI), based on 95% confidence level, after eliminating 2% outlier data with the highest standardized residuals

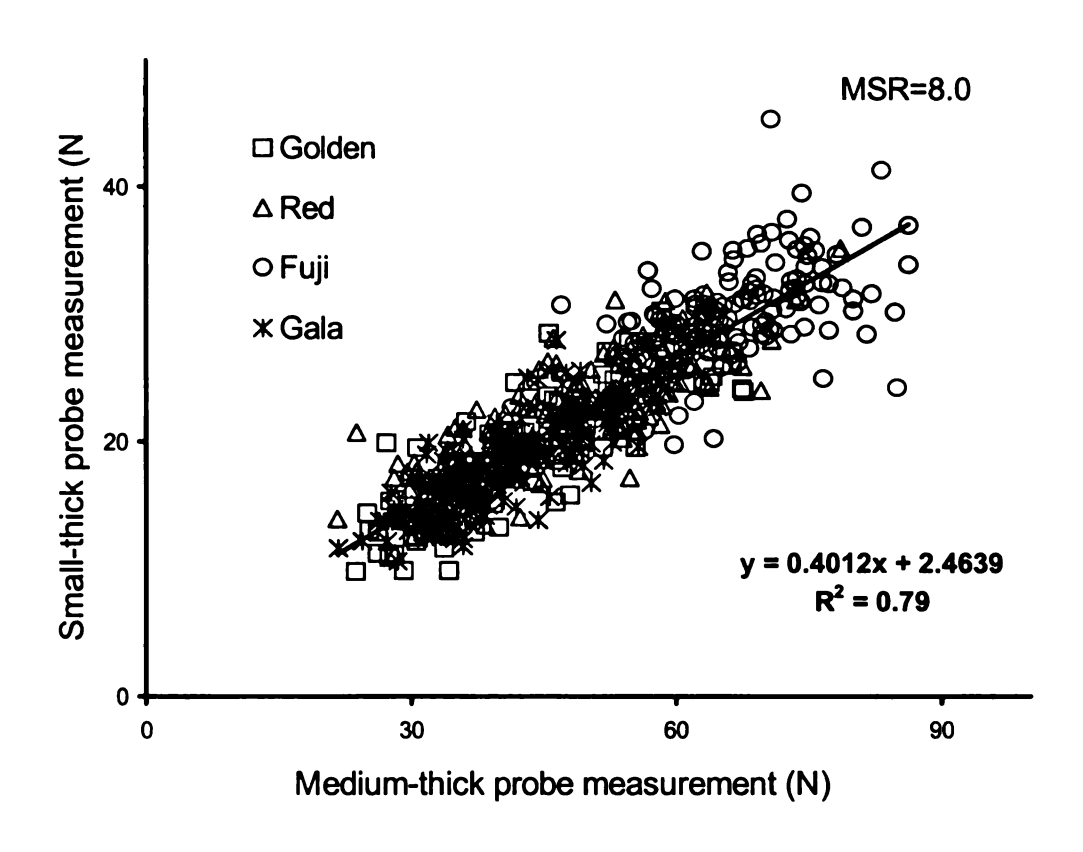


Fig. 5.21 Scatter plot of bioyield force measurements of the small-thick SK-probe and the medium-thick MK-probe

5.5 Summary and Conclusions

The fundamental material properties including both elastic and viscoelastic properties were measured. A generalized Maxwell rheological model composed of two simple Maxwell elements was constructed to explain the viscoelastic relaxation characteristics of average apple material. These priorities were used in the finite element simulation to assist in designing mechanical probes.

Based on the finite element study, six probes were built with three sizes and two rubber tip thickness to diameter ratios. The probes were investigated for nondestructive bioyield point detection. As the testing probe pressed against the fruit skin at a constant rate of 30 mm/min the contact load increased linearly with probe extension since the contact area was constant. The probe was stopped at the bioyield point, where a sharp drop of the load was demonstrated.

The bioyield point was well-defined in a majority of the tested samples. The rubber tip creates a uniform contact stress distribution, causing simultaneous failure of apple tissue under the contact area. When a probe with small rubber thickness of less than 2 mm was used, the resultant non-uniform stress distribution caused skin injury at the outer edge with gradual tissue failure that might complicate the bioyield point detection. On the other hand, mealy fruit didn't exhibit well-defined bioyield regardless of the probe,

which may be attributed to the changes of cellular structure and its greater capability of resisting cell rupture.

The stress at the bioyield point (or the force for a specific probe size) provided the best estimator of the Magness-Taylor firmness. In general, decreasing the probe diameter increased the correlation with firmness, which also reduced the effect of apple size on bioyield point measurement. Besides, probes with higher thickness to diameter ratio (t/d= ½) tended to have better firmness prediction, were more practical, and somewhat more accurate than those with lower thickness to diameter ratio ($t/d = \frac{1}{4}$). However, as the quasiuniform stress distribution is achieved, the correlation could not be improved further by increasing the thickness; the probe instability became a serious problem when too thick rubber is used. Moreover, the bruise volume was related to the cubic power of the probe diameter. For example, the bruise volume due to testing by a 1/4 inch diameter probe was less than one third that of 3/8 inch probe. These results and observations led to the conclusion that the small-thick (SK) probe with a diameter of ¼ inch and a rubber thickness to diameter ratio of t/d= ½ was the optimal design among the six probes evaluated. It produced a correlation coefficient with the MT firmness of r=0.853 after excluding only 2\% outlier data, in comparison with the ultimate correlation coefficient (r=0.919) of the MT firmness measurements on opposite sides of the fruit. The force at bioyield point occurs at an average probe displacement of 1.78 mm, including the deformation of the elastic rubber piece. Therefore, the proposed probe leaves only a tiny bruise, which is hardly noticeable and would not degrade the fruit. For sorting purposes, bruises may be completely avoided for the firm (good) apples by compressing up to a predetermined threshold value. Soft apples will bioyield below that value but the firm ones will not. Thus, firm fruits whose bioyield force are greater than the threshold value could be recognized without creating any bruise.

Since the standard deviation of the bioyield point measurement around the regression line was lower than that of the MT firmness, the of the bioyield point measurement was more repeatable than the MT firmness.

Chapter 6

Overall Summary, Conclusions and Recommendations

6.1 Summary

Fruit firmness is an important quality attribute of apples. It is the key to ensure consumer satisfaction, proper fruit storage, and shelf life. Therefore, it is considered a crucial parameter in the postharvest operations from the orchard to the consumer. Firmness is affected by many factors in the preharvest and postharvest stages and these effects are still uncertain. Determining and retaining apple fruit firmness are two major issues in the apple industry. The widely used Magness-Taylor firmness test requires penetration of a steel probe into the fruit flesh, which is destructive and cannot be used to inspect every individual fruit in a given lot that may have great variation in firmness.

The overall objective of the research was to develop a nondestructive sensor that is capable of estimating apple firmness. The estimate should correlate to the destructive Magness-Taylor measurement. Since firmness is a measure of apple tissue strength or integrity for resisting probe penetration, the bioyield strength of the fruit tissue appears to be a reasonable estimator for apple firmness.

Previous quasi-static studies were primarily based on evaluating the apparent modulus of elasticity and considered the elastic modulus to be a measure of firmness. Most studies had used a spherical rigid indenter that was characterized by non-uniform stress distribution and an unknown contact area. However, the elastic modulus does not correlate well with firmness.

A quasi-static method was used to detect the bioyield point by direct contact with apple skin. A rubber piece was bonded to the end of a circular steel probe, the deformability of rubber material produced a uniform contact stress distribution on the fruit.

The finite element simulation of the contact problem with the fruit suggested the use of rubber material with a modulus of elasticity of less than twice that of the apple material. A smaller size probe reduced the resulting bruise volume and the fruit curvature effect. A sharp edged probe eliminated the variability in the contact area. A rubber thickness greater than 2 mm was necessary for quasi-uniform contact stress distribution. The maximum critical strain and von Mises failure criteria were found to be useful in explaining the tissue failure.

The Instron Universal Testing Machine with a constant loading rate of 30 mm/min was used in all tests. The bioyield point test was conducted using six mechanical probes (3 diameters × 2 ratios of thickness to diameter). The probes were pressed against the fruit skin at a constant rate of deformation. The Instron was programmed to stop at the instant a small drop

in the contact force was detected. The force-deformation curve was linear due to the unchanging contact area after the full contact with skin was developed. The radial expansion of the rubber tip was neglected. The force at the bioyield point had a higher correlation coefficient with MT firmness measurement compared with the deformation, apparent modulus of elasticity, or compression energy necessary for tissue bioyielding. A rubber thickness below 2 mm was inadequate to detect the bioyield point due to the lack of uniform stress distribution. The study also found that mealy fruit did not exhibit tissue failure, so the bioyield phenomenon could not be measured regardless of the testing probe.

The small-thick probe of 1/4" in diameter and 1/8" tip thickness was concluded as the optimal probe for measuring the bioyield strength of the fruit tissue. The force at the bioyield point that was measured with this probe had the maximum correlation coefficient with the MT firmness measurement (r=0.853). The correlation coefficient of MT firmness measurements on opposite sides of the fruit was (r=0.919), which was considered the limit of the potential sensor.

6.2 Conclusions

The following conclusions can be drawn from this study:

1. The force at bioyield point was a satisfactory estimator of the firmness of apple fruit.

- 2. The bioyield point measurement was independent of the size of the fruit.
- 3. The skin of the fruit was an insignificant factor in the bioyield measurement.
- 4. The developed probe minimally destructive and did not degrade the fruit.
- 5. Bruise volume was proportional to the probe diameter raised to the power 3.
- 6. The effect of friction between the probe and the skin of the apple was negligible.
- 7. The critical strain and the von Mises stress were able to explain the failure of apple tissue underneath the contact area.
- 8. Increasing the rubber tip thickness enhanced the uniformity of the contact stress distribution. However, measuring instability due to misalignment became a serious problem when rubber thickness was equal to the probe diameter.

6.3 Recommendations

The following recommendations are suggested for further research:

- 1. For less bruise volume, a smaller probe size (diameter < 1/4 inch) with thickness to diameter ratio of 1/2 should be examined.
- 2. To meet the sorting rate requirement in the fruit industry, a higher loading rate should be investigated experimentally.
- 3. Development of a portable electronic hand held version of the probe would be a useful tool for detecting fruit firmness in the postharvest system.

References

- Ababneh, H.A., A. K. Srivastava, and R. Lu. 2000. Development of a Mechanical Probe for Nondestructive Apple Firmness Evaluation. *ASAE St. Joseph, MI.* Paper No. 006073.
- Abbott, J.A, J.S. Bachman, R. F. Childer J. V. Fitzgerald, and F. J. Matusik. 1968. Sonic techniques for measuring texture of fruit and vegetable. *Food Technology* 22: 635-646.
- Abbott, J. A. 1994. Firmness measurement of freshly harvested Delicious apples by sensory methods, sonic transmission, Magness-Taylor, and compression. J. American Soc. Hort. Sci. 119(3): 510-515.
- Abbott, J. A., Massie, D. R. Upchurch, B.L. and W.R. Hruschka. 1995. Nondestructive sonic firmness measurement of apples. *Transactions of the ASAE* 38(5): 1461-1466.
- Abbott, J.A, H. A. Affeldt, and L. A. Liljedahl. 1992. Firmness measurement of stored Delicious apples by sensory methods, Magness-Taylor, and sonic transmission. J. Am. Soc. Hort. Sci. 117(4): 590-595.
- Abbott, J. A., A. E. Watanda, and D. R. Massie. 1976. Effe-gi, Magness-Taylor, and Instron fruit pressure testing devices for apples, peaches and nectarines. J. Am. Soc. Hort. Sci. 101: 698-700.
- Abbott, J. A. and R. Lu. 1996. Anisotropic mechanical properties of apples. Transactions of the ASAE 39(4): 1451-1459.
- Abbott, J. A. and D. R. Massie. 1995. Nondestructive dynamic force / deformation measurement of Kiwifruit firmness. *Transactions of the ASAE* 38(6): 1809-1812.
- Armstrong, P. R., M. L. Stone, and G. H. Brusewitz. 1997. Peach firmness determination using two different nondestructive vibrational sensing instruments. *Transactions of the ASAE* 40(3): 699-703.
- Armstrong, P., H. R. Zapp, and G.K. Brown. 1990. Impulsive excitation of acoustic vibrations in apples for firmness determination. *Transactions of the ASAE* 33(4): 1353-1359.
- Bajema, R.W., G. M. Hyde, and A. L. Baritelle. 1998. Turgor and temperature effects on dynamic failure properties of potato tuber tissue. *Transactions of the ASAE* 41(3): 741-746.

- Bourne M.C. 1965. Studies of punch testing of apples. Food Technology 113-115.
- Bourne M. C. 1966. Measure of shear and compression components of puncture tests. *J. Food Sci.* 31: 282-291.
- Bourne, M.C. 1980. Texture evaluation of horticultural crops. *HortScience* 15(1): 51-57.
- Canada Extra Fancy Grade Standard. 2001. http://lois.justice.gc.ca/en/C-0.4/C.R.
 C.c.285/22317.html#rid-22381.
- Chen, H., and J. D. Baerdemacker. 1993. Effect of apple shape on acoustic measurements of firmness. J. Agric. Engng. Res. 56: 253-266.
- Chen, H., F. Duprat, M. Grotte, D. Loonis, and E. Pietri. 1996. Relationship of impact transmission wave to apple texture during ripening. *J. Texture studies* 27(2): 123-141.
- Chen, P., and Z. Sun. 1984. Critical strain criterion: pros and cons. *Transactions of the ASAE* 27(1): 278-281.
- Cherng, A. 1999. Approximation of force deformation relations using impact response data. ASAE St., MI. Paper No. 99-6004.
- Chowdhury, H. R. 1995. A study of blackspot bruising in potatoes. Ph.D. Thesis. *Michigan State University*, East Lansing, MI.
- Clevenger, Jr. J. T., and D. D. Humann. 1968. The behavior of apple skin under tensile loading. *Transactions of the ASAE* 11(1): 34-37.
- De Baerdemaeker, J. 1975. Experimental and numerical techniques related to the stress analysis of apples under static loads. Ph.D. Thesis. *Michigan State University*, East Lansing, MI.
- De Baerdemacker, J. and L. J. Segerlind. 1976. Determination of the viscoelastic properties of apple flesh. *Transactions of the ASAE* 19(2): 346-348, 353.
- Delwiche, M. J., H. Arevalo, and J. Mehlschau. 1996. Second generation impact force response fruit firmness sensor. *Transactions of the ASAE* 39(3): 1025-1033.
- Delwiche, M. J., T. McDonald, and S. V. Bowers. 1987. Determination of peach firmness by analysis of impact forces. *Transactions of the ASAE* 30(1): 249-254.

- Delwiche, M. J., S. Tang, and J. J. Mehlschau. 1989. An Impact force response of fruit firmness sorter. *Transactions of the ASAE* 32(1): 321-326.
- Dobrzanski, B. and R. Rybczynski. 1999. Stress-strain relationship for fruit firmness estimation. *Acta Hort*. 485: 117-123.
- Fekete, A. 1994. Firmness ranges of fruit and vegetables. ASAE St. Joseph, MI. Paper No. 94-6601.
- Finney, E. E. 1963. The viscoelastic behavior of the potato. Solanum Tubersom, under quasi-static loading. Ph.D. Thesis, *Michigan State University*, East Lansing, MI.
- Fridley, R. B. 1969. Firmness tester for fruit, U.S. Patent No. 3470737.
- Fridley, R. B., R. A. Bradley, J. W. Rumsey, and P. A. Adrin, 1968. Some aspects of elastic behavior of selected fruits. *Transactions of the ASAE* 11(1): 46-49.
- Fridley, R. B., P. Chen. J. J. Mehlschau, and L. C. Claypool. 1977. *Deformeter non-destructive maturity defector sorting device*, U.S. Patent No. 4061020.
- Garcia, J.L., M. Ruiz-Altisent, and P. Barreiro. 1995. Factors influencing mechanical properties and bruise susceptibility of apples and pears. J. Agric. Eng. London. 61(1): 11-18.
- Harker F.R and I.C. Hallett, 1992. Physiological changes associated with development of mealiness of apple fruit during cool storage. *HortScience*. 27 (12): 1291-1294.
- Harker, F. R., J. H. Maindonald, and P. J. Jackson. 1996. Penetrometer measurement of apple and kiwifruit firmness: Operator and instrument differences. J. American Soc. for Hort. Sci. 121(5): 927-936.
- Jeong, S. 1997. A rheological model of apple flesh failure during the Magness-Taylor puncture test. M.Sc. Thesis. *Michigan State University*, East Lansing, MI.
- Johnson, K.L. 1985. Contact Mechanics. Cambridge University Press. Cambridge.
- Khan, A. A., and J.F.V. Vincent. 1991. Bruising and splitting of apple fruit under uni-axial compression and the role of skin in preventing damage. *J. Texture Studies* 22 (3): 251-263.
- Krishnamachari, S. I. 1993. Applied stress analysis of plastics, a mechanical engineering approach. L. J. Broutman & Assoc. Ltd. Chicago, IL. USA.

- Lee, E. H. and J. R. M. Radok. 1960. The contact problem for viscoelastic bodies. Trans. of the ASME, J. Applied Mech. 27(9): 438-444.
- Magness, J. R. and G. F. Taylor. 1925. An improved type of pressure tester for the determination of fruit maturity. U.S. Dept. Agr. Cir. 350. 8pp.
- MARC Analysis Research Corporation. 2000. MARC user's manual. CA. USA.
- Mattus, G. E. 1965. Mechanical thumb tests of apple firmness. J. Am. Soc. Hort. Sci. 87:100-103.
- Mehlschau, J. J., P. Chen, L. L. Claypool, L.L. Fridley, R.B. 1981. A Deformeter for non-destructive maturity detection of pears. *Transactions of the ASAE* 24 (5): 1368-1371, 1375.
- Miles J., and G. E. Rehkugler. 1973. A failure criterion for apple flesh. *Transactions of the ASAE* 16: 1148-1153.
- MINITAB reference manual, release 10 for windows. 1994. *Minitab Inc.* State College, PA. USA.
- Mizrach, A., D. Nahir, and B. Ronen, 1992. Mechanical thumb sensor for fruit and vegetable sorting. *Transactions of the ASAE* 35 (1): 247-250.
- Mohsenin N. N. 1986. *Physical properties of plant and animal materials*. Gorden and Breach Sci. Publ., New York.
- Mohsenin. N. N., C. T. Morrow, and D. L. Tukey 1965. The "yield-point" non-destructive technique for predicting firmness of golden delicious apples. *Am. Soc. Hort. Sci.* 86:70.
- Peleg, M., L.G. Brito, and Y. Malevski. 1976. Compressive failure patterns of some juicy fruits. J. Food. Sci. 41(6): 1320-1324.
- Perry, J. S. 1977. A nondestructive firmness (NDF) Testing for fruit. *Transactions of the ASAE* 20(4): 762-767.
- Reddy, J. N. 1993. An introduction to the finite element method. McGraw-Hill, New York
- Rumsey, T. R., and R.B. Fridley. 1977. Analysis of viscoelastic contact stress in agricultural products using finite element method. *Transactions of the ASAE* 20(1): 162-167, 171.

- Schomer, H. A., and Olsen. 1962. A mechanical thump for determining firmness of apples. J. Am. Soc. Hort. Sci. 81: 61-66.
- Schomer, H. A., K. L. Olsen, and J. N. Yeatman. 1963. A mechanical thumb for measuring the firmness of fruits. U.S. Dept. Agr. Mkt Bul. No. 25: 1-4
- Segerlind L. J and I. D. Fabbro. 1978. A failure criterion for apple flesh. ASAE St. Joseph, MI. Paper No. 78-3556.
- Seymour G. B., J.E. Taylor, and G. A. Tucker 1993. *Biochemistry of fruit ripening*. Chapman & Hall, London.
- Sherif S. M. 1976. The quasi-static contact problem for nearly agricultural products. Ph.D. Thesis, *Michigan State University*, East Lansing, MI.
- Shewfelt R.L. and S. E. Prussia. 1992. Postharvest handling, a system approach. Academic Press, Inc. CA. USA.
- Shewfelt R. L. S. C. Myers, S. E. Prussia. J. L. Jordan. 1987. Quality of fresh market peaches within the postharvest handling system. *J. Food Sci.* 52: 361-364.
- Siyami, S., G. K. Brown, G. J. Burgess, J. B. Gerrish, B. R. Tennes, C. L. Burton, and H. R. Zapp. 1988. Apple impact bruise prediction models. *Transactions of the ASAE* 31(4): 1038-1046.
- Takao, H. and S. Ohmori. 1994. Development of device for nondestructive evaluation of fruit firmness. *JARQ* (Japan). 28(1): 36-43.
- Timm, E.J., P. R. Armstrong, G.K. Brown, and R.M. Beaudry. 1993. A portable instrument for measuring firmness of cherries and berries. *ASAE St. Joseph, MI*. Paper No. 93-6539.
- Timoshenko, S. and J. N. Goodier. 1951. *Theory of elasticity*. McGraw-Hill, New York.
- Tu K., J. De Baerdemaeker. 1995. Investigate apple mealy texture using instrumental methods. Agri-Food Quality, An Introdisciplinary Approach. The Royal Society of Chemistry. Cambridge, UK.204-207.
- Watkins, C. B., A. Leake, S. M. Hoggett and J. H. Bowen. 1995. Maturation and storage quality of six 'Golden Delicious' × 'Red Dougherty' apple selections. *New Zel. J. Crop Hort. Sci.* 23: 49-54.

- Wilkus S. 1980. Apple firmness tests and the penetrator shape choice for the measurement device (firmness-meter). Roczniki nauk roliczych, seria C. 74(3): 91-106.
- Wu, N. Q., M.J. Pitts, D. C. Davis, R. P. Cavalieri and S.R. Drake. 1994. Modeling mechanical behavior of apple with the finite element method. *ASAE St. Joseph, MI*. Paper no. 94-3585.
- USDA, 1976. Apples shipping point instructions. Inspectors guide for apple bruises at shipping point and market.
- Yakushiji, H., S. Ono, H. Takao and Y. Iba. 1995. Nondestructive measurement of fruit firmness with soft touch sensor in Japanese presimmon. *Bull. Tree Res. Stn.* 28: 39-50.

Appendices

Appendix A The Testing Codes

A.1 The Relaxation Testing Code

Batch Information
Batch descriptor 1 Relaxation test of cylindrical apple sample
Batch descriptor 2 for 120 second after compression to 0.25MPa
stress
Batch descriptor 3 24th April 2001
Gauge length 12.400 mm
Parameter File c:\hs\RELATN.CTP
Date Read 20 August 2001
Time Read 17:05:16
Specimen information required prior to test No
Specimen cross-sectional shape Circular
Diameter 20.0 mm
Number of sequence repetitions 1
Number of sequence repetitions Number of blocks defined 1
Number of markers in sequence 1
Sequence order
Marker 1 Block 1 : Relax
Block Number 1
Select block type Relaxation
Control mode Displacement
Limit type Strain
First level 0.00
Second level -0.10
Crosshead speed 500 mm/sec
End test/Break detect No action Dwell time 0.0 sec
Relaxation terminator Time
Relaxation time 120.0 sec
Transition to start level Yes
Crosshead action at end of block Crosshead return

Block number Is logging required for this block? Yes Should data be logged on basis of time? Yes Time increment 0.1 sec Should data be logged on basis of displacement? Should data be logged on basis of load? No Block number 1 Is a plot required for this block? Yes Realtime Plot Size Half Page Plot Grid Yes Yes Axes through Origin X axis Type Time Minimum 0.000 sec 120.000 sec Maximum Y axis **Stress** Type 0.000 MPa Minimum Maximum -0.250 MPa --- Results Selection |---Results Page 1 Column 1 **Peak Load** Column 2 **Peak Stress**

Strain at Peak Load

Specimen Area

Column 3 Column 4

A.2 The Bioyield Point Testing Code

! Batch	Information
•	est programming for bioyield point detection
	ubber tipped probe compresses apple until
bioyield point	ibboi appea probe compresses apple una
	mm/min bioviolding claimed when lead follo
· —	mm/min bioyielding claimed when load falls
by 0.01% and auto stop	IOOAIN OTD
Parameter File c:\hs\HU	
Date Read 10 July 200)1
Time Read 15:20:11	
	 nformation
Specimen information req	·
Specimen cross-sectional	l shape Circular
Diameter	11.11 mm [probe diameter]
	etup
Number of sequence repe	etitions 1
Number of blocks defined	1
Number of markers in sec	quence 1
Sequence order	
Marker 1	Block 1 : Preconditioning
	Test Control Data
Block Number	1
Select block type	Pre-conditioning
Control mode	Displacement
Crosshead speed	30.000 mm/min
End test/Break detect	Load falls by given % below peak load
Amount below neak load	

Dwell time	0.0 sec
Preload	-9.000 N
Anvil Height	8.00 mm
Upper limit given by:	Absolute Displacement
Displacement	6.00 mm
Number of Cycles	1
Action on Specimen Failure	Stop test
Below % of first cycle max load	1 %
Crosshead action at end of block	No action / Next block
	ging Selection ¦
Block number	1
Is logging required for this block?	Yes
Should data be logged on basis of	time? Yes
Time increment	0.05 sec
Should data be logged on basis of	displacement? No
Should data be logged on basis of	load? No
	up
Block number	1
Is a plot required for this block?	Yes
Realtime Plot Size	Half Page
Plot Grid	Ves

Appendix B The Bioyield Test Results

B.1 Golden Delicious

Test date: Feb. 12, 2001. Group: A Probe: MT_K MT_N MK LK LK MK SK LN MN MN SK LN SN SN Fy Ху Fy Χy Fy Ху Fy Χy Fy Ху F Ху (N) (N)No. (N) (mm) (N) (mm) (N) (mm) (N)(mm) (N)(mm) y(N)(mm) 25.0 25.1 26.6 2.03 23.7 28.5 1 1.97 1.32 1.68 15.5 1.29 12.4 9.8 1.17 2 33.9 35.7 41.4 2.22 34.1 1.87 14.9 1.27 24.1 1.39 24.1 1.13 12.5 0.84 3 35.5 33.7 39.6 2.22 29.4 2.17 14.0 1.42 32.5 1.47 25.8 1.19 12.3 0.86 4 34.9 37.6 2.14 34.6 2.17 34.4 15.0 1.42 27.0 1.39 33.5 1.54 14.6 0.97 5 34.0 32.7 36.8 1.94 33.7 2.32 11.7 1.19 32.9 1.37 21.4 1.22 0.96 11.0 6 29.1 27.5 30.3 21.8 1.54 1.86 9.9 0.99 25.7 28.6 15.2 1.14 1.64 1.06 7 34.6 32.0 47.9 2.39 40.8 2.27 1.54 30.4 17.8 1.34 27.7 1.19 13.8 0.82 8 29.0 30.3 34.4 2.12 31.9 1.97 16.0 1.55 32.8 1.44 24.4 1.24 10.7 0.91 9 40.4 42.5 42.9 2.39 44.7 2.67 19.0 1.59 42.7 1.71 42.0 1.46 19.7 1.29 10 33.2 36.3 34.1 40.2 2.04 2.12 13.9 1.24 28.4 1.32 33.0 1.27 18.1 1.08 32.7 2.29 2.39 11 34.7 37.9 34.4 13.9 1.31 36.7 1.74 27.0 1.59 12.3 1.09 12 34.3 36.2 36.0 2.05 36.2 2.22 31.9 1.54 23.3 16.7 1.04 14.9 1.44 1.09 13 41.3 32.0 40.2 2.34 30.8 47.0 2.59 19.0 1.64 1.79 22.0 1.22 12.6 0.97 14 29.0 32.1 35.3 1.91 33.0 2.05 13.1 1.27 34.6 1.46 25.5 1.14 13.2 0.97 15 37.9 38.2 48.1 2.47 40.6 2.31 17.7 1.54 35.7 1.72 29.1 1.39 16.7 1.02 42.6 30.3 62.9 36.2 2.24 33.5 22.6 16 3.14 21.6 1.59 1.56 1.17 14.3 0.94 26.9 17 26.6 25.4 1.72 27.5 1.99 10.9 1.21 26.6 1.05 12.2 0.89 1.37 18.4 18 37.0 30.5 42.6 2.52 29.1 45.4 2.44 19.1 1.49 1.34 23.4 1.22 15.4 1.06 19 29.4 36.0 2.02 32.4 1.95 42.8 1.29 33.8 13.4 1.24 1.52 23.0 15.3 1.17 20 30.2 34.3 34.0 1.77 25.2 1.64 13.1 1.21 36.4 1.60 18.7 1.14 15.0 0.99 21 39.7 40.7 58.0 2.67 41.9 2.54 20.9 1.72 44.4 1.68 26.5 1.30 17.7 1.16 22 34.9 32.0 45.3 2.57 31.8 2.06 16.8 1.49 33.6 1.59 22.8 1.47 12.3 0.96 23 32.2 2.29 33.2 2.24 0.99 34.1 37.3 13.0 1.32 26.5 1.53 26.2 1.76 14.2 24 32.2 32.1 41.2 2.32 31.4 2.49 12.9 1.29 34.2 1.63 31.4 1.59 13.8 1.19 25 32.1 29.5 26.4 1.54 37.4 2.31 15.7 1.47 27.2 1.42 22.1 1.12 12.6 1.04 30.7 36.9 26 33.6 30.7 51.6 2.60 1.74 19.6 1.54 1.49 29.2 1.24 14.9 1.02 27 27.6 28.9 36.3 28.8 1.32 24.3 23.3 1.34 14.5 0.89 1.89 1.77 14.4 1.27 28 39.7 36.2 45.1 2.29 36.4 2.17 15.4 1.36 31.2 1.44 29.7 1.34 16.0 0.97 29 36.5 35.8 48.7 2.39 34.9 2.04 17.4 1.54 34.9 1.49 25.8 1.27 15.1 1.09 30 30.5 33.4 26.2 28.1 2.02 11.1 1.17 33.9 1.44 20.7 1.12 11.7 1.09 1.79 31 35.0 34.4 44.1 2.26 32.0 2.19 1.37 36.7 1.44 1.01 13.0 0.92 14.5 17.3 32 33.8 33.6 40.8 2.22 31.6 2.04 14.5 1.34 38.6 1.78 26.3 1.22 16.4 1.03 33 34.8 33.0 42.1 2.24 37.7 2.09 1.62 24.1 1.22 28.6 1.59 15.0 0.99 17.0 34 32.0 30.0 38.2 2.02 32.0 1.87 16.2 1.44 29.8 1.31 17.4 1.04 11.5 0.87 35 32.7 33.0 40.2 2.24 35.7 2.29 14.9 1.47 26.0 1.62 25.1 1.37 14.0 1.12 36 33.4 29.5 40.0 2.29 32.7 2.17 13.9 26.5 1.27 21.3 1.14 12.1 0.92 1.45 37 32.5 35.1 2.09 28.4 40.1 1.82 15.5 1.46 31.3 1.44 30.5 1.26 11.3 0.84 38 33.9 35.9 39.4 2.02 37.8 2.02 1.42 41.8 1.69 1.39 1.22 15.1 31.1 14.5 39 33.5 33.4 45.6 2.42 33.8 2.02 14.4 1.39 38.9 1.57 26.3 1.39 15.5 1.13 40 32.8 32.8 39.6 2.02 30.1 1.89 12.6 1.19 27.2 1.39 23.5 14.2 0.96 1.17

Test date: Feb. 17, 2001. Group: B Probe: MT_K MT_N MK MK SK SK LK LK LN LN MN MN SN SN Xy Fy F Fy Ху Fy Ху Fy Xy Fy Ху Ху (N) No. (N)(N) (N) (mm) (N) (mm) (N)(N)<u>y(N)</u> (mm) (mm) (mm) (mm) 41 67.2 58.9 60.8 2.97 2.97 60.8 27.2 49.4 1.74 1.69 39.2 25.0 1.59 1.29 42 62.9 54.5 59.8 2.82 59.8 2.82 28.6 1.89 56.1 42.1 22.0 0.94 1.89 1.60 43 33.3 35.6 32.9 2.02 32.9 2.02 15.6 1.37 33.2 1.39 22.0 1.19 14.1 0.99 44 67.0 64.4 67.7 2.79 67.7 2.79 24.0 1.69 58.1 1.67 47.5 1.54 21.5 1.09 45 68.4 71.0 52.2 2.79 52.2 2.79 27.2 1.97 62.3 1.92 48.5 1.81 23.5 1.14 46 67.8 70.8 66.4 3.06 66.4 3.06 26.1 1.74 57.5 1.92 47.4 22.2 1.14 1.61 47 61.1 61.5 45.5 2.44 45.5 2.44 23.6 1.72 54.3 1.72 25.5 31.7 1.49 1.44 48 73.5 64.8 45.7 2.14 45.7 2.14 28.6 1.92 60.3 1.92 48.0 1.52 21.5 1.07 49 64.3 63.5 61.1 2.87 61.1 2.87 24.6 1.82 57.7 1.67 49.5 1.59 27.2 1.19 50 82.9 80.2 55.5 2.59 55.5 2.59 19.5 1.67 46.7 1.39 44.6 1.42 20.6 1.02 51 63.3 74.7 58.3 2.69 2.69 58.3 25.1 1.77 69.2 2.02 50.2 25.9 1.27 1.54 52 65.0 69.0 51.7 2.89 51.7 2.89 25.3 1.79 52.9 1.99 22.9 46.2 1.46 1.19 53 87.5 91.0 54.7 3.09 54.7 27.9 63.0 22.0 3.09 2.19 2.42 47.4 1.89 1.36 54 66.1 63.2 59.3 2.87 59.3 2.87 25.7 1.87 55.7 1.59 42.6 1.49 27.5 1.22 55 65.2 68.0 58.0 2.66 58.0 2.66 27.3 1.79 45.4 1.67 47.7 1.64 25.5 1.14 56 69.7 73.8 65.4 2.92 65.4 2.92 26.1 60.2 22.0 1.84 1.77 51.5 1.77 1.12 57 90.7 92.3 63.9 3.19 63.9 3.19 24.7 2.27 67.4 2.54 27.4 1.69 56.4 2.09 58 68.6 60.9 48.2 2.54 48.2 56.4 2.54 22.3 1.57 1.84 45.9 24.3 1.19 1.49 59 54.2 59.4 2.49 50.3 50.3 2.49 24.5 1.77 56.0 1.92 49.4 1.57 20.1 1.09 60 82.2 84.9 53.0 2.59 53.0 2.59 23.0 1.64 61.5 1.78 44.6 1.92 22.2 1.07 61 61.7 63.9 48.8 2.56 48.8 2.56 23.5 1.79 62.2 1.69 42.9 21.9 0.99 1.39 62 35.9 32.5 35.3 2.17 35.3 2.17 18.0 1.57 28.7 1.37 25.0 1.34 13.0 1.02 63 59.2 66.0 55.1 2.47 55.1 2.47 25.8 1.87 42.1 35.9 19.8 1.19 1.44 1.64 1.13 64 30.4 31.0 34.5 2.04 34.5 2.04 13.3 1.39 29.9 1.21 19.2 12.9 0.94 65 38.8 41.2 37.2 2.09 37.2 2.09 15.3 1.26 33.7 1.54 35.3 1.27 17.8 0.94 66 37.9 37.1 34.5 2.22 2.22 1.32 37.8 25.9 15.6 0.94 34.5 13.3 1.52 1.39 67 29.4 28.2 34.3 2.04 34.3 2.04 9.9 1.04 23.8 1.12 21.4 1.19 11.8 0.84 46.8 68 35.1 36.0 33.7 2.17 33.7 2.17 16.5 1.44 1.79 27.4 1.39 14.0 0.92 69 38.5 38.2 36.9 2.04 36.9 2.04 16.6 1.54 36.2 1.49 28.2 1.29 14.3 0.89 70 32.0 33.3 33.5 2.02 33.5 2.02 34.1 12.1 15.7 1.36 1.47 24.6 1.23 1.04 71 34.7 34.1 28.2 31.4 1.99 31.4 1.99 14.1 1.29 1.39 22.6 1.14 13.5 1.09 72 33.0 36.6 33.8 2.17 33.8 2.17 16.4 1.47 28.3 1.44 22.9 1.24 13.0 0.79 73 42.9 37.0 49.7 2.49 49.7 2.49 20.2 49.8 29.5 14.6 1.37 1.57 1.24 0.94 74 34.0 33.8 43.8 2.34 43.8 2.34 16.9 1.56 47.6 1.74 28.6 1.24 19.1 1.07 75 37.7 37.7 40.8 35.6 37.7 2.32 2.32 15.3 1.44 1.46 26.2 1.39 15.3 0.89 76 31.1 37.7 29.7 1.84 29.7 1.84 14.4 1.44 44.5 1.64 24.9 1.21 14.3 1.07 77 38.5 28.9 39.3 2.52 39.3 2.52 18.9 1.64 26.7 1.39 22.6 1.14 12.5 0.87 78 28.5 33.9 30.6 1.87 30.6 1.87 12.1 31.1 1.27 19.5 0.82 1.18 1.16 11.8 79 32.2 33.7 33.8 1.97 33.8 1.97 40.8 29.8 13.6 1.18 1.71 1.17 16.8 1.09

16.9

1.43

39.5

1.54

29.3

1.29

15.0

0.94

80

35.4

35.7

38.6

2.29

38.6

2.29

Test date: March 14, 2001. Group: C

Probe:	MT_K		LK	LK	MK	MK	SK	SK	LN	LN	MN	MN	SN	SN
			Fy	Ху	Fy	Ху	Fy	Ху	Fy	Ху	Fy	Ху	F	Ху
No.	(N)	(N)	(N)	(mm)	(N)	(mm)	(N)	(mm)	(N)	(mm)	(N)	(mm)	y(N)	(mm)
81	47.9	44.6	59.7	2.79	49.7	2.87	20.0	1.72	46.0	1.74	38.3	1.62	15.3	1.07
82	39.2	41.2	47.1	2.39	40.1	2.49	20.2	1.84	43.0	1.79	32.9	1.51	13.6	0.97
83	35.2	32.6	39.1	2.21	26.3	1.72	12.9	1.17	36.2	1.37	21.2	1.17	14.4	0.92
84	29.6	34.5	49.0	2.32	27.6	1.87	15.4	1.42	37.1	1.39	32.7	1.32	15.1	1.01
85	29.4	31.7	37.2	2.07	25.0	2.07	14.4	1.44	31.9	1.59	23.4	1.42	13.4	1.03
86	36.4	37.9	48.0	2.59	38.8	2.22	20.7	1.82	32.0	1.37	25.9	1.47	14.4	0.92
87	36.0	35.9	49.9	2.44	37.1	2.29	18.2	1.49	45.6	1.96	27.4	1.34	17.7	0.99
88	31.2	34.9	34.8	2.22	32.9	1.94	14.1	1.41	38.5	1.59	25.7	1.37	13.2	0.99
89	42.7	40.6	54.1	2.69	38.6	2.41	17.7	1.67	38.4	1.61	31.5	1.39	16.9	1.22
90	33.8	31.2	36.6	2.21	34.6	2.07	16.5	1.49	19.1	1.27	21.2	1.19	12.8	0.89
91	42.4	40.9	47.6	2.30	43.5	2.54	19.3	1.84	47.2	2.12	29.4	1.29	16.4	1.09
92	32.6	38.3	33.9	2.07	26.2	1.92	11.3	1.24	32.5	1.52	23.4	1.24	13.7	0.99
93	38.2	35.2	45.1	2.29	33.0	2.09	17.2	1.54	37.2	1.56	26.1	1.27	11.0	0.87
94	37.4	33.2	42.4	2.54	33.5	2.32	13.9	1.44	27.0	1.34	27.2	1.29	13.4	0.92
95	36.8	36.7	47.1	2.19	35.0	2.04	16.0	1.47	38.2	1.47	25.0	1.37	15.0	0.94
96	36.4	31.0	42.2	2.24	35.9	2.29	17.5	1.62	27.7	1.32	25.7	1.27	12.0	0.99
97	36.6	32.5	45.1	2.27	40.4	2.26	18.9	1.52	33.3	1.35	29.4	1.29	13.6	0.94
98	45.7	41.7	58.9	2.69	43.5	2.36	23.5	1.74	46.3	1.69	36.6	1.44	18.6	1.02
99	41.9	51.7	48.2	2.59	36.6	2.27	16.9	1.52	52.7	1.62	34.6	1.57	19.9	1.17
100	43.5	39.8	63.7	2.99	46.1	2.54	23.3	1.82	43.6	1.66	36.9	1.27	18.5	0.99
101	37.8	40.8	41.9	2.02	27.2	1.77	20.0	1.72	42.2	1.54	35.8	1.34	19.9	1.04
102	37.0	35.5	38.1	2.07	35.6	2.13	16.3	1.49	37.5	1.77	28.8	1.27	12.2	0.99
103	52.6	57.0	82.3	3.34	58.4	2.92	30.3	2.05	69.8	2.36	48.2	1.69	24.2	1.34
104	54.4	49.7	74.1	3.24	62.2	3.54	27.6	2.04	61.8	1.97	45.9	1.77	22.0	1.17
105	43.9	52.5	51.0	2.49	36.9	2.39	16.9	1.52	44.9	2.24	36.5	1.37	19.0	1.07
106	55.8	51.7 52.0	54.0	2.61	42.9	2.41	20.8	1.72	47.6	1.69	28.1	1.42	16.5	1.19
107	44.9	52.0	48.7	2.52	39.2	2.44	19.3	1.64	42.9 75.2	1.64	35.3	1.43	19.1	1.07
108	51.1	62.0 40.1	68.7	2.84	53.0	2.67	24.9	1.92	75.2	2.12	43.5	1.71	24.2	1.19 1.29
109	54.1	49.1	78.7	3.39	59.6	2.97	26.0	1.78	45.4 57.0	1.76 1.74	40.3 39.7	1.54 1.59	18.1 22.5	1.47
110	56.8 54.2	50.2	58.3	2.82	51.9 52.6	2.89	22.8 22.6	1.76	57.0 64.8	2.07	39.7 48.3	1.59	22.5 23.4	1.47
111	54.2	57.9 43.6	62.0 73.6	2.99 3.24	52.6 54.8	2.82 3.17	23.2	1.69 1.82	04.6 42.2	2.07 1.79	46.3 28.5	1.07	23.4 15.9	1.24
112 113	50.6	43.0 46.2	73,6		54.6 53.6	3.17 2.87	20.9	1.82	42.2 53.4	1.79	26.5 34.1	1.54 1.64	15.9 21.5	1.14
114	42.6 39.4	40. <i>2</i> 42.6	49.4 40.7	3.02 2.17	32.1	2.04	20.9 16.5	1.74	52.5	2.29	34.1 30.2	1.67	21.5 15.1	0.91
115	39.4 46.2	42.0 49.7	40.7 49.5	2.17	37.0	2.0 4 2.57	18.4	1.74	32.3 48.7	1.88	31.5	1.52	13.1 18.6	1.13
116	41.3	49.7 42.3	49.5 47.5	2.59	37.0 39.3	2.37 2.24	15.1	1.74	40.7 47.2	1.72	28.3	1.52	17.6	1.13
117	41.3 37.6	42.3 49.9	51.4	2.42	38.0	2.2 4 2.27	18.5	1.64	55.5	1.72	26.3 36.9	1.40	21.7	1.12
118	43.4	49.9 45.3	65.4	3.12	49.2	2.79	23.0	1.89	50.7	1.84	31.9	1.42	18.2	1.09
119	34.2	45.5 33.1	46.1	2.39	49.2 42.4	2.73	17.7	1.59	40.2	1.61	24.4	1.34	15.6	1.03
120	50.5	33.1 49.4	62.4	2.74	49.9	2.54	21.3	1.67	40.2 57.4	1.82	38.4	1.62	22.6	1.12
120	JV.J	73.4	UZ.4	4.14	77.7	2.04	41.3	1.07	37.4	1.02	30.4	1.02	22.0	1.14

Test date: March 26, 2001. Group: D Probe: MT_K MT_N MK MK SK LK SK LN LK LN MN MN SN SN Fy Ху F Ху Fy Fy Χy Fy Ху Fy Ху Ху No. (N) (N)(N) (mm) (N) (mm) (N)y(N)(N) (mm) (mm) (N) (mm) (mm) 121 36.6 36.5 43.4 3.27 33.8 2.64 13.1 1.76 45.4 2.44 30.6 1.97 11.4 1.59 122 41.0 38.4 50.6 2.66 40.8 2.57 18.6 1.62 49.7 2.04 30.2 1.37 18.1 1.29 123 45.1 52.0 55.3 2.50 37.2 2.17 12.9 1.42 48.9 1.77 34.4 1.37 27.5 1.99 124 38.8 45.7 2.24 32.4 2.20 1.59 35.8 16.7 48.8 1.87 33.0 1.39 15.4 1.04 125 43.8 42.3 40.5 2.47 30.0 2.04 17.2 1.59 41.1 1.71 35.7 1.47 16.9 1.21 41.1 2.29 126 36.8 51.0 3.81 37.5 3.29 17.5 47.4 2.99 42.4 2.62 17.4 1.77 127 35.3 35.2 32.7 2.32 34.4 2.29 12.7 1.62 41.9 28.1 1.64 1.57 14.1 1.17 128 39.7 37.2 44.2 2.24 35.1 2.14 17.3 1.44 37.6 23.0 1.39 1.14 17.1 1.04 35.2 37.7 58.5 2.09 18.2 129 2.54 36.2 16.9 1.67 40.4 1.52 31.4 1.37 1.19 36.3 130 33.0 44.1 3.84 31.6 2.97 12.8 1.81 42.5 2.94 35.1 2.64 1.77 16.1 131 50.2 43.7 54.8 2.69 48.0 2.63 15.8 1.59 32.3 1.34 31.4 1.64 16.1 1.02 132 54.7 51.9 56.3 41.8 2.44 3.09 24.7 2.12 48.5 2.04 36.7 1.74 25.1 2.27 133 45.7 49.1 39.9 2.37 53.6 2.64 18.0 1.77 49.0 1.62 33.0 1.47 1.01 16.0 134 37.0 42.4 45.5 2.49 36.6 2.54 15.9 1.49 34.7 1.77 29.9 1.29 13.2 0.97 135 52.1 42.5 66.3 2.96 64.2 3.09 25.1 1.97 50.9 1.81 43.3 1.59 19.7 1.17 136 40.2 38.6 44.6 2.56 43.4 2.59 17.8 1.72 43.2 1.79 32.7 1.49 14.4 1.24 137 42.1 55.0 56.6 2.77 43.5 2.32 21.3 1.77 58.6 1.92 47.4 1.72 26.5 1.29 43.7 138 47.9 62.3 2.85 44.9 2.72 19.6 1.64 45.7 1.57 37.5 1.49 13.1 0.99 139 44.3 49.7 63.9 3.02 46.8 2.57 21.3 1.74 56.1 1.98 35.5 1.52 23.0 1.34 1.04 140 41.8 46.4 53.4 41.5 2.42 17.0 1.54 44.4 30.1 2.84 1.49 1.47 16.5 141 41.1 37.4 49.7 2.64 47.2 2.66 1.72 18.9 41.0 1.57 21.0 1.04 15.4 1.02 43.9 38.2 142 46.2 58.3 3.04 2.32 16.5 1.69 38.2 1.77 31.4 1.54 13.4 1.11 48.1 2.86 143 46.2 60.3 2.92 46.4 15.3 1.77 56.9 1.92 37.0 1.39 17.9 1.14 43.8 44.6 57.6 2.76 46.4 2.54 19.0 1.69 42.1 41.4 1.04 144 1.64 1.67 16.3 55.3 2.84 48.8 37.8 145 49.5 54.6 3.14 47.2 18.0 1.77 2.17 1.64 19.3 1.36 146 49.7 48.1 75.8 3.39 55.0 2.82 25.9 1.97 49.7 1.79 40.7 1.49 18.9 1.12 45.3 47.1 54.6 2.74 34.0 2.09 18.4 1.67 48.7 1.87 30.2 1.34 17.8 1.13 147 148 43.1 36.7 45.1 2.34 36.5 2.34 17.7 1.72 35.6 1.69 27.7 1.39 14.8 1.09 48.2 28.2 149 55.1 45.0 2.33 39.6 2.72 16.3 1.44 39.0 1.67 1.24 13.7 1.16 46.7 2.94 150 61.4 55.6 53.2 3.01 23.2 2.01 56.1 1.69 35.2 1.59 17.3 1.24 151 38.2 37.0 45.6 2.57 28.3 2.09 14.1 1.49 40.3 1.74 27.8 1.42 14.4 1.34 152 44.4 44.9 55.5 2.99 42.6 2.72 37.8 19.0 1.81 46.4 1.74 1.64 16.0 1.17 49.2 2.87 48.6 2.87 20.9 35.8 153 46.5 58.6 1.77 43.1 1.86 1.49 14.8 1.14 154 39.9 35.9 42.7 2.59 29.2 2.02 13.8 1.47 26.1 1.32 26.6 1.37 12.9 1.04 155 39.3 49.2 2.54 43.0 49.6 3.17 19.1 1.63 43.1 1.69 24.8 1.17 17.8 1.04 37.3 36.6 53.1 2.39 41.7 2.44 18.8 1.64 38.2 1.39 21.4 1.09 16.0 1.02 156 59.7 46.4 74.5 3.27 67.5 24.2 2.03 47.3 39.5 157 3.42 1.74 1.42 19.1 1.12 158 42.1 40.9 48.4 2.44 40.0 2.54 13.3 1.44 45.1 1.59 22.9 1.09 15.8 1.02 159 46.2 44.6 64.4 2.94 51.8 2.87 19.5 1.64 55.9 1.84 45.2 1.54 22.0 1.14 2.58 160 44.4 39.2 56.1 2.67 46.6 20.3 1.77 44.4 1.44 34.4 1.42 18.6 1.22

B.2 Red Delicious

Test date: Feb. 8, 2001. Group: A Probe: MT_K MT_N LK LK MK MK SK SK LN LN MN MN SN SN Fy Ху Fy Xy Fy Χy Fy Ху Fy Ху F Xy (N) No. (N)(N) (mm) (N) (mm) (N)(mm) (N) (mm) (N)(mm) y(N)(mm) 49.6 57.7 2.62 42.1 1 51.6 2.48 20.2 1.59 67.9 1.97 41.5 1.49 20.9 1.17 2 51.6 54.0 62.6 2.79 48.2 2.49 18.9 48.7 33.6 18.4 0.92 1.56 1.64 1.35 3 61.3 55.8 84.4 3.41 63.4 3.06 69.0 24.6 1.87 1.84 45.7 1.48 19.5 1.12 4 60.3 59.3 82.2 3.27 53.6 2.87 26.1 46.6 1.89 1.62 40.0 1.60 18.3 0.89 5 57.1 62.8 73.5 3.00 57.9 2.71 23.1 1.67 70.2 2.34 49.6 1.69 24.1 1.16 6 61.3 53.7 75.7 3.13 45.5 2.66 26.4 2.09 45.7 1.64 1.44 20.0 1.22 41.7 7 63.0 50.1 81.3 3.50 58.8 3.07 23.8 1.69 48.4 1.84 41.0 1.52 19.6 1.04 8 1.84 53.0 58.3 69.3 3.18 49.2 2.99 21.1 61.3 2.47 20.5 1.09 36.7 1.59 9 50.3 52.4 70.0 3.09 54.8 2.97 25.3 1.78 56.1 1.79 46.0 1.59 19.6 0.94 10 56.1 60.2 2.54 48.0 23.5 51.5 2.64 1.79 51.5 1.89 42.1 1.53 21.0 1.24 11 64.0 57.1 65.6 2.79 50.9 2.69 23.5 1.79 57.9 2.14 20.2 1.79 56.9 1.31 12 71.0 60.1 70.9 3.14 62.0 3.22 26.1 1.87 59.4 1.74 48.3 1.84 23.5 1.18 13 51.6 55.6 61.1 2.69 47.4 2.74 22.8 1.72 61.7 2.19 45.8 1.69 23.7 1.19 3.14 14 61.7 57.9 66.4 58.5 3.04 23.8 1.94 59.9 2.14 51.5 2.07 20.8 1.09 15 61.5 60.4 58.1 54.0 3.22 23.0 69.0 2.07 1.54 24.2 2.77 1.84 42.2 1.12 16 58.5 60.0 3.26 55.9 79.5 2.89 22.4 1.87 55.3 45.8 1.59 25.9 1.67 1.14 17 59.0 57.0 53.2 2.34 40.3 2.34 18.1 1.57 45.2 1.57 41.1 1.59 20.9 1.05 18 62.8 55.7 82.9 3.42 67.6 3.17 25.9 1.77 57.1 1.82 48.5 1.48 25.2 1.09 19 51.3 53.1 49.5 2.51 43.8 2.52 20.5 1.69 48.1 1.96 39.9 1.49 22.7 1.04 20 57.1 57.1 50.8 2.89 45.8 2.52 63.2 1.97 21.0 1.07 21.7 1.61 45.3 1.64 21 56.6 55.9 60.4 63.0 2.79 3.02 24.7 1.84 58.1 1.94 43.2 1.47 23.7 1.27 22 60.6 63.1 74.7 3.12 57.9 2.84 26.4 1.87 64.1 1.97 43.3 1.79 24.0 1.21 23 58.1 62.5 75.1 3.07 48.1 2.92 23.0 1.69 66.9 1.87 45.1 1.69 22.7 1.29 24 58.6 54.2 55.4 2.54 56.9 2.76 24.2 1.84 56.7 1.69 45.5 1.42 25.2 1.82 25 59.6 52.4 78.8 3.39 50.5 2.99 25.7 1.89 59.6 2.14 48.9 1.66 22.9 1.27 26 53.2 2.77 2.39 55.2 54.2 63.4 2.54 31.2 54.6 1.67 45.8 1.49 18.1 1.06 27 56.8 2.97 20.3 61.9 70.1 3.02 51.9 23.5 1.74 54.6 1.77 41.5 1.57 1.04 28 47.9 56.1 54.6 2.49 38.8 2.62 20.8 1.82 51.9 1.81 47.3 1.91 21.1 1.12 29 56.4 52.4 59.2 2.69 41.7 2.34 18.2 1.57 61.7 2.19 41.1 1.74 18.7 1.17 1.91 30 68.3 54.2 71.3 2.97 55.4 2.93 20.9 1.84 61.6 39.3 1.39 16.5 1.04 50.5 1.22 31 56.3 63.7 73.9 3.12 2.82 23.2 1.89 65.1 1.92 51.4 1.54 23.0 32 61.6 57.9 66.3 2.88 53.8 2.84 21.0 1.74 59.4 1.82 45.2 1.60 20.2 1.04 33 53.9 59.9 65.4 2.96 37.4 2.34 22.6 1.76 62.4 2.12 43.1 1.72 21.6 1.17 53.9 39.2 2.19 34 54.5 65.6 2.86 2.47 20.8 1.67 59.4 44.8 1.57 20.0 1.27 35 59.5 70.9 71.9 3.25 63.9 2.84 24.3 1.72 66.8 1.94 46.1 1.59 23.3 1.24 36 54.3 62.5 77.8 3.59 55.6 2.97 20.8 1.67 66.8 1.94 42.2 1.59 22.4 1.07 37 53.2 2.89 53.2 54.7 51.0 61.0 2.89 24.3 1.72 1.89 40.1 1.58 16.4 1.04 38 64.4 62.9 67.6 3.26 44.5 2.54 25.7 1.82 54.6 1.99 52.4 1.56 20.9 1.09 39 29.2 2.38 34.2 2.24 20.6 1.74 36.5 47.0 31.9 1.32 20.0 0.99 16.1 0.97 40 26.7 29.0 33.6 1.79 28.0 2.02 17.2 1.79 36.0 1.47 27.6 1.17 13.6 0.86

Test date: Feb. 20 & 21, 2001. Group: B Probe: MT_K MT_N MK MK SK SK LK LK LN LN MN MN SN SN Fy Ху Fy Ху Fy Ху Fy Ху Χy F Ху Fy No. (N) (N)(N)(N) (N) (mm) (mm) (mm) (N)(mm) (N) (mm) y(N)(mm) 41 40.1 39.4 50.3 2.84 35.1 2.49 21.2 1.69 43.9 1.81 31.8 1.39 14.7 1.19 42 34.8 43.2 36.0 2.59 31.1 1.92 16.9 1.49 33.4 1.36 26.8 1.34 14.1 0.92 43 44.6 43.3 56.2 2.64 23.8 1.84 20.7 1.67 31.0 1.77 33.8 1.39 18.3 1.09 44 43.2 44.2 35.2 2.17 34.4 2.32 17.1 27.7 30.3 1.67 1.59 1.42 18.2 1.17 45 38.5 38.2 32.9 2.16 21.6 1.74 13.9 1.49 31.3 2.17 27.7 1.44 0.97 13.6 46 44.3 49.6 48.4 2.42 40.3 2.39 20.2 1.74 32.6 1.36 32.4 1.48 17.6 1.09 47 38.2 41.9 39.1 2.14 32.5 1.89 12.9 1.19 36.2 1.54 29.0 1.22 15.6 0.92 48 45.5 40.8 40.2 2.32 37.2 2.24 16.2 1.52 35.1 1.44 28.8 1.42 0.89 15.9 2.04 49 37.5 38.7 36.4 40.4 2.54 17.4 1.54 39.6 1.79 25.8 1.61 20.1 1.42 50 37.3 38.9 41.0 2.64 33.4 16.2 1.41 32.6 2.19 29.2 1.44 1.39 17.7 1.12 51 2.52 24.3 27.0 34.0 28.2 1.87 11.2 1.16 42.5 2.67 25.0 1.17 13.7 0.77 52 42.0 41.0 2.07 42.4 35.1 2.57 14.0 1.32 35.5 1.47 31.4 1.29 15.5 1.14 53 43.9 48.3 53.4 2.49 53.0 2.67 24.2 1.79 45.0 37.0 1.09 1.64 1.52 19.9 54 40.3 43.1 38.5 2.32 31.8 2.09 15.9 1.39 27.6 1.32 26.3 1.17 0.84 10.7 55 49.1 46.7 35.0 1.89 29.8 2.07 13.9 1.19 26.4 1.39 19.7 1.13 12.9 0.92 42.3 40.9 42.1 56 55.9 2.64 2.44 20.0 1.69 45.5 28.6 1.21 1.44 21.3 1.04 57 47.4 46.0 2.36 29.3 1.92 38.4 14.4 1.24 28.9 1.37 25.4 1.19 14.7 1.14 58 36.8 39.2 52.5 2.47 34.9 2.47 18.5 1.47 41.3 33.7 1.29 19.0 1.07 1.61 59 29.0 26.3 2.24 35.4 30.3 2.29 12.5 1.27 42.9 2.49 25.4 1.17 14.0 1.14 60 38.9 31.9 33.9 1.97 28.5 2.31 18.3 1.59 34.0 29.4 1.24 1.57 15.0 1.14 61 42.8 39.3 46.1 2.54 34.4 2.44 19.3 1.59 41.1 36.2 1.54 1.22 1.69 17.6 62 32.9 33.1 39.4 2.12 29.6 29.9 0.87 1.72 17.7 1.44 42.9 1.87 1.17 17.9 2.29 63 41.1 43.4 38.6 30.4 1.94 18.3 1.57 33.6 1.62 31.6 1.42 17.3 1.09 64 45.6 41.3 48.1 2.39 44.0 2.37 20.2 1.56 44.2 1.64 34.1 1.29 16.2 0.99 65 44.9 40.6 58.8 2.64 39.5 2.57 22.0 1.67 33.3 1.59 33.4 1.36 19.0 1.04 66 42.6 41.9 2.06 34.2 2.29 19.4 1.72 36.1 27.2 1.22 1.17 44.7 1.49 19.3 67 43.0 40.2 50.9 2.72 42.3 2.52 38.1 22.7 1.67 46.5 1.82 1.34 18.0 1.07 68 2.13 0.99 37.2 31.1 46.6 41.0 2.04 17.8 1.41 37.7 1.29 23.3 1.07 16.6 2.27 69 42.1 42.0 46.1 30.6 2.24 17.6 1.54 37.6 1.72 30.0 1.39 18.3 0.98 70 42.4 42.2 43.1 2.49 29.8 1.89 16.2 1.56 30.0 1.27 25.5 1.32 0.89 15.7 71 50.4 50.1 2.57 45.9 46.2 2.64 22.4 1.64 44.4 1.54 28.6 1.24 17.3 0.89 72 42.3 43.6 2.39 19.8 1.49 1.02 44.2 41.3 2.11 46.3 1.86 27.2 1.56 19.1 73 40.2 40.8 46.3 2.57 38.4 2.36 13.5 1.29 36.3 1.64 16.2 34.3 1.44 1.14 74 51.4 46.0 36.6 1.99 38.1 2.02 15.8 1.29 40.4 1.47 32.9 1.29 19.2 1.09 75 46.4 39.0 43.7 2.49 41.1 2.24 19.0 1.67 33.1 1.59 27.9 1.21 17.5 1.04 39.6 76 47.7 44.4 2.19 36.2 2.19 19.7 1.64 40.9 1.64 31.3 1.29 17.1 0.88 76.7 77 65.8 57.1 4.04 62.4 3.42 28.5 2.17 62.8 2.92 51.0 2.49 27.0 1.79 78 50.3 56.7 69.8 3.47 46.5 2.54 23.4 1.91 70.8 2.59 49.0 1.77 22.2 1.39 79 56.9 61.1 54.8 63.2 3.42 3.09 27.9 1.99 74.3 2.44 50.2 2.02 25.6 1.42

22.6

2.20

66.2

2.57

48.9

1.83

22.7

1.29

80

57.1

51.0

68.3

3.61

50.1

3.14

Test date: Feb. 24, 2001. Group: C

	MT_K		, 200 LK	LK	MK	MK	SK	SK	LN	LN	MN	MN	SN	SN
			Fy	Ху	Fy	Ху	Fy	Ху	Fy	Ху	Fy	Ху	F	Ху
No.	(N)	(N)	(N)	(mm)	(N)	(mm)	(N)	(mm)	(N)	(mm)	(Ň)	(mm)	y(N)	(mm)
81	66.9	64.5	75.7	2.64	69.6	3.34	24.1	1.57	56.1	1.94	42.1	1.39	22.1	0.92
82	47.2	53.3	58.4	2.57	51.7	2.76	22.7	1.82	47.9	1.64	40.2	1.39	20.8	0.94
83	59.7	63.7	77.7	2.79	52.9	2.32	27.4	1.74	57.2	1.51	45.8	1.29	21.0	0.94
84	66.6	75.6	88.5	3.12	78.6	2.96	35.2	1.94	49.0	1.42	39.2	1.14	16.8	0.94
85	74.6	75.2	65.1	2.87	51.2	2.34	22.4	1.59	52.0	1.77	31.4	1.22	19.6	1.04
86	75.0	74.2	67.2	2.62	59.7	2.59	24.7	1.82	35.6	1.19	36.2	1.32	20.1	1.07
87	82.2	73.4	63.1	2.52	43.2	1.99	22.6	1.54	63.7	1.77	41.8	1.19	24.4	0.99
88	63.7	59.7	65.1	2.59	53.3	2.12	21.2	1.54	59.6	1.80	40.9	1.34	19.0	0.96
89	41.2	53.1	68.4	2.89	44.7	2.25	16.7	1.29	40.2	1.22	42.2	1.26	21.5	0.87
90	79.3	67.1	64.7	2.72	54.0	2.54	23.3	1.57	46.7	1.56	42.0	1.24	21.5	0.94
91	73.6	70.8	80.2	2.87	54.5	2.27	25.3	1.69	66.8	1.92	60.0	1.72	23.3	1.24
92	75.4	58.3	70.4	2.49	60.8	2.29	29.7	1.72	60.5	1.39	47.5	1.24	24.6	0.99
93	63.4	79.8	55.7	2.19	48.9	2.29	24.6	1.64	62.1	1.92	43.7	1.42	24.0	1.07
94	72.2	79.4	66.9	2.54	63.3	2.84	30.1	1.89	81.4	2.12	45.2	1.41	25.0	0.99
95	70.0	67.3	72.8	2.79	46.1	2.42	28.2	1.69	49.9	1.59	37.0	1.15	18.5	0.92
96	67.5	64.8	82.2	2.80	52.9	2.44	26.8	1.67	63.3	1.36	47.0	1.39	20.7	0.97
97	59.4	62.8	60.8	2.54	49.0	2.26	17.7	1.26	56.9	1.74	36.2	1.34	20.6	0.79
98	69.6	75.5	73.3	2.76	57.5	2.94	25.0	1.69	41.9	1.44	42.0	1.49	27.7	1.66
99	69.4	79.7	74.3	2.67	56.3	2.49	28.4	1.84	62.9	1.62	47.1	1.42	23.9	0.89
100	60.8	58.9	66.9	2.59	48.4	2.24	24.1	1.64	47.0	1.27	39.1	1.36	17.2	0.87
101	72.8	72.1	74.0	2.71	58.3	2.57	21.4	1.46	66.4	1.69	38.0	1.33	19.6	0.84
102	65.9	65.1	75.3	2.69	54.1	2.49	23.4	1.54	57.3	1.51	37.7	1.24	19.5	1.12
103	71.9	68.8	63.4	2.67	48.4	2.27	21.0	1.52	38.9	1.11	37.7	1.09	15.7	0.74
104	62.3	62.8	60.7	2.62	48.5	2.29	22.7	1.59	49.9	1.21	39.7	1.14	18.0	0.89
105	65.0	68.5	92.7	3.07	70.9	2.89	28.0	1.65	84.0	1.96	46.5	1.62	26.4	1.22
106	77.5	72.6	68.1	2.39	58.4	2.56	29.0	1.74	65.6	1.91	49.2	1.52	23.5	1.07
107	67.5	71.2	73.6	2.99	54.0	2.49	20.2	1.67	60.7	1.57	37.2	1.24	19.0	1.02
108	65.8	67.6	72.4	2.69	48.8	2.24	22.3	1.52	61.3	1.87	46.2	1.77	16.3	0.82
109	71.4	74.2	63.7	2.64	49.4	2.44	21.6	1.49	67.7	1.69	39.7	1.33	23.1	0.89
110	48.0	70.3	56.8	2.32	44.9	2.09	18.6	1.39	40.3	1.24	50.1	1.56	21.5	0.92
111	68.8	77.5	46.2	2.09	46.7	1.97	18.5	1.27	46.9	1.47	36.3	1.14	23.5	0.87
112	61.2	57.3	79.8	3.21	73.6	3.09	31.2	1.87	61.1	1.56	41.9	1.24	20.3	0.91
113	66.7	58.3	75.4	2.98	54.5	2.27	22.5	1.54	61.7	1.44	46.0	1.39	23.3	0.94
114	76.1	66.0	54.8	2.39	45.5	2.07	22.4	1.54	60.2	1.57	40.9	1.47	19.0	1.14
115	63.5	68.5	80.5	2.87	63.5	2.84	31.7	2.17	63.2	1.79	52.1	1.42	22.9	1.02
116	66.9	59.4	66.2	2.52	58.5	2.61	22.8	1.49	50.2	1.36	36.8	1.04	18.6	0.89
117	75.2	74.3	52.2	2.06	45.0	2.14	17.1	1.26	44.0	1.24	32.4	1.06	16.0	0.77
118	72.3	71.9	53.2	2.43	55.5	2.50	22.7	1.64	50.9	1.37	42.4	1.39	18.9	0.89
119	77.2	80.4	80.0	2.94	57.7	2.90	23.1	1.59	58.0	1.49	41.0	1.24	18.8	0.89
120	73.6	78.5	87.9	3.19	62.9	2.64	29.8	1.87	62.7	1.66	60.0	1.82	29.0	1.09

Test date: March 20, 2001. Group: D

	MT_K	MT_N	ĹK	LK	MK	MK	SK	SK	LN	LN	MN	MN	SN	SN
		_ _	Fy	Ху	Fy	Ху	Fy	Ху	Fy	Ху	Fy	Ху	F	Xy
No.	(N)	(N)	(Ň)	(mm)	(Ň)	(mm)	(Ň)	(mm)	(Ń)	(mm)	(Ń)	(mm)	y(N)	(mm)
121	59.2	58.0	73.7	3.19	66.1	3.09	27.2	1.94	61.9	2.32	38.5	1.27	20.4	0.99
122	55.8	54.0	57.9	2.67	54.2	2.56	23.8	1.59	51.4	1.64	35.2	1.24	26.2	1.59
123	48.9	50.7	57.9	2.99	56.5	2.74	24.7	1.84	64.6	1.94	39.4	1.29	23.4	1.07
124	59.8	61.9	61.1	2.69	40.3	2.29	19.6	1.56	43.6	1.34	41.9	1.37	18.3	1.04
125	61.3	58.9	65.6	3.04	52.7	2.84	24.1	1.79	50.0	1.69	38.3	1.44	20.5	0.94
126	69.1	71.0	77.1	3.07	60.0	3.22	24.8	1.77	51.3	1.79	42.9	1.29	22.7	0.94
127	57.2	60.7	57.1	2.59	43.7	2.39	18.9	1.54	58. 6	1.84	42.3	1.29	24.3	1.14
128	63.3	70.6	58.8	2.39	40.7	2.27	22.3	1.59	56.5	1.84	34.4	1.16	20.0	1.12
129	58.4	57.1	59.5	2.64	45.9	2.51	20.9	1.57	49.5	1.69	45.7	1.42	19.3	0.94
130	63.6	64.2	73.7	3.14	49.3	2.52	23.0	1.77	73.5	2.22	48.9	1.37	26.2	1.19
131	74.7	58.4	66.8	2.92	46.5	2.44	26.2	1.99	<i>58.5</i>	1.87	40.1	1.37	20.6	1.07
132	57.3	58.4	62.9	3.32	55.7	2.74	21.7	1.56	54.4	1.69	38.5	1.38	18.4	0.92
133	55.2	53.6	73.7	3.39	61.7	3.49	25.9	2.19	68.7	2.69	50.9	2.09	25.0	1.29
134	61.8	60.4	73.1	3.27	58.6	2.64	27.4	1.97	53.6	1.69	36.9	1.27	20.2	1.09
135	51.5	63.0	63.9	2.84	52.7	2.69	21.2	1.59	47.7	1.59	38.1	1.62	17.3	0.92
136	53.1	57.4	44.1	2.29	53.5	2.74	22.3	1.72	53.7	1.69	40.3	1.49	21.0	1.12
137	55.6	54.6	53.9	2.32	44.4	2.27	20.2	1.59	61.0	1.89	44.1	1.47	19.2	1.09
138	57.5	44.6	60.1	2.52	42.2	2.14	23.6	1.72	43.8	1.64	37.1	1.24	21.0	1.02
139	57.5	66.2	53.3	2.57	54.9	2.72	17.2	1.49	53.4	1.77	45.7	1.39	23.7	1.09
140	62.1	58.8	67.8	2.91	58.1	2.84	27.8	1.94	61.7	1.77	43.7	1.62	25.3	1.22
141	59.9	62.5	73.2	3.79	55.3	3.24	24.4	2.04	70.7	2.61	49.5	2.19	21.0	1.67
142	54.4	53.0	51.5	2.66	59.3	3.07	23.8	1.89	57.9	2.32	49.5	1.82	25.7	1.47
143	66.8	67.3	60.4	2.62	54.1	2.74	26.0	1.82	49.0	1.57	40.4	1.44	19.6	1.04
144	60.0	63.7	52.7	2.54	45.2	2.69	22.2	1.61	47.6	1.54	36.7	1.14	15.7	0.99
145	46.6	53.0	54.1	2.42	47.6	2.52	22.7	1.71	51.3	1.67	42.9	1.26	21.3	0.99
146	49.3	52.2	74.7	3.59	56.9	3.19	22.0	2.04	60.5	2.44	52.2	2.29	20.2	1.41
147	71.4	77.1	51.5	2.64	49.4	2.52	24.5	1.77	56.1	1.87	39.2	1.39	21.4	0.99
148	56.6	56.7	60.9	2.72	43.9	2.27	20.2	1.62	47.3	1.56	50.9	1.66	22.1	1.06
149	58.1	58.9	63.7	3.49	57.3	3.09	23.9	1.92	67.2	2.27	52.7	2.27	21.7	1.39
150	62.3	48.6	86.8	3.84	58.8	3.37	31.1	2.29	46.8	1.97	36.8	1.47	21.4	1.22
151	58.5	64.2	70.6	3.17	56.5	3.09	24.9	1.79	64.3	2.17	43.3	1.52	22.9	1.22
152	60.9	57.6	57.4	2.49	47.1	2.42	25.5	1.76	58.3	2.12	39.4	1.42	17.8	1.07
153	60.9	68.9	62.1	2.84	48.4	2.54	24.2	1.77	70.5	2.27	51.1	1.32	23.1	1.22
154	58.9	67.6	71.9	2.89	51.9	2.64	27.0	1.97	72.2	1.92	51.2	1.47	24.5	0.99
155	65.1	69.5	72.4	2.87	47.7	2.56	23.0	1.72	59.4	1.97	40.0	1.29	21.4	0.89
156	58.7	59.4	71.9	2.97	52.7 25.0	2.57	24.0	1.82	47.9	1.54	35.2	1.27	17.3	1.17
157	61.8	60.6	46.8	2.37	35.9	2.29	21.0	1.69	49.0	1.77	32.1	1.34	22.2	1.14
158	59.6	57.8 57.0	69.8	3.67	55.7	3.64	23.7	2.19	63.0	2.37	50.4	1.99	21.7	1.19
159	65.2	57.8	56.0	2.52	44.2	2.26	23.2	1.77	60.5	1.84	39.7	1.39	23.3	1.49
160	61.0	55.5	57.8	2.87	47.0	2.59	21.2	1.81	31.0	1.49	35.1	1.24	18.5	1.12

B.3 Fuji

Test o	date: F	eb. 15	, 200	1						_			Grou	p: A
Probe:	MT_K	MT_N	LK	LK	MK	MK	SK	SK	LN	LN	MN	MN	SN	SN
			Fy	Ху	Fy	Ху	Fy	Ху	Fy	Ху	Fy	Ху	F	Ху
No.	(N)	(N)	<u>(N)</u>	(mm)	(N)	(mm)	(N)	(mm)	(N)	(mm)	(N)	(mm)	y(N)	(mm)
1	64.7	66.3	64.3	2.93	56.6	2.94	20.9	1.72	60.1	1.82	44.9	1.48	28.7	1.22
2	61.5	61.4	87.3	3.14	58.8	2.72	26.1	1.69	68.6	2.07	59.7	1.79	29.1	1.17
3	57.5	47.6	74.0	3.09	84.7	3.32	30.2	1.97	54.5	1.72	46.0	1.44	27.1	1.17
4	63.2	60.3	88.1	3.57	71.1	3.04	31.3	1.94	58.2	1.69	41.6	1.41	25.3	1.34
5	69.1	69.7	74.5	2.87	63.2	2.64	28.2	1.77	80.9	2.09	45.6	1.49	28.2	1.22
6	51.1	54.0	84.7	2.94	74.5	3.24	29.0	2.12	80.0	2.04	45.9	1.41	24.1	1.14
7	60.2	65.1	63.2	2.46	62.1	2.82	23.2	1.72	55.7	1.91	43.2	1.49	22.9	1.16
8	62.2	72.2	67.0	2.82	59.9	2.74	31.2	1.89	49.9	1.52	47.9	1.37	24.7	1.07
9	61.8	57.8	89.0	3.34	52.1	2.62	29.3	1.79	51.5	1.87	63.6	1.94	23.5	1.01
10	56.0	51.4	73.2	2.99	55.4	2.79	21.5	1.59	58.3	1.74	41.3	1.44	23.5	1.14
11	68.3	55.1	94.0	3.34	76.5	2.99	33.7	2.14	64.5	1.68	61.7	1.58	26.5	1.19
12	56.8	56.8	61.8	2.64	41.4	2.19	22.7	1.74	54.1	1.79	56.2	2.42	22.2	1.29
13	73.7	62.7	103.1	3.31	81.0	3.17	36.9	2.07	75.6	1.89	56.9	1.69	29.6	1.22
14	61.9	61.5	70.5	2.89	59.5	2.89	28.7	1.92	60.3	1.99	40.8	1.44	23.0	0.99
15	50.4	70.0	60.3	2.69	54.0	2.57	28.1	1.87	68.7	2.09	65.8	1.82	29.4	1.37
16	62.6	67.2	75.3	3.07	66.2	2.82	26.8	1.92	53.9	1.54	52.9	1.62	23.8	0.99
17	65.2	58.7	77.3	2.76	54.2	2.69	26.4	1.72	53.7	1.59	47.5	1.57	25.1	1.09
18	52.0	52.0	71.6	2.94	62.5	2.82	28.3	1.87	73.7	2.54	40.9	1.32	27.8	1.82
19	52.3	62.3	80.7	3.19	69.7	2.89	29.2	1.89	53.2	1.82	57.1	1.72	28.7	1.26
20	52.1	59.3	70.7	3.06	64.5	2.96	29.8	1.97	67.3	2.02	40.6	1.52	26.8	1.17
21	54.8	65.2	84.7	3.27	62.1	2.79	31.2	2.09	69.4	2.09	55.8	1.59	24.5	1.17
22	69.8	57.3	93.9	3.19	73.0	3.17	31.9	2.02	67.0	1.87	49.3	1.49	26.5	1.17
23	51.0	55.1	69.1	2.72	55.0	2.91	29.5	1.86	<i>56.0</i>	1.92	42.4	1.62	22.1	1.14
24	62.7	66.9	75.3	2.99	65.2	3.09	27.1	1.84	64.2	2.07	43.8	1.67	27.7	1.14
25	58.2	55.0	80.5	3.27	72.9	3.29	32.0	2.09	64.4	1.87	52.7	1.77	29.1	1.24
26	70.2	53.5	85.3	3.29	63.0	2.99	30.1	2.14	48.3	1.62	43.0	1.67	23.0	1.19
27	55.4	57.4	60.3	2.72	62.0	2.67	28.1	1.82	62.1	1.87	37.5	1.33	22.8	1.07
28	59.8	57.6	78.8	2.96	67.1	3.14	26.2	1.89	52.4	1.69	54.8	1.52	26.4	1.09
29	67.7	76.8	98.7	3.29	75.7	2.94	35.1	1.97	70.3	1.89	58.3	1.70	24.5	1.09
30	63.5	57.1	81.3	3.09	74.2	3.34	31.1	1.94	66.3	1.99	55.9	1.47	25.0	1.12
31	58.4	56.3	80.6	3.19	60.5	2.77	26.6	1.87	58.1	1.86	47.6	1.52	27.7	1.37
32	63.3	63.2	69.1	2.77	59.7	2.77	25.3	1.79	63.9	1.79	49.4	1.46	29.2	1.37
33	67.4	68.7	69.0	2.77	63.3	2.82	24.6	1.74	69.0	2.01	49.1	1.54	33.6	1.22
34	57.7	57.5	78.7	3.17	74.0	3.27	31.0	2.09	66.9	2.19	56.3	1.74	30.8	1.27
35	67.3	53.1	83.9	3.07	69.8	2.87	28.5	2.07	50.4	1.72	39.2	1.24	19.3	0.97
36	68.1	55.7	86.8	3.07	59.7	2.87	29.1	2.01	52.3	1.54	37.3	1.22	24.2	0.97
37	66.7	75.2	94.1	3.27	71.1	2.97	28.8	2.04	79.2	2.34	55.8	1.82	36.1	1.34
38	61.8	51.6	82.7	3.34	66.9	2.83	28.2	1.87	64.2	2.67	37.7	1.27	23.6	1.04
39	61.3	72.8	76.7	2.77	64.8	2.86	28.1	1.84	51.4	1.80	51.0	1.47	24.9	1.22
40	57.7	58.3	77.4	3.09	64.1	2.83	30.2	1.87	51.7	1.67	41.1	1.44	24.6	1.14

Test date: Feb. 22, 2001. Group: B

Probe:	MT_K	MT_N	LK	LK	MK	MK	SK	SK	LN	LN	MN	MN	SN	SN
			Fy	Ху	Fy	Ху	Fy	Ху	Fy	Ху	Fy	Ху	F	Ху
No.	(N)	(N)	(N)	(mm)	(N)	(mm)	(N)	(mm)	(N)	(mm)	(N)	(mm)	<i>y</i> (N)	(mm)
41	70.6	68.1	91.3	3.62	67.4	2.84	31.2	2.07	64.6	1.66	56.6	1.67	28.8	1.22
42	85.8	74.3	81.9	2.92	57.4	2.62	28.0	1.84	68.1	1.87	56.3	1.54	27.7	1.12
43	78.3	87.6	87.1	2.92	73.7	2.91	32.8	1.97	73.2	1.99	61.7	1.54	33.9	1.22
44	75.6	82.7	98.4	3.27	65.9	2.74	33.3	1.87	68.9	1.72	55.7	1.44	25.7	0.99
45	72.7	78.6	75.1	2.62	68.4	3.42	27.4	1.82	70.1	1.82	49.9	1.34	22.7	1.02
46	64.5	67.3	80.8	2.82	61.8	2.74	28.6	1.87	56.2	1.44	59.3	1.54	21.9	1.09
47	77.2	81.1	83.0	2.89	73.7	2.77	35.2	1.94	83.3	1.92	59.5	1.39	32.4	1.09
48	78.6	87.9	83.2	2.66	64.5	2.74	30.4	1.77	76.9	1.66	54.2	1.37	25.5	1.17
49	68.0	78.3	79.5	2.76	64.9	2.74	28.0	1.69	64.7	1.52	36.3	1.26	25.3	0.99
50	76.6	77.6	69.2	2.67	56.2	2.44	25.2	1.72	68.2	1.79	48.5	1.37	25.7	1.09
51	78.6	80.2	73.8	2.64	58.6	2.62	25.7	1.67	49.5	1.32	43.9	1.32	26.7	1.09
52	74.1	78.0	95.7	3.19	70.8	2.79	36.5	1.99	86.0	2.04	54.1	1.32	29.0	1.16
53	84.1	91.7	93.0	3.09	62.2	2.79	30.9	1.79	69.6	1.61	55.7	1.64	28.7	1.19
54	81.3	86.8	77.3	2.89	68.3	2.79	31.8	1.92	66.4	1.62	49.5	1.27	24.6	1.01
55	76.0	74.5	82.7	2.97	69.3	2.92	31.5	1.82	81.4	1.89	57.5	1.42	32.1	1.12
56	78.7	86.3	60.8	2.37	57.7	2.49	27.9	1.74	68.3	1.62	57.3	1.49	25.5	1.12
57	78.0	68.3	65.6	2.52	59.7	2.62	26.3	1.64	56.6	1.67	50.9	1.44	25.8	1.07
58	83.6	82.0	114.4	3.61	75.2	3.04	36.0	2.42	66.8	1.84	57.1	1.57	30.3	1.29
59	69.5	73.1	80.1	2.96	57.5	2.47	30.0	1.94	81.4	2.02	44.0	1.27	27.0	1.14
60	71.6	70.4	82.9	3.07	78.2	3.17	34.7	2.02	75.6	1.82	55.1	1.49	24.7	0.94
61	78.5	71.2	84.3	2.84	76.2	2.87	30.8	1.87	60.7	1.47	48.7	1.22	30.5	1.14
62	85.1	74.1	92.0	2.94	72.8	3.02	35.9	2.04	78.2	1.99	49.6	1.39	29.5	1.04
63	82.5	77.6	67.8	2.49	58.6	2.62	25.4	1.67	79.4	1.92	50.7	1.47	27.7	1.19
64	74.5	77.2	69.9	2.57	60.1	2.54	29.3	1.87	59.6	1.54	46.2	1.19	23.4	0.97
65	77.2	81.7	96.0	3.52	63.4	2.69	30.8	1.89	61.7	1.67	42.9	1.44	28.3	1.22
66	66.6	80.9	79.4	2.74	70.7	2.97	28.9	1.74	67.3	1.74	56.5	1.34	26.8	1.06
67	86.5	78.5	90.3	3.02	74.7	3.14	32.4	1.97	56.5	1.59	45.3	1.19	23.2	1.19
68	76.3	73.9	78.8	3.26	68.7	2.79	29.1	1.84	54.1	1.54	42.2	1.19	21.1	1.04
69	78.7	98.6	87.4	3.87	72.6	3.37	37.5	2.49	80.9	1.96	54.4	1.42	33.6	1.19
70	77.0	72.7	72.7	2.82	50.9	2.32	21.7	1.77	60.4	1.52	40.2	1.19	29.6	1.27
71	73.4	82.5	71.3	2.77	55.5	2.37	27.3	1.79	61.1	1.52	46.9	1.44	24.7	0.96
72	83.9	72.9	83.0	3.04	81.5	3.34	28.5	1.96	72.8	1.79	51.7	1.52	27.7	1.07
73	67.0	80.0	76.5	2.72	65.9	2.79	29.7	1.87	82.3	1.92	57.0	1.52	35.8	1.27
74	86.0	81.2	67.7	2.64	67.1	2.87	27.9	1.84	58.9	1.66	49.1	1.24	23.3	0.99
75	73.1	87.9	99.2	3.32	71.3	2.89	34.1	1.89	73.8	1.77	59.2	1.47	33.3	1.14
76	101.2	92.3	88.6	3.14	74.7	3.22	33.8	1.96	65.3	1.77	62.3	1.59	27.7	1.09
77	76.8	83.3	76.0	2.84	58.9	2.77	29.7	1.84	62.0	1.56	43.5	1.32	25.1	0.94
78	74.6	94.5	70.0	2.89	68.5	2.84	31.1	1.84	76.4	1.77	57.1	1.54	29.7	1.27
79	76.2	87.4	57.8	2.21	61.2	2.64	27.8	1.79	84.7	1.79	60.9	1.44	30.6	1.29
80	78.9	78.2	73.7	3.19	63.2	2.97	28.9	1.89	70.8	3.74	53.2	2.14	32.3	2.32

Test date: Feb. 27, 2001. Group: C

	MT_K		, 2001	LK	MK	MK	SK	SK	LN	LN	MN	MN	SN	SN
1 1000.		1411 _14	Fy	Xy	Fy	Xy	Fy	Xy	Fy				F	
No.	(N)	(N)	(N)	(mm)	(N)	∧y (mm)	(N)	∧y (mm)	гу (N)	Xy (mm)	Fy (N)	Xy (mm)	.г у(N)	Xy (mm)
81	69.5	58.7	89.1	3.94	66.5	3.17	35.0	2.27	64.2	2.07	36.9	1.76	23.9	1.41
82	57.8	58.9	63.2	3.59	56.0	3.44	28.0	2.42	61.0	2.69	42.4	2.47	22.8	1.57
83	67.6	73.2	93.6	4.94	82.1	5.11	31.7	3.24	93.8	3.57	56.5	2.77	30.4	1.94
84	64.7	75.5	80.5	3.69	65.0	3.87	29.6	2.34	78.3	2.42	61.8	2.14	33.0	1.47
85	77.2	75.2	89.2	4.84	68.1	4.54	35.2	3.17	84.2	3.24	62.9	2.67	30.8	1.89
86	58.5	66.1	70.0	3.47	65.7	3.41	29.2	2.32	71.2	2.59	64.0	2.49	30.2	1.64
87	59.9	72.4	77.6	3.92	73.1	3.79	32.7	2.72	84.5	2.84	59.9	2.31	31.0	1.89
88	63.9	69.5	77.7	4.29	70.2	4.09	29.5	2.67	70.4	2.94	54.8	2.69	25.8	1.79
89	66.3	71.8	89.4	4.57	63.5	4.09	30.0	2.77	78.2	3.34	53.2	2.72	26.6	1.84
90	63.0	59.1	77.8	3.59	66.6	3.57	27.2	2.14	75.6	2.59	57.1	2.07	28.5	1.49
91	83.1	86. 9	105.0	5.04	74.2	4.74	39.6	3.19	95.9	3.89	66.2	3.09	32.1	2.14
92	70.6	63.3	82.4	4.57	64.1	4.32	28.2	2.79	76.1	3.12	50.6	2.77	28.0	2.04
93	62.8	62.9	77.4	3.62	63.2	3.49	28.7	2.27	67.9	2.29	62.1	2.19	28.5	1.44
94	59.5	57.8	99.0	4.44	73.0	3.97	28.5	2.59	64.7	2.59	54.4	2.32	24.5	1.54
95	78.2	78.9	98.2	4.89	74.6	4.09	35.4	2.94	73.8	3.07	64.5	2.59	29.3	1.69
96	63.4	66.2	75.3	4.52	62.8	3.97	27.6	2.59	59.4	2.94	49.2	2.69	26.6	2.12
97	72.8	69.7	79.7	4.39	77.3	3.64	32.4	2.42	67.1	2.44	54.7	2.07	27.7	1.39
98	62.2	59.7	77.3	3.72	56.6	3.29	27.7	2.36	72.6	2.64	48.8	2.07	25.4	1.64
99	64.4	72.4	80.3	3.69	63.3	3.34	26.1	2.09	87.3	3.02	56.9	2.06	30.5	1.85
100	59.6	63.1	76.9	3.54	63.7	3.12	27.1	2.24	72.8	2.29	53.4	1.82	26.3	1.41
101	66.2	69.4	94.3	4.74	80.0	4.44	30.3	2.52	93.2	3.34	60.2	2.57	31.6	1.87
102	67.0	79.9	96.7	4.61	74.2	4.02	31.0	2.59	84.9	3.04	61.3	2.44	29.2	1.82
103	67.0	61.7	91.9	4.39	66.1	3.96	32.6	2.74	71.6	2.71	57.3	2.34	25.7	1.79
104	78.1	77.6	100.0	3.77	63.0	2.74	35.0	2.27	74.9	2.02	52.7	1.57	31.9	1.39
105	75.3	76.9	100.1	5.12	63.8	4.14	30.6	2.77	84.3	3.47	71.2	3.04	28.9	2.09
106	64.3	61.4	76.3	3.54	55.6	3.44	25.0	2.14	87.0	2.77	43.0	1.97	25.0	1.44
107	71.1	65.4	98.0	4.17	76.5	3.66	32.5	2.49	78.6	2.32	53.3	1.82	27.8	1.34
108	76.8	74.7	98.6	3.82	70.9	3.26	30.4	2.24	81.8	2.42	52.7	1.89	26.8	1.29
109	63.1	62.7	76.5	3.72	63.9	3.24	28.7	2.24	71.9	2.34	50.1	1.79	29.2	1.54
110	74.6	64.1	95.7	4.84	86.3	4.54	37.0	2.92	73.1	3.52	61.9	2.71	23.8	1.71
111	62.2	72.2	70.1	3.54	60.3	3.17	22.1	2.09	80.0	2.74	46.3	1.82	25.3	1.52
112	75.8	72.6	102.0	4.22	78.9	3.89	32.2	2.72	72.1	2.62	70.0	2.49	31.5	1.52
113	67.4	91.8	93.5	4.47	73.6	4.04	32.1	2.62	110.7	3.78	62.3	2.42	36.6	1.89
114	76.3	67.2	112.4	4.12	68.7	3.21	32.5	2.21	78.4	2.22	58.5	1.84	30.0	1.57
115	59.1	66.2	67.6	3.29	61.1	3.44	25.9	2.11	65.3	2.17	54.2	1.89	26.0	1.34
116	83.4	70.9	100.0	5.52	69.2	4.99	36.3	3.59	95.3	4.10	62.4	3.39	31.9	2.21
117	67.6	64.1	83.8	3.49	65.4	3.19	30.7	2.22	74.0	2.06	47.8	1.84	26.7	1.57
118	80.3	80.4	104.0	4.64	72.5	4.04	30.5	2.56	78.8	3.19	54.6	2.47	26.1	1.82
119	74.3	64.5	93.9	4.29	73.7	3.69	31.4	2.49	83.7	2.81	65.4	2.46	33.0	1.66
120	65.1	61.5	79.2	4.47	64.8	4.04	27.3	2.62	71.6	3.22	44.1	2.39	24.1	1.89

Test date: March 19, 2001. Group: D MK Probe: MT_K MT_N LK LK MK SK SK ĹŃ LN MN MN SN SN Fy Xy Fy Ху Fy Ху Fy Ху Fy Ху F Xy No. (N) (N)(N) (mm) (N) (mm) (N) (N)(N)<u>y</u>(N) (mm) (mm) (mm) (mm) 121 81.0 76.0 73.3 60.6 2.92 60.3 3.17 29.1 1.96 1.72 49.9 25.3 1.18 1.46 122 89.2 94.6 91.4 3.19 70.8 3.02 45.4 2.94 85.1 2.14 59.1 1.59 30.6 1.24 123 80.6 83.4 61.5 2.59 54.5 2.66 29.4 1.92 67.1 1.94 43.2 1.34 27.6 1.09 71.5 124 81.7 96.9 3.66 69.7 3.17 2.79 35.6 66.0 1.79 46.7 1.34 27.4 1.02 125 74.5 78.6 76.7 2.76 64.3 2.89 20.3 1.67 59.9 1.54 44.4 1.32 25.7 1.04 126 80.2 78.2 81.1 3.06 69.1 2.99 32.0 2.02 55.8 35.8 25.9 1.57 1.19 1.09 127 84.1 86.1 81.3 70.2 2.92 28.4 3.12 2.00 67.3 1.64 47.1 1.49 23.0 1.06 128 79.4 73.0 67.6 2.49 54.9 2.69 24.2 55.6 43.3 1.64 1.54 1.42 22.0 0.99 129 85.2 85.1 64.1 2.86 76.6 2.99 25.0 1.74 53.7 1.54 44.0 1.31 24.8 1.15 130 86.8 81.3 83.7 3.12 80.0 3.44 31.2 2.14 75.0 1.84 62.9 1.74 29.7 1.22 131 82.7 81.5 78.0 2.96 62.2 3.07 30.6 1.99 67.1 2.01 46.0 1.47 27.8 1.37 132 84.7 86.1 90.7 3.42 69.9 2.84 31.6 2.12 55.9 1.59 49.9 1.39 27.4 1.09 133 79.1 78.7 92.2 3.29 2.04 3.52 86.2 33.9 64.0 1.24 23.3 1.92 41.8 1.12 134 73.5 65.6 77.6 2.86 55.6 2.47 26.4 1.87 66.4 1.61 50.5 1.64 28.3 1.19 135 77.0 78.6 74.6 3.12 61.3 2.71 25.7 2.07 43.8 27.6 1.27 1.84 38.6 1.39 136 78.6 77.7 72.3 2.76 57.0 2.54 24.4 1.87 59.6 1.75 66.7 2.34 29.4 1.09 137 80.3 73.9 79.9 3.02 69.1 2.99 32.9 54.6 2.12 46.0 1.42 1.47 23.8 1.09 2.04 138 84.0 70.4 81.0 3.01 66.7 2.82 30.8 69.6 1.94 43.2 1.52 30.2 1.32 139 82.4 79.6 71.5 2.67 64.7 2.96 31.0 2.04 70.3 1.64 50.6 1.54 23.0 1.01 140 75.7 68.1 71.8 2.64 57.8 2.77 65.0 41.4 1.34 29.9 1.97 1.74 21.7 1.30 141 95.4 98.1 83.2 3.22 2.34 111.0 3.72 41.4 83.3 2.09 42.4 1.44 32.9 1.34 142 72.1 81.3 81.6 2.94 59.0 2.64 28.5 1.96 60.0 1.42 73.1 1.76 27.8 1.19 143 76.6 77.0 77.4 2.94 67.7 2.92 31.2 2.12 54.0 1.84 59.3 1.52 26.2 1.07 144 78.5 83.0 66.6 2.14 83.9 2.89 2.97 34.4 77.7 1.91 44.5 1.46 28.8 1.24 145 90.1 84.1 83.9 3.34 55.3 2.69 27.8 2.09 56.9 1.67 41.9 1.37 23.1 1.07 146 72.5 77.1 78.5 3.19 56.9 3.21 33.4 2.24 96.6 2.29 44.6 1.37 28.3 1.14 147 81.2 86.5 87.6 77.2 3.22 28.8 3.17 1.92 77.4 1.82 51.4 1.66 36.7 1.61 148 82.0 103.7 71.4 2.89 58.2 2.77 29.6 1.94 55.9 1.67 54.5 1.57 21.7 0.91 149 81.6 78.7 76.4 2.99 61.2 2.87 27.1 1.99 72.4 2.19 49.1 1.64 36.8 1.84 150 78.9 77.5 92.2 3.37 63.3 2.79 2.02 57.1 26.7 31.6 1.44 46.9 1.41 1.19 151 76.5 80.1 66.5 2.61 60.5 2.89 26.4 54.3 49.9 1.52 21.5 1.84 1.64 1.12 152 78.0 77.7 85.8 3.12 47.1 2.59 30.8 2.42 60.3 1.82 46.0 1.47 23.7 0.94 153 76.1 75.4 76.7 3.07 59.9 2.79 19.8 1.64 80.7 1.99 43.6 1.42 30.8 1.21 154 80.9 79.5 59.8 3.02 71.2 27.5 83.7 3.21 28.4 1.97 1.82 50.4 1.44 1.14 155 93.5 76.5 84.3 3.17 62.3 2.72 29.2 1.92 62.5 2.09 45.9 1.67 25.3 1.06 156 76.1 81.7 85.6 3.24 65.2 2.84 25.8 1.84 88.8 1.80 1.47 29.4 1.23 41.0 80.9 157 79.6 82.0 2.92 57.3 2.54 32.0 2.07 55.3 1.37 57.7 1.52 23.1 0.92 49.6 158 73.8 89.4 87.4 3.22 84.9 3.24 24.3 88.5 1.34 22.1 1.79 1.99 1.14 159 74.8 86.6 110.9 4.02 74.9 3.24 34.7 2.34 83.1 1.74 1.42 29.2 1.09 57.9 160 68.1 2.70 58.0 2.79 27.0 1.64 19.7 64.3 72.2 1.87 63.8 1.64 54.4 1.06

B.4 Gala

		<u> Iarch</u>	1, 200										Gro	up: A
Probe:	MT_K	MT_N	LK	LK	MK	MK	SK	SK	LN	LN	MN	MN	SN	SN
			Fy	Ху	Fy	Ху	Fy	Ху	Fy	Ху	Fy	Ху	F	Ху
No.	(N)	(N)	(N)	(mm)	(N)	(mm)	(N)	(mm)	(N)	(mm)	(N)	(mm)	y(N)	(mm)
1	36.6	38.2	38.3	2.22	35.3	2.24	17.3	1.44	33.6	1.37	22.6	1.10	17.2	0.99
2	51.4	49.5	67.5	3.62	53.0	3.32	23.0	2.06	35.5	1.68	43.2	1.84	18.7	1.19
3	41.1	40.6	49.2	2.84	39.3	2.69	19.7	1.79	39.9	1.72	34.2	1.37	18.8	1.04
4	52.5	55.2	56.5	2.84	48.6	2.79	20.9	1.82	51.6	2.11	40.5	1.56	20.1	1.42
5	46.6	53.0	51.4	3.24	51.9	3.09	18.5	1.74	44.6	2.12	36.5	1.77	20.9	1.47
6	46.8	52.8	47.3	2.54	41.2	2.69	19.4	1.64	43.4	1.87	37.0	1.61	21.7	1.22
7	39.1	39.8	36.6	2.14	35.9	2.17	12.4	1.32	20.1	1.14	26.6	1.22	13.0	0.91
8	50.7	55.6	56.0	2.94	47.7	2.86	18.3	1.62	48.4	1.94	39.5	1.67	20.3	1.09
9	38.7	39.1	38.8	2.50	37.1	2.44	15.5	1.55	38.3	1.59	21.2	1.42	13.5	1.04
10	41.8	38.8	41.8	2.22	34.9	2.32	12.3	1.34	30.8	1.19	23.8	1.04	15.4	1.02
11	51.6	52.6	56.7	3.03	32.0	2.54	19.9	2.09	40.4	1.79	32.2	1.44	17.6	1.19
12	43.6	45.2	58.0	2.94	37.6	2.44	17.2	1.82	55.9	2.19	31.7	1.64	18.6	1.29
13	67.6	70.1	74.8	3.84	57.8	3.52	25.3	2.33	62.0	2.64	48.2	2.34	26.5	1.89
14	54.0	46.2	59.8	2.67	49.5	2.59	21.4	1.77	38.7	1.54	36.1	1.29	18.4	0.92
15	32.5	34.7	42.0	3.19	27.9	1.87	13.7	1.37	32.4	1.59	25.9	1.29	15.4	1.16
16	39.8	41.3	43.6	2.56	34.7	2.24	14.8	1.62	35.7	1.72	24.5	1.34	13.3	1.07
17	34.1	40.7	45.6	2.32	34.8	2.04	14.1	1.36	36.4	1.44	31.9	1.19	13.9	0.91
18	39.3	32.2	45.6	2.67	36.7	2.74	17.1	1.67	37.8	1.69	31.8	1.51	13.3	1.22
19	32.8	30.8	30.3	2.14	29.7	1.94	13.0	1.31	26.9	1.29	20.0	1.12	12.5	0.87
20	59.5	53.2	59.8	3.37	52.7	3.12	20.9	1.82	48.2	2.06	36.4	1.62	21.0	1.28
21	61.4	48.3	59.8	2.96	52.3	3.07	22.5	1.84	52.8	2.01	41.7	1.67	19.9	1.24
22	47.5	54.2	52.2	2.77	45.1	2.89	19.0	1.82	52.8	2.07	34.8	1.99	18.2	1.04
23	47.2	37.9	43.7	2.62	35.9	2.17	15.6	1.47	29.1	1.32	26.8	1.34	19.3	2.17
24	49.5	50.0	59.9	2.87	48.5	2.59	22.2	1.74	39.3	1.64	29.1	1.36	19.0	1.27
25	48.8	53.7	52.1	2.84	41.6	2.67	18.0	1.72	45.6	1.94	27.1	1.41	17.2	1.22
26	48.2	59.9	53.0	2.54	39.8	2.34	19.6	1.66	48.6	1.84	37.0	1.51	22.0	1.37
27	42.4	37.7	57.0	3.46	45.3	3.37	18.5	1.96	45.8	1.91	32.5	1.94	16.8	1.27
28	25.7	27.1	26.2	1.62	21.7	1.56	11.6	1.29	19.1	1.34	25.7	1.36	9.7	0.94
29	36.0	37.6	43.6	2.46	32.3	2.32	14.4	1.44	29.6	1.36	23.7	1.06	15.6	0.99
30	62.7	44.8	45.3	2.56	47.6	2.94	21.4	1.95	29.9	1.48	24.9	1.27	13.4	0.84
31	69.5	66.9	74.3	3.44	52.0	2.99	23.5	1.99	52.5	1.91	42.8	1.69	22.5	1.34
32	41.2	46.1	55.8	3.07	35.8	2.29	20.9	1.99	31.0	1.37	28.8	1.29	15.1	1.02
33	43.7	59.1	48.6	3.09	44.1	2.77	20.0	2.09	51.0	2.41	39.9	2.03	21.0	1.41
34	67.6	71.9	62.6	3.36	47.1	2.57	24.5	2.06	74.2	2.72	50.7	1.96	25.6	1.67
35	46.8	37.2	48.1	2.37	42.4	2.44	19.3	1.82	45.6	1.84	29.0	1.36	18.5	1.06
36	45.2	39.3	40.8	2.14	40.5	2.27	15.3	1.44	28.7	1.27	25.4	1.27	13.9	0.87
37	42.3	43.9	50.1	2.59	30.0	2.14	17.1	1.69	34.1	1.73	27.2	1.37	16.3	1.34
38	64.7	41.2	69.4	3.72	46.5	2.89	28.0	2.34	49.3	1.81	30.2	1.42	20.0	1.14
39	55.3	57.2	65.4	3.04	50.1	2.84	22.3	1.77	62.6	2.24	44.3	1.74	22.3	1.44
40	53.7	55.4	70.9	3.19	52.7	2.94	21.7	2.04	47.0	1.93	33.0	1.46	20.0	1.29

Test date: March 11, 2001. Group: B

Probe:	MT_K	MT_N	LK	LK	MK	MK	SK	SK	LN	LN	MN	MN	SN	SN
			Fy	Ху	F	Ху								
No.	(N)	(N)	(N)	(mm)	y(N)	(mm)								
41	51.8	45.9	48.0	2.94	49.5	3.17	20.7	1.94	32.2	1.79	32.2	1.49	16.3	1.12
42	60.5	50.6	53.8	3.12	44.5	2.97	24.9	2.32	46.5	2.32	34.7	1.63	18.3	1.36
43	50.1	51.1	41.3	2.37	41.7	2.44	17.1	1.59	40.6	1.77	30.0	1.46	17.3	1.03
44	64.5	58.9	76.4	3.94	54.9	3.32	26.7	2.36	65.7	2.62	35.4	1.79	20.8	1.60
45	36.5	35.9	31.3	2.19	28.0	2.22	14.7	1.64	30.5	1.84	30.7	1.75	14.3	1.19
46	40.6	45.5	54.6	2.89	38.6	2.62	17.7	1.77	33.9	1.59	31.0	1.60	18.5	1.22
47	56.5	58.2	59.8	3.59	43.2	2.89	25.1	2.07	57.0	2.09	40.1	1.87	18.9	1.27
48	54.2	51.4	56.5	3.12	47.3	2.77	19.9	1.72	36.5	1.97	34.1	1.49	15.4	1.19
49	30.7	38.5	40.1	2.72	32.1	2.41	13.0	1.69	32.6	2.02	24.5	1.54	15.6	1.27
50	34.9	44.4	40.8	2.54	40.8	3.02	17.3	1.84	36.9	1.79	32.7	1.56	15.7	1.17
51	46.2	54.2	63.4	3.64	52.9	3.59	20.0	2.02	52.1	2.69	39.0	2.37	22.6	1.84
52	40.9	39.0	43.9	2.42	35.9	2.22	20.2	1.87	30.7	1.62	31.6	1.39	16.3	1.24
53	43.1	48.4	60.1	3.39	51.3	3.12	23.1	2.02	48.1	2.07	36.8	1.67	17.2	1.37
54	48.8	38.5	65.2	3.92	48.9	3.47	21.6	2.29	45.7	2.39	30.0	1.97	16.4	1.54
55	57.9	61.0	66.2	3.59	57.9	3.37	22.7	2.04	46.6	2.04	40.8	1.99	17.4	1.29
56	49.4	40.6	52.2	2.84	50.5	2.84	19.8	1.92	38.9	1.72	28.8	1.44	17.9	1.05
57	43.3	44.2	67.6	3.19	49.5	2.86	22.9	2.04	44.8	1.97	33.9	1.61	17.3	1.22
58	41.8	40.1	44.9	2.42	42.5	2.64	17.3	1.53	44.7	1.86	29.6	1.44	17.5	1.12
59	29.6	24.0	28.0	1.84	28.5	2.01	10.6	1.34	20.7	1.49	16.5	1.29	11.2	0.92
60	35.4	45.6	46.5	2.62	35.7	2.42	17.3	1.69	35.2	1.79	30.7	1.57	16.2	1.24
61	38.4	38.4	54.4	3.19	41.4	3.24	21.0	2.34	37.4	2.04	30.2	1.74	13.0	1.42
62	40.3	47.1	48.7	3.02	40.3	2.79	20.0	1.97	49.6	2.12	38.9	1.92	18.5	1.27
63	35.2	36.0	44.2	2.49	34.5	2.17	16.2	1.62	43.6	1.74	29.1	1.42	14.6	1.16
64	42.1	37.5	55.1	3.14	44.2	2.96	22.7	2.12	44.0	2.29	26.6	1.74	16.2	1.39
65	55.9	65.3	61.2	3.14	47.1	2.79	21.8	2.09	60.5	2.32	36.6	1.82	19.0	1.39
66	52.8	59.8	58.6	3.34	47.0	2.89	19.7	2.08	46.3	2.29	43.2	2.12	20.1	1.84
67	37.7	39.5	36.7	2.29	34.7	2.67	16.5	1.71	35.2	1.64	20.8	1.29	10.2	1.14
68	30.8	27.5	47.7	2.87	31.0	2.44	14.0	1.62	36.8	2.11	31.9	1.89	12.9	1.19
69	41.3	45.3	38.6	2.17	37.9	2.59	18.4	1.62	47.1	1.96	31.4	1.57	17.4	1.19
70	55.7	60.2	59.3	3.19	41.2	3.02	20.5	1.97	41.3	2.22	39.4	1.72	19.5	1.54
71	54.9	46.4	57.3	2.84	49.1	2.74	20.3	1.72	53.7	2.07	37.3	1.74	18.3	1.46
72	36.5	40.0	41.9	2.59	32.3	2.24	13.0	1.66	26.9	1.49	20.7	1.32	13.7	1.04
73	46.4	50.0	45.3	2.59	48.1	3.02	19.0	1.88	41.5	2.14	29.4	1.74	17.0	1.42
74	43.7	37.0	38.5	2.62	36.1	2.51	13.9	1.62	34.8	1.87	26.8	1.59	11.9	1.19
75	39.3	41.7	33.2	2.19	38.0	2.29	15.6	1.65	27.1	1.42	23.0	1.22	12.6	0.96
76	38.3	49.3	55.5	3.54	37.5	2.79	18.5	1.97	44.4	2.39	35.3	1.96	16.9	1.52
77	40.4	38.2	41.7	2.47	42.3	3.07	18.7	1.79	39.1	2.14	29.2	1.67	15.2	1.14
78	35.6	33.5	44.9	2.64	37.6	2.64	15.4	1.86	30.1	1.52	26.2	1.54	12.9	1.12
79	30.1	32.7	37.7	2.67	34.0	2.64	13.7	1.64	28.1	1.67	19.8	1.32	14.4	1.11
80	49.6	56.5	66.7	3.39	57.4	3.27	23.3	1.87	51.6	2.63	44.2	1.92	20.9	1.54

Test date: March 12, 2001. Group: C

	MT_K	MT_N	LK	LK	MK	MK	SK	SK	LN	LN	MN	MN	SN	SN
	-		Fy	Ху	F	Ху								
No.	(N)	(N)	(Ň)	(mm)	(Ň)	(mm)	(Ň)	(mm)	(Ń)	(mm)	(Ń)	(mm)	y(N)	(mm)
81	38.1	44.9	46.4	2.82	34.1	2.47	17.8	1.77	35.3	1.79	39.2	1.69	21.0	1.37
82	42.6	50.7	54.2	2.69	34.1	2.19	19.2	1.69	39.4	1.74	30.5	1.32	15.7	1.21
83	45.2	51.9	49.3	2.62	27.7	2.09	16.0	1.57	46.1	1.74	36.4	1.69	15.2	1.22
84	56.0	50.0	59.8	3.04	46.0	2.96	25.6	2.17	41.5	1.64	23.2	1.47	18.2	1.34
85	44.0	36.7	36.0	2.02	39.1	2.60	16.7	1.62	27.4	1.22	22.2	1.29	13.6	1.14
86	56.2	58.3	79.6	3.37	57.3	2.97	26.8	2.04	49.3	1.70	52.1	1.79	21.5	1.22
87	36.8	42.5	60.1	3.09	35.7	2.42	18.8	1.92	39.9	1.84	34.1	1.67	19.0	1.49
88	36.1	35.5	33.0	1.99	29.2	1.90	14.4	1.34	28.4	1.44	18.1	1.14	13.9	1.07
89	38.7	38.7	38.4	2.22	31.0	2.07	15.1	1.54	32.7	1.49	26.9	1.15	14.9	1.29
90	46.5	40.2	41.3	2.39	39.4	2.34	20.7	1.71	45.3	1.84	26.5	1.29	15.9	1.17
91	46.2	46.1	53.4	2.87	46.0	2.72	20.5	1.77	47.1	1.79	32.8	1.69	19.4	1.42
92	49.9	49.2	51.1	2.74	40.1	2.41	17.1	1.54	42.9	1.74	35.4	1.61	17.3	1.46
93	38.8	36.0	51.4	2.77	47.9	2.87	19.0	1.79	36.5	1.69	30.8	1.39	18.4	1.22
94	33.0	35.8	53.2	2.62	40.1	2.31	17.5	1.57	35.2	1.47	20.3	1.32	15.8	0.97
95	40.9	41.9	55.3	2.82	42.0	2.49	14.9	1.44	42.7	1.81	39.3	1.82	20.4	1.47
96	44.1	51.2	55.1	2.97	40.4	2.76	17.2	1.79	41.7	1.99	29.0	1.69	15.1	1.12
97	53.7	59.1	63.7	2.94	42.5	2.69	21.8	1.77	38.1	1.82	33.9	1.62	20.7	1.37
98	59.2	66.5	55.9	2.69	41.8	2.72	17.8	1.64	52.5	1.84	35.2	1.49	23.3	1.24
99	37.7	36.7	34.0	2.09	26.5	2.01	13.8	1.26	21.3	1.12	18.6	1.04	12.8	0.99
100	47.8	55. 4	55.7	2.84	44.5	2.53	18.8	1.69	61.3	2.87	35.7	1.47	18.7	1.17
101	61.3	59.4	71.5	3.17	55.8	3.14	19.6	1.62	48.6	1.93	32.8	1.44	19.0	1.04
102	41.2	41.3	51.1	2.56	31.8	2.14	19.0	1.67	36.6	1.77	28.2	1.34	13.3	1.07
103	43.5	45.4	50.1	2.51	41.4	2.74	19.6	1.67	33.8	1.32	27.4	1.27	13.3	0.94
104	41.8	46.2	44.4	2.34	39.2	2.59	17.1	1.66	36.9	1.41	27.2	1.17	11.9	1.07
105	64.5	50.5	67.5	3.02	49.6	2.67	18.1	1.82	41.0	1.72	35.8	1.79	18.2	1.34
106	22.1	27.6	30.3	1.79	24.5	1.87	12.1	1.24	24.6	1.42	22.2	1.39	11.7	0.94
107	38.5	38.7	29.3	1.89	38.4	2.49	14.1	1.61	25.7	1.39	23.5	1.19	12.3	1.19
108	37.7	46.4	41.9	2.47	36.6	2.39	13.4	1.67	56.7	2.14	36.6	1.72	19.2	1.38
109	41.9	49.1	71.7	3.69	41.9	2.82	20.9	2.09	46.2	2.06	32.6	1.72	14.9	1.49
110	43.0	40.8	53.5	2.64	50.5	2.74	16.8	1.62	37.1	1.59	39.0	1.54	12.6	1.12
111	38.8	43.4	34.7	1.89	34.1	2.14	13.7	1.39	22.5	1.17	19.4	1.12	13.1	0.87
112	42.8	41.6	42.3	2.19	31.2	2.14	14.7	1.30	23.1	1.27	23.0	1.22	12.7	0.87
113	46.8	42.9	44.3	2.57	40.1	2.74	16.0	1.82	36.9	1.92	26.4	1.56	16.8	1.24
114	58.2	58.4	61.9	3.17	54.6	3.04	23.9	2.19	57.0	2.04	40.5	1.72	20.2	1.52
115	46.2	45.5	42.1	2.22	40.2	2.32	17.8	2.14	33.3	1.39	26.5	1.39	16.7	1.12
116	34.2	35.2	35.6	2.07	27.1	1.99	13.8	1.41	33.9	1.44	23.5	1.27	13.0	1.04
117	52.3	52.1	60.4	2.82	42.7	2.47	20.0	1.79	42.6	1.77	31.1	1.41	14.0	1.19
118	51.5	66.2	46.9	2.34	42.2	2.54	17.1	1.64	54.7	1.79	33.4	1.49	19.0	1.14
119	36.8	38.3	35.9	2.12	31.8	1.94	12.4	1.42	22.3	1.24	23.5	1.24	11.0	0.89
120	45.0	37.7	44.0	2.47	35.9	2.37	18.6	1.69	35.0	1.54	33.0	1.39	14.6	1.33

Test date: March 13, 2001. Group: D

Probe:	MT_K	MT_N	LK	LK	MK	MK	SK	SK	LN	LN	MN	MN	SN	SN
	_		Fy	Ху	F	Ху								
No.	(N)	(N)	(N)	(mm)	y(N)	(mm)								
121	32.0	35.1	40.0	2.31	32.5	2.32	13.2	1.44	31.4	1.44	21.6	1.44	15.0	1.12
122	43.9	38.4	56.1	3.11	46.9	3.29	21.4	1.99	40.7	2.20	24.4	1.39	15.6	1.27
123	36.6	40.1	45.8	2.69	33.6	2.44	18.5	1.84	29.9	1.84	22.2	1.42	13.2	1.24
124	51.6	50.4	48.9	2.63	39.8	2.29	19.5	1.64	45.4	1.69	33.9	1.37	20.4	1.34
125	41.5	40.4	51.8	2.82	33.3	2.12	17.1	1.55	44.2	1.94	30.7	1.64	15.1	1.17
126	35.1	36.7	39.9	2.09	34.2	2.14	14.2	1.36	28.9	1.39	24.2	1.39	12.7	0.92
127	52.4	51.5	75.8	3.79	53.2	3.24	21.8	2.29	54.7	2.27	52.9	2.12	27.5	1.62
128	52.3	58.2	64.1	3.46	50.0	2.89	23.5	1.99	49.7	2.14	41.9	1.64	23.2	1.34
129	42.2	45.0	57.2	3.27	39.7	2.39	18.4	1.87	48.6	2.19	27.3	1.51	16.1	0.99
130	38.0	36.5	44.5	2.44	32.4	2.32	12.5	1.27	40.4	1.54	26.4	1.29	15.2	1.07
131	51.9	59.5	69.4	4.19	49.2	3.17	25.6	2.39	53.5	2.79	50.3	2.24	25.8	1.67
132	34.5	28.5	36.7	2.44	33.1	2.24	14.3	1.57	25.9	1.84	20.2	1.59	13.4	1.16
133	49.1	58.3	49.5	2.52	41.6	2.51	18.2	1.66	46.0	1.72	28.1	1.29	18.1	1.39
134	38.0	41.3	44.2	2.49	34.7	2.16	12.5	1.37	27.4	1.56	29.2	1.36	14.4	1.19
135	43.1	35.2	45.5	2.84	39.0	2.64	20.1	1.84	41.0	1.74	35.0	1.47	15.9	1.04
136	54.2	43.3	49.1	2.84	37.3	2.31	13.7	1.38	43.2	1.74	24.7	1.44	16.3	1.22
137	29.4	55.0	60.0	3.02	44.1	2.79	18.4	1.82	52.4	2.19	37.4	1.93	19.8	1.39
138	41.0	29.7	38.2	2.57	27.3	2.17	12.2	1.46	31.7	1.64	20.2	1.44	11.6	1.39
139	44.9	39.8	39.3	2.32	32.4	2.06	17.1	1.39	39.2	1.39	28.2	1.22	15.0	1.01
140	43.9 42.7	59.7 45.8	52.5 56.4	2.77 2.84	49.3 48.6	2.87	19.2	1.73	69.8	2.66	42.8	1.99	21.4	1.40
142	41.3	45.6 46.8				2.78	19.5	1.89	50.8	2.11	36.4	1.84	19.3	1.37
143	41.3 46.1		37.2 48.1	2.14	45.7 35.9	2.64	15.6	1.59	38.2	1.59	32.7	1.42	15.7	0.97
143	46.1	50.6 44.9	48.5	2.57 2.92	35.9 44.5	2.31	11.8 13.9	1.31	39.2 44.4	1.67	29.7 28.2	1.62 1.62	15.2	1.17 1.32
145	38.0	47.4	46.5 47.7	2.39	36.7	2.79 2.31	14.6	1.57 1.54	44.4 45.0	1.97 1.74	20.2 31.3	1.57	17.7 22.4	1.47
146	36.0 46.4	43.3	58.5	3.04	38.8	2.42	15.0	1.79	50.5	1.81	30.2	1.62	20.8	1.47
147	36.7	38.5	66.3	3.64	40.7	2.57	20.4	1.73	34.8	1.79	28.8	1.69	17.6	1.29
148	32.7	41.6	47.8	2.77	39.8	2.74	16.6	1.69	47.9	2.22	32.9	1.62	20.7	1.48
149	32.7	45.0	40.6	2.57	33.3	2.27	15.7	1.57	43.9	1.94	35.9	1.76	20.7	1.48
150	45.0	52.0	55.0	2.54	48.5	2.72	19.8	1.62	51.5	1.79	36.6	1.56	17.2	1.02
151	43.7	41.8	59.9	3.44	48.9	3.26	24.8	2.24	42.5	2.19	31.6	1.87	18.5	1.09
152	66.6	44.8	61.2	3.39	47.6	2.87	25.4	2.17	44.4	1.77	33.4	1.44	18.2	1.24
153	47.0	46.9	67.5	3.67	52.1	2.89	22.9	2.04	60.0	2.29	44.7	1.87	17.6	0.99
154	47.4	46.5	54.1	3.06	39.7	2.49	21.4	1.87	56.8	2.37	32.0	1.60	19.5	1.32
155	44.4	35.3	50.8	2.67	42.8	2.42	16.7	1.49	28.7	1.52	32.3	1.37	20.2	1.40
156	49.0	56.9	52.0	2.74	37.1	2.34	16.9	1.62	57.8	2.19	46.7	1.96	21.0	1.30
157	72.4	68.5	77.0	4.17	58.3	3.64	24.6	2.19	54.1	3.02	44.8	2.22	21.4	1.72
158	53.8	62.6	72.8	3.34	49.1	3.04	21.5	1.94	42.8	1.82	42.5	1.91	21.5	1.57
159	60.5	61.1	55.5	2.89	42.6	2.62	19.1	1.84	54.2	2.16	35.6	1.69	19.8	1.27
160	78.0	84.0	72.8	3.02	52.3	3.04	21.5	1.99	63.3	2.65	43.9	1.81	21.5	1.39

